

**MICRORNAS IN NORMAL AND MALIGNANT COLON STEM CELLS
AND THEIR POSSIBLE ROLE IN STEM CELL ORIGIN
OF COLON CANCER**

by

Vignesh Viswanathan

A dissertation submitted to the Faculty of the University of Delaware in partial fulfillment of the requirements for the degree of Doctor of Philosophy in Biological Sciences

Summer 2014

© 2014 Vignesh Viswanathan
All Rights Reserved

UMI Number: 3642367

All rights reserved

INFORMATION TO ALL USERS

The quality of this reproduction is dependent upon the quality of the copy submitted.

In the unlikely event that the author did not send a complete manuscript and there are missing pages, these will be noted. Also, if material had to be removed, a note will indicate the deletion.



UMI 3642367

Published by ProQuest LLC (2014). Copyright in the Dissertation held by the Author.

Microform Edition © ProQuest LLC.

All rights reserved. This work is protected against unauthorized copying under Title 17, United States Code



ProQuest LLC.
789 East Eisenhower Parkway
P.O. Box 1346
Ann Arbor, MI 48106 - 1346

**MICRORNAS IN NORMAL AND MALIGNANT COLON STEM CELLS
AND THEIR POSSIBLE ROLE IN STEM CELL ORIGIN
OF COLON CANCER**

by

Vignesh Viswanathan

Approved:

Randall L. Duncan, Ph.D.
Chair of the Department of Biological Sciences

Approved:

George H. Watson, Ph.D.
Dean of the College of Arts and Sciences

Approved:

James G. Richards, Ph.D.
Vice Provost for Graduate and Professional Education

I certify that I have read this dissertation and that in my opinion it meets the academic and professional standard required by the University as a dissertation for the degree of Doctor of Philosophy.

Signed:

Bruce Boman, M.D., Ph.D.
Co-Advisor in charge of dissertation

I certify that I have read this dissertation and that in my opinion it meets the academic and professional standard required by the University as a dissertation for the degree of Doctor of Philosophy.

Signed:

Deni Galileo, Ph.D.
Co-Advisor in charge of dissertation

I certify that I have read this dissertation and that in my opinion it meets the academic and professional standard required by the University as a dissertation for the degree of Doctor of Philosophy.

Signed:

Pamela Green, Ph.D.
Member of dissertation committee

I certify that I have read this dissertation and that in my opinion it meets the academic and professional standard required by the University as a dissertation for the degree of Doctor of Philosophy.

Signed:

Greg Gonye, Ph.D.
Member of dissertation committee

I certify that I have read this dissertation and that in my opinion it meets the academic and professional standard required by the University as a dissertation for the degree of Doctor of Philosophy.

Signed:

Gary Laverty, Ph.D.
Member of dissertation committee

ACKNOWLEDGEMENTS

I would like to thank my advisor Dr. Bruce Boman for giving me this really interesting project on miRNAs and cancer stem cells. I thank for him for his constant support and guidance through the course of dissertation. He looked at the smallest progress with a lot of enthusiasm and promise. He taught me how to think like an independent investigator and come up with ideas and sound reasoning for new findings in lab. His idea of having social gatherings in our lab was a great opportunity to take your mind off science once in a while and just sit and brainstorm with your colleagues.

I would like to extent my gratitude to Dr. Lynn Opdenaker, who played a very important role in completion of my dissertation. Her prior scientific experience guided me with my experiments such as troubleshooting and setting up the right controls. I am grateful to her for training me how to use the Flow cytometer, which was used extensively for my work. She was always very prompt in reminding me of small deadlines regarding conferences and trainings, which helped keeping up with such important things. She provided valuable inputs and criticism for my dissertation and I thank her for that.

I would like to thank Dr. Deni Galileo for his constant encouragement and guidance in my project. I am thankful to him for letting me use his lab space for work that was crucial for my experiments. His input was very valuable in all my committee meetings, which made me rethink the design of my proposed experiments in a proper

well-directed fashion. He and his lab helped me extensively with the chick embryo model, which was used for my *in vivo* experiments.

I would like to acknowledge Dr. Pamela Green for being greatly involved in my project and introducing the world of RNA SEQ to me. She was always very enthusiastic about the progress I made in my work and provided me with great tips to help me plan my experiments better to support my hypothesis. She was very generous to help me perform RNA SEQ analysis, which turned out to be a crucial part of my work. She was always welcoming to discuss problems I was facing during the course of my PhD.

I would like to thank Dr. Greg Gonye, for his insight on miRNAs, profiling and having set goals in a time dependent fashion. He was always concerned about my timeline and the feasibility of completion of my proposed work, which was a good source of support and encouragement. I thank him for all the positive criticism I received regarding my data presentation skills. He also helped me understand simple bioinformatics tools to represent my miRNA profiling data in a better way.

I would like to acknowledge Dr. Gary Lavery for his valuable input regarding my progress of my work in all the committee meetings. He was very prompt in getting back to my queries and helped me understand what was expected of me to accomplish.

I extend my gratitude to Dr. Kirk Czymmek for his valuable help with my immunostaining and microscopy work. He always encouraged new ideas and was available to discuss the feasibilities about making them work.

I would like to thank Dr. Nicholas Petrelli, for his support and motivation during my PhD work. He provided us with constant source of funding which made sure I never faced a roadblock or lag in my progress. He provided me with valuable

opportunities to present my work as a young investigator with clinicians that eventually helped bridge the gap between the two and established a more definite and tailored research goals.

I would like to thank my lab mate Shirin Modarai for her immense help during the course of my PhD. We learned and optimized conditions for a lot of experiments together such as tissue processing, soft agar assay and flow cytometry. She was always there to assist me with small steps of my experiment when I was preoccupied with something else and I am really grateful to her for that. She and her family especially her mother was very supportive, welcoming, included me in their festivities and made me feel at home away from home.

I would like to acknowledge Seema Bhatlekar for her immense help and support during my PhD work. I thank her for all the appreciated help she provided with tissue processing and isolation of cells, which was used for later for my miRNA profiling experiments.

I would like to thank Brenda Rabeno and Pat Swanson for their help with procurement of fresh patient matched normal and tumor tissue. Their hard work resulted in a constant supply of patient samples to our lab, which was used for a lot of downstream applications.

Thanks to Vishnu Mohanan and Karma Pace McDuffy for their immense contribution towards completion of my experiments. Vishnu guided me well with the transformation, transduction and cloning experiments. Karma helped me a lot with my chick embryo experiments and I thank her sincerely for that.

I would like to acknowledge Monica Accerbi and Skye Schmidt of Dr. Green's lab for all their invaluable time and help with my RNA SEQ experiment and analysis.

Thanks to Dr. Jennifer Sims Mourtada and Dr. Swati Pradhan Bhatt for the much appreciated inputs towards my work. I would like to thank other current and past lab members Dan, Kevin, Brian, Pawel, Jayasree, Anu, Matt and Kim of CTCR at Helen F Graham Cancer Center and Research Institute, for all their support.

I would like to strongly acknowledge Rosemarie Pope and Betty Cowgill's efforts in regards to scheduling my committee meetings and follow-ups to meet my deadlines.

I would like to thank Poonam (Ivy) for her unconditional love and support over the last five years. Her unparalleled determination and hard work to achieve her career and personal goals always inspired me. I would like to thank my friends Montu, Su, Aditya, Praveen, Siddharth, Pratima, Arul, Suresh and Sandy for being there for me all these years. Special gratitude to my friends Anindita Gupta and Vimal Gangadharan for all their support, the brainstorming discussions and helpful feedbacks.

Last but not the least, I would like to extend my sincere gratitude to my family back in India, who have been truly motivating and inspiring me for the longest time I remember.

TABLE OF CONTENTS

LIST OF TABLES	xiv
LIST OF FIGURES	xv
ABSTRACT	xviii

Chapter

1	BACKGROUND	1
1.1	Colon Anatomy and Physiology:	1
1.2	Colon Diseases:	6
1.2.1	Ulcerative Colitis:	6
1.2.2	Crohn's Disease:	6
1.2.3	Irritable Bowel Syndrome (IBS):	6
1.2.4	Diverticular disease:	7
1.2.5	Colorectal cancer:	7
1.3	Types of Colon Cancer:	9
1.4	Progression and Staging of the Disease:	9
1.5	Molecular Basis of Progression of Colon Cancer:	13
1.5.1	Genomic Instability:	13
1.5.2	Activation of Oncogenes:	14
1.5.3	Inactivation of Tumor Suppressor Genes:	15
1.6	Stem Cell Model for Carcinogenesis:	16
1.7	Cancer Stem Cell Model using Colon as an Example:	17
1.8	Colon Cancer Stem Cell Markers:	19
1.9	Role of MicroRNAs in Colon Cancer:	23
1.9.1	Synthesis and Function:	23
1.9.2	Deregulation of MiRNAs in Cancer:	26
1.9.3	Mechanism of Deregulation of MiRNAs:	26
1.9.3.1	Genomic Abnormalities:	27
1.9.3.2	Histone Modification and CpG Island methylation:	27
1.9.3.3	Regulation by Transcription Factors:	27

1.9.3.4	Abnormal Maturation of MiRNAs:	28
1.9.4	Differential Expression of MiRNAs in Colorectal Cancer:	28
1.9.5	MiRNAs as Biomarkers in Colorectal Cancer:	31
1.9.6	MicroRNAs Target Signaling Pathways affected in Colorectal Cancer:.....	32
1.10	MiRNAs in Cancer Stem Cells:	34
2	MiRNA23B REGULATES SELF-RENEWAL AND CHEMORESISTANCE PROPERTIES OF COLON CANCER STEM CELLS.....	36
2.1	Introduction:	36
2.2	Methods:.....	39
2.2.1	Cell Lines used:	39
2.2.2	ALDEFUOR assay:	39
2.2.3	Cell Sorting by Flow Cytometry:	39
2.2.4	Taqman MiRNA Assay:.....	40
2.2.5	Transient Transfection:.....	41
2.2.6	Proliferation Assay:	41
2.2.7	Cell Cycle Analysis by PI Staining:	42
2.2.8	Soft Agar Assay:.....	42
2.2.9	Colony Sphere Assay:	43
2.2.10	Protein Isolation:	43
2.2.11	BSA Colorimetric Protein Estimation Assay:	43
2.2.12	SDS PAGE Electrophoresis:	44
2.2.13	Western Blot:.....	44
2.2.14	RNA Isolation:.....	45
2.2.15	RNA Quantification:	46
2.2.16	cDNA Synthesis:	46
2.2.17	Realtime PCR:	47
2.2.18	Immunocytochemistry:.....	47
2.2.19	Invasion Assay:	48
2.2.20	Transformation, Transfection and Transduction:	48
2.2.21	Luciferase Assay:	49
2.2.22	Determination of IC ₅₀ for 5-FU for HT29:.....	50
2.2.23	RNA SEQ analysis:	50
2.3	Results:	50
2.3.1	MiR23b is Upregulated in Colon Cancer Stem Cells and Has an Effect on Proliferation and Cell Cycle:	51

2.3.2	Mir23b Causes a G0/G1 Arrest In Cells and Decreases Proliferation:	51
2.3.3	Mir23b is Important for Self-Renewal Function of Colon Cancer Stem Cells:	52
2.3.4	Mir23b Promotes EMT and Invasion in Colon Cancer Cells: ...	56
2.3.5	Stable Expression and Knockdown of MiR23b Modulates Proliferation, Cell Cycle and Self-renewal Function:	56
2.3.6	Mir23b Knockdown Promotes Chemoresistant Properties in HT29 cells Against 5-FU Drug via the Up-regulation of LGR5:.....	60
2.3.7	LGR5 and ALDH Positive Cells are Two Different Sub-populations in Colon Cancer Cell Line HT29:.....	60
2.3.8	RNA SEQ Analysis Identified Novel Targets of MiR23b:	61
2.4	Discussion:	66
3	IDENTIFICATION, ISOLATION AND MiRNA PROFILING OF COLON CANCER STEM CELLS	71
3.1	Introduction:	71
3.1.1	Musashi 1:	72
3.1.2	CD133:.....	72
3.1.3	CD166:.....	73
3.1.4	ABCG2:.....	74
3.1.5	LGR5:.....	75
3.1.6	LRIG1:.....	75
3.1.7	BMI1:.....	76
3.1.8	Telomerase:	77
3.1.9	ALDH1:.....	77
3.2	Methods:	78
3.2.1	Immunofluorescence:	78
3.2.2	Cell Lines:	80
3.2.3	Immunostaining and Flow Cytometry Analysis for CD166:	80
3.2.4	Tissue Microarray (TMA) Immunofluorescence Study:	81
3.2.5	Isolation of Crypts and Dissociation of Normal and Tumor Tissue to Single Cells:	83
3.2.6	Aldefluor Assay, Propidium Iodide Staining and EpCAM Staining of Normal and Tumor cells:	83
3.2.7	Cell Sorting by Flow Cytometry:	84
3.2.8	RNA Isolation:.....	85
3.2.9	RNA Quantification:	86

3.2.10	MiRNA Profiling:.....	86
3.2.11	Taqman MiRNA Assay:.....	87
3.2.12	Transient Transfection:.....	87
3.2.13	Proliferation Assay:.....	88
3.3	Results:.....	88
3.3.1	Multiple Stem Cell Markers Stain Specific Cells in Normal Crypt Base as Well as in Tumor:.....	88
3.3.2	Normal and Cancer Stem Cells were Identified and Sorted from Fresh Tissue Samples:.....	106
3.3.3	Cancer Stem Cells have Differential MiRNA Expression Pattern as Compared to the Normal Stem Cells:.....	110
3.3.4	Microrna92a Show Differential Expression in ALDEFLUOR Positive Cancer Stem Cells and Target LRIG1 Gene:.....	114
3.4	Discussion:.....	116
4	DISCUSSION.....	119
5	FUTURE WORK.....	134
6	REFERENCES.....	138
Appendix		
A	SUPPLEMENTARY INFORMATION.....	154
A.1	POSITIVELY AND NEGATIVELY CORRELATED GENES WITH ALDH1A1 WITH SHARED TRANSCRIPTIONAL REGULATORY ELEMENTS (TREs) IN NORMAL COLON AND CANCER TISSUE: A BIOINFORMATICS STUDY.....	154
A.2	VALIDATION OF MIR23B OVEREXPRESSION AND KNOCKDOWN IN HT29 CLONES.....	158
A.3	EXPRESSION ANALYSIS OF THREE DIFFERENT CD44 ISOFORMS IN NORMAL COLONIC CRYPT AND TUMOR TISSUES.....	160
A.4	ANALYSIS OF MRNA LEVELS OF PREDICTED TARGETS FOR DIFFERENTIALLY EXPRESSED MIRS AT THE NORMAL STEM CELL ENRICHED REGION.....	164
A.5	VALIDATION OF RNA SEQ DATA BY LOOKING AT EXPRESSION OF 3 PREDICTED TARGETS.....	166
B	PERMISSIONS.....	169

LIST OF TABLES

Table 3.1: List of antibodies and their dilutions tested for expression in normal and tumor colonic tissue.....	80
Table 3.2: Clinicopathological features of patient tissues used for the tissue microarray study.....	82
Table 3.3: Summary of expression pattern of different SC markers analyzed by immunofluorescence.	101
Table 3.4: List of patients matched normal and tumor colon samples with successful sorting of ALDEFLUOR positive cells.	111
Table 3.5: List of differentially expressed microRNAs in tumor ALDEFLUOR positive compared to normal ALDEFLUOR positive cells from one patient.	113
Table 4.1: miR23b expression and its targets in cancer..	125
Table A.1: List of primers of genes used for Real time PCR studies.....	168

LIST OF FIGURES

Figure 1.1: Anatomy of colon and the colon wall.....	2
Figure 1.2: Colonic crypt architecture.....	5
Figure 1.3: TNM classification of colorectal cancer stages.....	12
Figure 1.4: ALDH1 as a marker for colon cancer stem cells.....	22
Figure 1.5: miRNA biosynthesis.....	25
Figure 1.6: Differential expression of miRNAs at different stages of colorectal cancer.....	30
Figure 1.7: miRNA expression at various stages of colon cancer.....	33
Figure 2.1: miRNA expression in stem cell enriched crypt bottom.....	38
Figure 2.2: ALDEFUOR assay for HT29 and SW480 and miR23b expression in ALDEFUOR positive cells in HT29 and SW480 cells.....	53
Figure 2.3: MiRNA23b inhibits proliferation via promoting G0/G1 cell cycle checkpoint.....	54
Figure 2.4: MiR23b promotes self-renewal.....	55
Figure 2.5: MiR23b promote Epithelial-Mesenchymal transition.....	58
Figure 2.6: Effects of long-term manipulation of miR23b.....	59
Figure 2.7: MiR23b inhibition promotes chemoresistance to 5-FU.....	62
Figure 2.8: MiR23b targets 3' UTR of LGR5 mRNA.....	63
Figure 2.9: LGR5 and ALDH1 expression do not overlap in cancer cells.....	64
Figure 2.10: RNA SEQ analysis to identify novel targets of miR23b.....	65
Figure 2.11: Proposed model of existence of hierarchy in colon CSCs.....	70
Figure 3.1: Expression of ALDH1 in normal colonic crypt and tumor tissue.....	91

Figure 3.2: Expression of ABCG2 in normal colonic crypt and tumor tissue.	92
Figure 3.3: Expression of CD166 in normal colonic crypt and tumor tissue.	93
Figure 3.4: Expression of LRIG1 in normal colonic crypt and tumor tissue.	94
Figure 3.5: Expression of BMI1 in normal colonic crypt and tumor tissue.	95
Figure 3.6: Co-staining of ALDH1 and CD166 in normal colonic crypt and tumor tissue.	96
Figure 3.7: Co-staining of ALDH1 and LRIG1 in normal colonic crypt and tumor tissue.	97
Figure 3.8: Co-staining of LRIG1 and CD166 in normal colonic crypt and tumor tissue.	98
Figure 3.9: Co-staining of ALDH1 and BMI1 in normal colonic crypt and tumor tissue.	99
Figure 3.10: Co-staining of CD166 and BMI1 in normal colonic crypt and tumor tissue.	100
Figure 3.11: Staining patterns of ALDH1 and LRIG1 in colon tumors tissues from 75 patients.	102
Figure 3.12: Staining pattern of ALDH1 and LRIG1 in colon tumors tissues from 75 patients.	103
Figure 3.13: FACS analysis of multiple marker expression in colon cancer cell lines.	104
Figure 3.14: FACS analysis of multiple marker expression in colon normal and cancer cells from patients.	105
Figure 3.15: ALDH activity in the bottom of fresh normal isolated crypts.	107
Figure 3.16: ALDH activity in fresh dissociated patient tumor cells.	108
Figure 3.17: Isolation of stem cells from fresh patient normal and tumor samples.	109
Figure 3.18: Differential expression of microRNAs in normal and tumor ALDEFLUOR positive and negative cells.	112

Figure 3.19: MiR92a is overexpressed in ALDEFLUOR positive cells and regulate the LRIG1 gene expression.....	115
Figure 4.1: Network map of miR23b and its targets.....	126
Figure 4.2: Role of microRNAs in colon cancer stem cells.....	133
Figure A.1: List of correlated genes with <i>ALDH1A1</i> with shared TREs in healthy colon.....	155
Figure A.2: List of correlated genes with <i>ALDH1A1</i> with shared TREs in colon cancer.....	156
Figure A.3: List of correlated genes with <i>ALDH1A1</i> with shared TREs in all samples.....	157
Figure A.4: Validation of miR23b levels in overexpressing and knockdown miR23b clones by looking at its functional target <i>SMAD3</i>	159
Figure A.5: CD44 staining (4077) of normal and tumor colon tissue.....	161
Figure A.6: CD44 staining (4080) of normal and tumor colon tissue.....	162
Figure A.7: CD44 staining (4081) of normal and tumor colon tissue.....	163
Figure A.8: mRNA levels of common predicted targets of miR25 and miR7.....	165
Figure A.9: Expression levels of predicted targets after altered miR23b expression.....	167

ABSTRACT

The role of miRNAs in colon cancer development pertaining specifically to the stem cell origin of cancer is yet to be elucidated. We hypothesized that perturbation of miR expression levels contributes to changes in target gene belonging to self-renewal pathways, which initiate colon tumorigenesis. Our miR profiling studies to identify miRs that regulate colon cancer stem cells (CSCs) were broadly divided in two parts. In one study we profiled the normal crypt bottom subsection that is enriched in stem cells and identified miR23b to be one of the miRs to have a significant differential expression. MiR23b has already been identified as having a role in renal, prostate, bladder, breast and colon cancers involving cell migration, invasion and apoptosis. Recently, a role for miR23b in ovarian CSCs and response to chemotherapy has also been elucidated. Consequently, I postulated that miR23b regulates colon CSCs. My results showed that miR23b is overexpressed in the ALDEFLUOR high sub-population of HT29 and SW480 colon cancer cells. It was shown to control the colon CSC phenotype and significantly affects proliferation, cell cycle, self-renewal, EMT, invasion and chemoresistance to the anti-cancer drug 5- FU. I validated that the colon CSC marker LGR5 is a target of miR23b, showing its role in modulating Wnt signaling. MiR23b also influences the transcription of multiple gene targets such as ATF2 and AKT2, which were identified by our extensive RNA SEQ analysis. The other aspect of the study was to identify miRs, which are differentially expressed in the CSCs as compared to the normal SCs from fresh patient samples. Normal and tumor tissue were initially screened for the expression of multiple putative CSC

markers (ALDH1, LRIG1, CD166, ABCG2, BMI1, Telomerase) with an aim to decide which markers should be used alone or in combination to isolate SCs. My results indicated for the first time that SC markers ALDH1, LRIG1 and CD166 do not co-stain cells in tumors suggesting a co-existence of subpopulations of CSCs in tumor. MiR profiling identified miRs such as miR200c, miR92a, miR20a and miR93 that had a significant differential expression in ALDEFLUOR high tumor cells as compared to ALDEFLUOR high normal cells. MiR92a was also significantly upregulated in ALDEFLUOR high cells of colon cancer cell lines HT29 and regulated its proliferation. Future studies have to be done on the other newly recognized candidate miRs that show differential expression in primary tumor SCs. Understanding the role of miRs in CSCs could contribute to identification of new targets for therapeutic intervention.

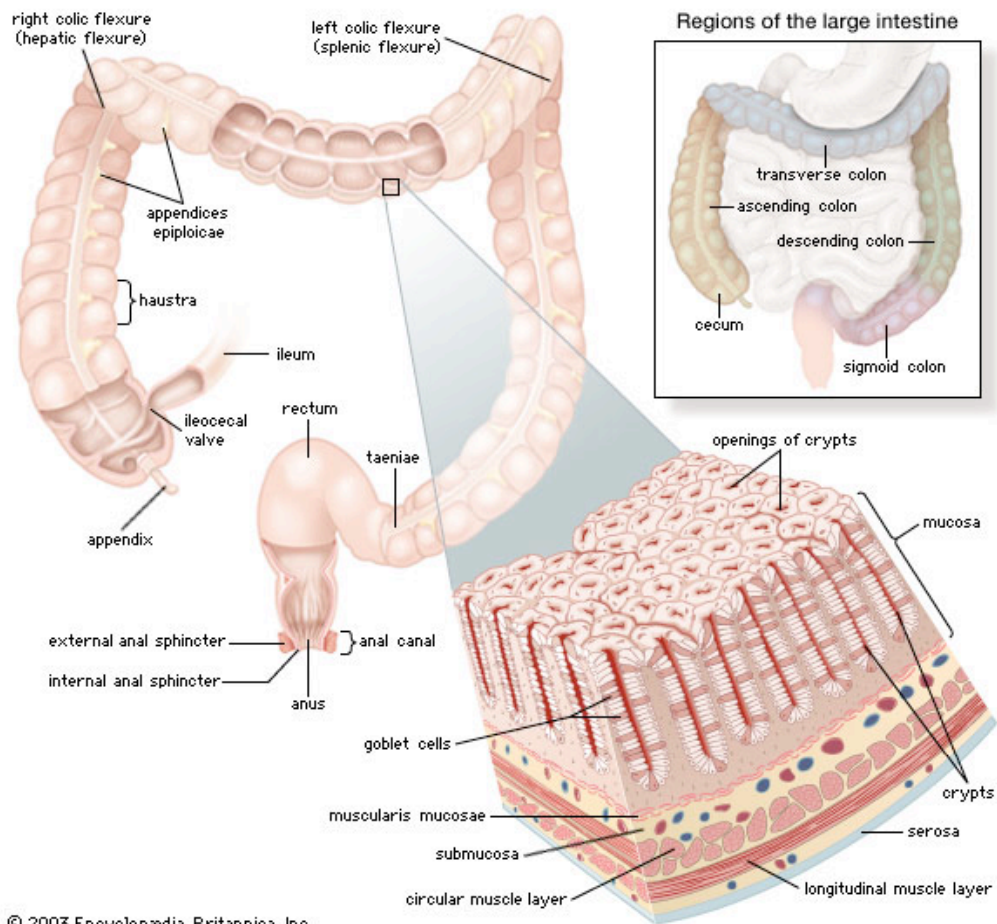
Chapter 1

BACKGROUND

1.1 Colon Anatomy and Physiology:

The colon is a 1.5-meter long muscular tube that forms the penultimate part of the digestive system. It is comprised of the ascending, transverse, descending and sigmoid segments. The right colon terminates into the caecum, which is also identified located by the appendix, a vestigial organ that protrudes out as a small appendage with the help of three longitudinal muscles of taeniae coli. The right and the left colon are connected by the transverse colon, which runs horizontally. The two junctions where the transverse colon meets the right or the left colon are called the hepatic flexure and splenic flexure, respectively. The left colon runs down from the splenic flexure and connects the sigmoid colon to the transverse colon. The sigmoid colon gets its name from its appearance, which is in the form of a letter 'S'. **(Figure 1.1)**

At the tissue level, the colon wall is composed of four prominent layers: mucosa, submucosa, muscularis and serosa. The mucosa, which is the innermost layer of the colon, is composed of glandular epithelium, lamina propria and muscularis mucosae. The submucosa is a layer of fibrous connective tissue, which connects the muscularis mucosae and muscularis propria. It harbors cells like fibroblasts, mast cells and also blood and lymphatic vessels. The next layer is the muscularis propria, which consists of two layers of smooth muscle cells that run in a circular and longitudinal fashion. The outermost layer, also called the serosa, is a single layer of mesothelial cells that lines the organ **(Figure 1.1)**[1].



© 2003 Encyclopædia Britannica, Inc.

Figure 1.1: Anatomy of colon and the colon wall. Colon is composed of the ascending, transverse, descending and the sigmoid colon. A cross-section of the colon wall displays different layers from outside towards the lumen, which are serosa, muscle layers, submucosa, muscularis mucosae and epithelial layer. By courtesy of Encyclopædia Britannica, Inc., copyright 2003; used with permission.

The colon, as an organ, plays a role in digestion in spite of the fact that the majority of the digestion has already been taken place in the stomach and the small intestine. The colon harbors around 400 species of the bacteria, out of which the majority are obligate anaerobes. They carry out fermentation of complex carbohydrates primarily in the ascending and the proximal transverse colon, whereas the undigested proteins are digested in the distal colon. The residual products by fermentation are absorbed or passed along with the feces. One of the final products, short chain fatty acids, are derived and provided predominantly by the colon and are responsible for meeting around 10 to 15 % of the daily caloric requirement of an individual. The primary source of energy of the colonic epithelial cell (i.e. colonocyte) is also met by a fatty acid molecule butyrate. Butyrate promotes absorption of water, sodium and chlorine from the lumen and also has been shown to play a role in colon carcinogenesis. The colon is integral in the absorption of water and electrolytes from the lumen by absorbing about 90% of the water fed to it (1.5 to 2.0 gallons), and the rest is extruded with feces. Surface epithelial cells of the ascending colon mainly carry out the absorption process by creating an osmotic gradient. The absorption occurs primarily through a paracellular pathway and to some extent transcellular with the help of different proteins. The colon at the expense of the loss of potassium and bicarbonate carries out sodium and chloride ions conservation [2].

The functional unit of the colon wall is composed of numerous finger-like invaginations called crypts of Leiberkuhn, which are lined by epithelial cells or colonocytes. There are pluripotent cells at the base of the crypt, which are responsible

for renewing the lining of the crypt every 5-6 days. This idea was postulated in 1974 by Cheng and Leblond as the Unitarian theory [2]. The stem cells, through symmetric and asymmetric divisions, give rise to various differentiated cells of the colonic crypt. There are four different terminally differentiated cells present in the colon: absorptive cells, mucus secreting goblet cells, peptide hormone secreting endocrine cells and less abundant Paneth cells. The absorptive cells are elongated columnar cells and are contain microvilli, whereas the goblet cells are oval or round cells with basally-placed nuclei. The crypts also possess few specialized endocrine function called enteroendocrine or neuroendocrine cells (**Figure 1.2**).

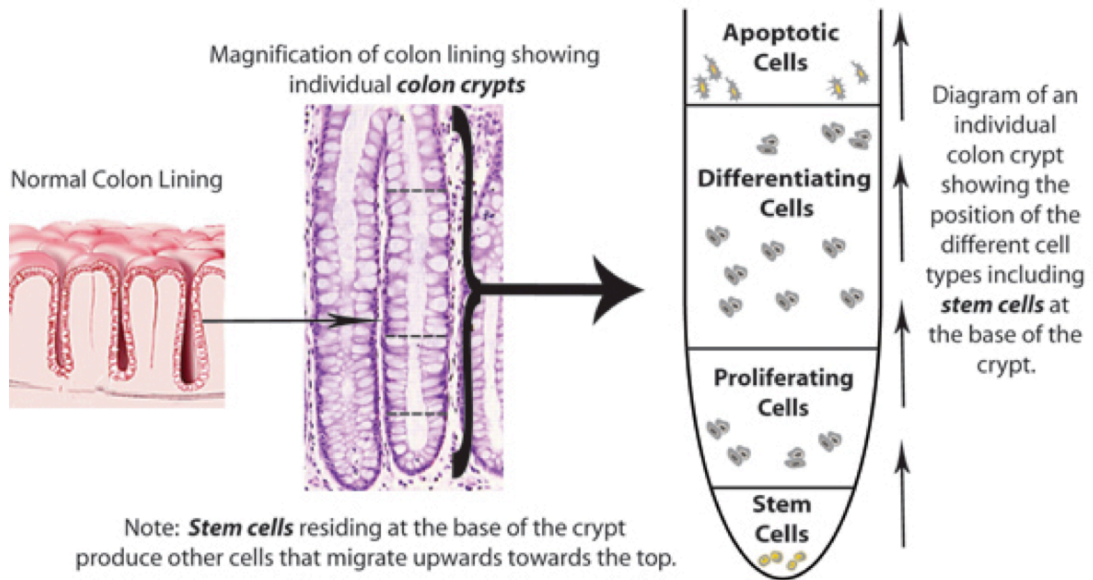


Figure 1.2: Colonic crypt architecture. Colonic crypts have stem cells residing at the base of the crypt, which is responsible for giving rise to committed progenitor and differentiated cells as they move up the crypt. Image reproduced from Johns Hopkins colon cancer center website with permission.

1.2 Colon Diseases:

There is a broad range of ailments that could be associated with the colon. The symptoms of the various conditions are quite overlapping, which could lead to misinterpretation or misdiagnosis. The major diseases associated with this organ are:

1.2.1 Ulcerative Colitis:

It is an inflammatory disease of the colon, which affects about 500,000 people under the age of 30 per year. Typical symptoms presented in this condition include bleeding with defecation, abdominal pain, constipation or diarrhea. While no specific treatment exists, medical help or even surgery is prescribed for chronic cases. A newer form of surgery called the ileoanal procedure replaces the colon and the rectum with a small bowel pouch, which is fused with the anus to collect waste [3].

1.2.2 Crohn's Disease:

It is a chronic inflammatory condition, which involves the intestinal tract and affects young individuals between the ages of 16 and 40. The disease is diagnosed with the help of a physical examination, such as colonoscopy or sigmoidoscopy, barium X-ray test of the upper and lower intestinal tract and analysis of the family history since 20% of all treated individuals present with an affected family member. Treatment involves use of anti-inflammatory drugs or surgery to remove the diseased portion of the intestine and join the adjoining ends together (resection and anastomosis) [3].

1.2.3 Irritable Bowel Syndrome (IBS):

This condition affects around 30% of Americans at some point of their lives. It is an intestinal muscle functioning disorder, which results in diarrhea, constipation or

both with abdominal pain. Because the symptoms of IBS are similar to other conditions such as colon cancer or colitis, medical examination of the intestine or a fecal sample is recommended to rule out such possibilities. Typically, dietary changes such as increased fluid intake or bulk food to soften the stool may provide relief to the patients or else medical intervention is prescribed [3].

1.2.4 Diverticular disease:

Also called Diverticulosis, this condition affects half of all Americans between the ages of 60 and 80. This disease is characterized by infection or inflammation of the pockets, or diverticuli, in the colon wall. It can be diagnosed by routine colon and rectal examinations, and treatment usually involves a high fiber/low fat diet as well as antibiotics and stool softeners [3].

1.2.5 Colorectal cancer:

Cancer is defined as the uncontrolled proliferation of cells. Cancer of the colon and rectum is the third leading cause of death in both sexes in the United States. The lifetime risk of developing this type of cancer is 1 in 20 or 5%. The main risk factors that may increase the chances of developing colon cancer are:

Age: The chances of developing colon cancer increases markedly after the age of 50.

History of polyps: If an individual has a history of adenomatous polyps, it increases the chances of developing cancer.

History of Inflammatory Bowel Disease: If a person presents with either Crohns' disease or Irritable Bowel Syndrome actually can present with dysplasia (abnormal cells), which could lead to cancer.

Family History of Colorectal Cancer or Polyp: One in five individuals diagnosed with colon cancer demonstrates a family history where they have an affected first-degree relative (siblings, parents).

Inherited Syndromes: Around 5 to 10 percent of individuals who have colorectal cancer have inherited gene defects. The two most common inherited forms of colorectal cancer are Familial Adenomatous Polyposis (FAP) and Hereditary Non Polyposis Colorectal Cancer (HNPCC). In addition, there are other rare disorders such as Turcot Syndrome, Peutz-Jeghers Syndrome and *MUTYH* associated syndrome that will increase the risk for developing colon cancer. **FAP** is caused by a mutation in the *APC* (Adenomatous polyposis coli) gene and is responsible for approximately 1% of all colorectal cancer cases. Individuals with this mutation develop thousands of polyps in the colon wall as at early age and one of them eventually grows to a full-blown disease. **HNPCC**, also known as Lynch Syndrome, accounts for 2-4% of all colorectal cases and is due to a mutation in the *MLH1* and *MSH2* genes, which are involved in DNA repair pathways. An individual with such a mutation can have hundreds of polyps and carry a high risk (80%) of developing colorectal cancer.

There are other risk factors associated with the development of colorectal cancer such as ethnicity, diabetes, diet, physical activity, smoking and alcohol abuse [4].

1.3 Types of Colon Cancer:

Colon cancer typically develops from the formation of small benign growth in the colon wall called a polyp. This polyp could be adenomatous (pre-cancerous) or hyperplastic (typically non-cancerous). There are several types of cancer that can start in the colon and the rectum:

Adenocarcinomas: This type of cancer accounts for 95% of all the cancer cases. These arise from the glandular cells of the crypt.

Carcinoid tumors: This type of tumor arises from specific hormone producing cells of the intestine called the neuroendocrine or enteroendocrine cells.

Gastrointestinal Stromal tumors: The intestinal cells of Cajal, a specialized group of cells present in the intestine, are responsible for giving rise to this type of cancer.

Lymphomas: The cells of the lymph nodes found in the colon are the source of lymphomas. Non-Hodgkin's Lymphoma is a typical example of one found in the intestine.

Sarcomas: These rare forms of colon cancer start in the muscle and connective tissue of the wall of the colon [5].

1.4 Progression and Staging of the Disease:

Colorectal cancer usually starts from a small lump of tissue called a polyp. It may cause changes in bowel habits, rectal bleeding and abdominal cramping. The disease starts in the inner wall of the colon and can potentially metastasize to distant organs via the blood stream or lymphatic system (**Figure 1.3**). Depending upon the extent of progression of the cancer, it can be categorized into four stages:

Stage 0: This is the presence of dysplastic or abnormal cells in the colon wall and is called Carcinoma in situ.

Stage I: Cancer has grown into the mucosa and possibly the submucosa or muscle layer.

Stage II: Cancer has developed into the mucosa and has started to penetrate into the submucosa layer. This stage is further divided into IIA, IIB and IIC.

IIA: Cancer has reached the serosa (outermost layer) through the muscle layer.

IIB: The cancer has spread out of the serosa but has not metastasized to nearby organs.

IIC: The cancer has spread out of the serosa and into the nearby organs.

Stage III: This is further divided into IIIA, IIIB, and IIIC.

IIIA: Cancer has spread through the mucosa, submucosa and into the muscle layer and also to 1-3 nearby lymph nodes. This stage is also used to describe cancer that has spread into the submucosa and 4-6 nearby lymph nodes.

IIIB: Cancer has spread through the serosa and into not more than 3 lymph nodes, or the cancer has spread into the muscle layer below the submucosa and into not more than 6 nearby lymph nodes. If the cancer has grown into the mucosa and 7 or more nearby lymph nodes, it falls in this category.

IIIC: Cancer has spread out the serosa and into not more than 6 nearby lymph nodes, or the cancer has spread to the serosa layer via the muscle layer and into 7 or more nearby lymph node. The cancer is grown out of the serosa and into nearby organs.

Stage IV: Can be further divided into stage IVA and IVB.

IVA: Cancer has basically spread to distant organ and lymph node.

IVB: Cancer has spread into multiple distant organs, away from colon or into the lining of the abdominal wall [6].

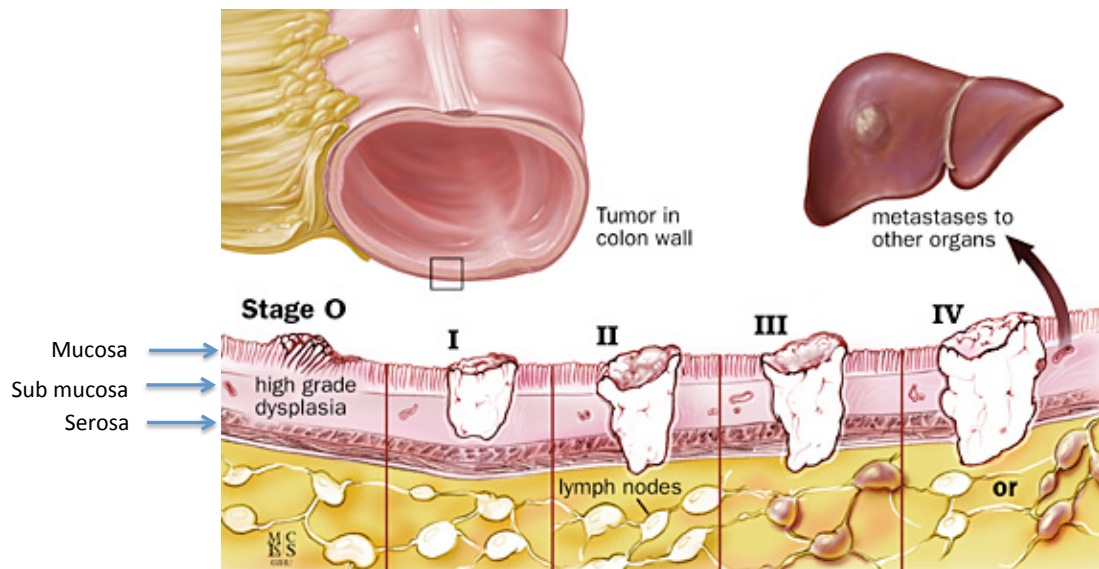


Figure 1.3: TNM classification of colorectal cancer stages. The progression of colon cancer involves the tumor growing outwards extruding out of the colon wall and metastasizing to nearby lymph nodes as well as distant organs such as liver. Image reproduced from Johns Hopkins colon cancer center website with permission

1.5 Molecular Basis of Progression of Colon Cancer:

The progression of the disease is controlled by the interplay of various factors, which operate at a multistep level. There are various molecular events, which direct the outcome or behavior of the colon cancer cells in this disease. Here is a small summary of the major molecular factors involved in this disease:

1.5.1 Genomic Instability:

Genomic integrity is crucial for normal cell function and can be challenged due to factors such as chromosomal instabilities or impairment of DNA repair capacity.

Chromosomal Instability: This anomaly is the most common genetic factor found in colorectal cancer (around 85% of cases), which is due to the changes in the number and structure of chromosomes. Efficient silencing of the working copy of genes like *APC*, *TP53* and *SMAD4* results in loss of their tumor suppressor role and could lead to cancer [7].

DNA repair gene defects: The genes that are involved in the DNA mismatch repair pathway are mutated and lose their function in some cases of colon cancer. HNPCC, as described above, is a classic example of such a defect where the genes *MLH1* and *MSH2* are affected. This occurs from germline inactivation of one allele of the gene, and later due to somatic inactivation of the other allele in HNPCC patients. Because of the defect in DNA repair, genomic instability becomes more frequent in

these patients.[8],[9]. In non-familial colorectal cancer cases, 15% of patients demonstrate inactivation of the *MLHI* gene due to promoter hypermethylation [10]. Mutations in this pathway primary result in colon cancer and tend to occur more frequently in older individuals and females. Other proteins like *TGFBR2* and *BAX*, which harbor functional bi or tri-nucleotide repeat sequences can get inactivated because of faulty repair mechanisms [8]. Alternatively, proteins involved in the base excision repair pathway, such as *MYH*, are inactivated due to germline mutations and are prominent in some cases associated with the development of at least 15 adenomas[11, 12].

Disturbed Gene methylation: Methylation of the promoter region is an epigenetic mechanism to silence gene expression. In colorectal cancer, there is a subgroup, or locus, in the genome, which is frequently associated with aberrant methylation patterns. This phenomenon is called CpG island methylator phenotype (CIMP) and is found in about 15% of all colon cancer cases. The *MLHI* gene is one of the important genes silenced by this mechanism, resulting in its loss of function [12].

1.5.2 Activation of Oncogenes:

The activation of oncogenes such as *K-RAS* and *B-RAF* are most commonly associated with the disease. *KRAS* activation is present in about 37% of all the cases, and is associated more with hyperplastic polyps and proximal cancer [13]. *KRAS* is involved in the MAPKinase pathway, which governs cell signaling to proliferate. *BRAF* activation, on the other hand, is observed in 13% of all cases and involves

BRAF serine threonine kinase activity, a part of the MAPKinase signaling cascade [14]. *BRAF* activation is seen in early small polyps, unlike *KRAS*. *PI3K* signaling promotes cell survival, and is constitutively activated in one third of all the colorectal cancer cases. This is due to the activation of the catalytic subunit of the *PI3K* protein, activation of their downstream targets *AKT* and *PAK 4*, or inhibition of its inhibitor *PTEN* [15].

1.5.3 Inactivation of Tumor Suppressor Genes:

The mutation of the *APC* protein found in the FAP patients is a good example of tumor suppressor gene silencing. It is involved in the initiation of colorectal cancer through modulation of the *WNT* signaling cascade. *WNT* signaling, which involves beta-catenin (an oncoprotein), is responsible for the activation of a lot of downstream gene targets, thus promoting cell proliferation and inhibiting apoptosis. The *APC* protein is responsible for the turnover of beta-catenin by promoting its degradation through proteolysis. When the *APC* protein is not functional due to an inactivating mutation, the beta-catenin accumulates in the cell and Wnt signaling becomes constitutively activated [16]. The protein *TP53* regulates cell cycle arrest and is activated under different types of stress. This protein is inactivated in most tumors by a double hit mechanism, which explains that the first allele is inactivated because of a missense mutation and the other due to chromosomal deletion at the 17p location. This inactivation step is the second step in tumor progression and goes hand in hand with the conversion of adenomas to invasive carcinomas in colon cancer [17]. *TGFBR2*

receptor, a primary component of the TGF-beta signaling pathway as mentioned before is inactivated due to the mismatch repair defects. This protein inactivation constitutes the third big step in cancer progression in the colon [18].

The molecular events predominant in the various steps of the progression of the disease are discussed later and are represented in **Figure 1.7**. There are signaling pathways affected as a whole, which is evident in the cancer cells. For example, in growth factor pathways, up-regulation of *COX-2*, which is responsible for inducing the synthesis of prostaglandin E2, is observed in most of the early stages of colorectal cancer [19]. Similar pathways like *EGF* and *VEGF* pathways are also seen to be involved in the disease. Stem cell pathways, which regulate the self-renewal ability of the normal stem cells of the colonic crypt, could also be disrupted and initiate colorectal cancer. This newer mechanism of colon cancer initiation and maintenance is explained by the cancer stem cell theory.

1.6 Stem Cell Model for Carcinogenesis:

Tumor heterogeneity is a hallmark for all types of cancers whether it is leukemic or a solid tumor. Heterogeneity can be defined by the characteristic morphology, expression of specific markers and response to therapy. Two models have explained this phenomenon: the stochastic model and the more recent cancer stem cell model. The stochastic model explains that a tumor is a homogenous system in which each tumor cell is influenced by intrinsic factors such as the level of gene expression, status of the cell cycle and by extrinsic factors such as the tumor niche.

Each cell is equally sensitive and is able to revert randomly into a different state of as maturation, cell cycle changes in response to temporary cues [20]. This results in the observed heterogeneity. On the other hand, the stem cell model or hierarchical model explains that the tumor is maintained by a specific group of cells called the progenitor cells or cancer stem cells. This model suggests that a tumor consists of a hierarchy of cells, in which a small sub-population of cells called ‘Cancer Stem Cells’ (CSCs) are responsible for the generation and maintenance of rest of the tumor. CSCs by definition are ‘a small subset of cancer cells within a cancer that constitute a reservoir of self-sustaining cells with the exclusive ability to self-renew and to differentiate into the heterogeneous lineages of cancer cells that comprise the tumor’ [21]. Studying acute myeloid leukemia, John Dick *et al.* were the first to report that CSCs have tumor-initiating ability when transplanted into immunocompromised mice [22]. CSCs were later identified in various solid tumors as well such as breast [23], liver and colon [24, 25].

1.7 Cancer Stem Cell Model using Colon as an Example:

The CSC hypothesis has been extended to the colon, in part because of the existence of normal stem cells in colon tissue. The lumen of the colon consists of millions of finger-like invaginations called the Crypts of Lieberkuhn (crypts). New cells replace the epithelial linings of the crypts every 5 days, suggesting a highly controlled proliferative capacity of the organ. SCs reside at the bottom and, through symmetric and asymmetric divisions, gives rise to the differentiated cells of the crypt

(mucus secreting goblet cells and enterocytes) (**Figure 1.2A**). The proliferating, differentiating and apoptotic cells in the colonic crypt are spatially organized within the crypt. The stem cells at the bottom can divide asymmetrically and give rise to transit amplifying cells, which occupy the bottom one third of the crypt; these eventually migrate up the crypt as they undergo maturation and differentiation (**Figure 1.2B**). The terminally differentiated cells at the top of the crypt undergo cell death and are extruded into the lumen of the colon [26].

The self-renewal capacity of these SCs is tightly regulated in order to maintain crypt homeostasis. When this regulation is disrupted by genetic mutations, the cells can be transformed into cancer ‘stem cells’. A mathematical model made and validated by Boman *et al.*, suggests that overpopulation of stem cells leads to tumor initiation and tumor growth [27]. Via this model, the authors describe that self-renewal pathway as a closed loop steady state system, and perturbation of S phase kinetics of the stem cell compartment can cause an increase in the SC numbers at the bottom of the crypt. This shift overlapped strongly with the biological data provided by label retaining experiments in APC^{min} mice (with a mutation in APC found in FAP patients). On the basis of comparison of normal and FAP crypt dynamics, they conferred that its not the change in the proliferation status of the non SCs which intitates cancer, but its due to the increase in SC compartment which disturbs the steady state of crypts.

Huang *et al.*, provided biological evidence (**Figure 4**) supporting this model. With the use of the SC marker *ALDH1* (aldehyde dehydrogenase1), they found that SC overpopulation occurred in the premalignant colon (from FAP patients) and

increased with the development of adenomas and carcinomas. When tumor-derived cells enriched for ALDH⁺ cells were transplanted into NOD-SCID mice, new tumors arose [28].

1.8 Colon Cancer Stem Cell Markers:

The cancer stem cell paradigm has ignited a lot of interest in identifying CSCs in various tumors. The isolation of SC-like entities from tumors requires the identification of specific molecular markers that distinguish these SCs from the rest of the non-stem cell population. There have been various approaches used to identify and isolate cancer stem cells based on the expression of specific markers. The first stem cell marker to be identified in solid tumors was *CD133* in brain tumors. Singh *et al.*, isolated CD133⁺ cells that were able to give rise to new brain tumors when transplanted into NOD-SCID mice [29]. Breast cancer stem cells were also found to have a unique pattern of expression of CD44^{high}/CD24^{low}/EpCAM^{high} and showed high tumor initiating capabilities when isolated and transplanted into the mammary pads of NOD-SCID mice [23].

In the colon, *CD133* was used to isolate a colorectal cancer (CRC) cell population and researchers were able to demonstrate the tumor-initiating phenotype of these cells in immunodeficient mice (O'Brien *et al.*, 2007; Ricci-Vitiani *et al.*, 2007; [25]. This initial recognition of *CD133* as a marker for CRC stem cells has been challenged by reports that showed that even *CD133* negative cells from metastatic colon cancer can form colonospheres in vitro and initiate tumors in mice [30]. In 2007,

Dalerba *et al.*, isolated tumor cells based on the expression of *EpCAM* (Epithelial cell adhesion molecule) and *CD44*, a cell adhesion protein and determined that the $EpCAM^+/CD44^+$ population gave rise to the tumor in NOD/SCID mice and was enriched in other surface stem cell markers such as *CD133*. They also identified *CD166 (ALCAM)*, previously reported as a mesenchymal stem cell marker, to be enriched in $EpCAM^+/CD44^+$ segment {Dalerba, 2011 #42}. The belief that SCs from different tissues are similar has led to the perception that common markers exist between these stem cells. Hematopoietic stem cells are known to have high aldehyde dehydrogenase 1 (*ALDH1* enzyme) activity, which confers on the cells protection against alkylating agents belonging to the oxazaphosphorines family [31, 32]. There are reports stating *ALDH1* as a SC marker for normal colon and neoplastic colon [28] (**Figure 1.4**). Aldehyde dehydrogenases are NAD(P)⁺ dependent enzymes that play a role in the metabolism of a wide spectrum of aliphatic and aromatic aldehydes. The isoform *ALDH1* is involved in a two-step process of irreversible conversion of retinaldehyde to retinoic acid (RA). Retinoic acid is essential for many developmental processes, and it serves as a ligand for retinoid signaling pathways [33]. Thus, high *ALDH1* levels confer resistance to these cells and give them the ability to differentiate via the synthesis of RA. High *ALDH1* expression was first reported in acute myeloid leukemia (AML) as a marker for leukemic SCs [34]. Wicha *et al.*, provided the first evidence of high *ALDH1* expression in solid tumors. He studied breast cancer stem cells in which *ALDH1* was found to be more specific marker than the $CD44^+/CD24^{low}/ESA^+$ phenotype. Similarly, *ALDH1* has been reported as a

promising marker for stem cells in normal and tumor tissue in the colon, as well as in other tissues such as lung, liver, prostate and ovary [35-38].

Multitude of factors plays an important role in colon carcinogenesis as discussed above. One such factor is MicroRNAs, which have been shown to play a role in the implication of different human ailments including colorectal cancer.

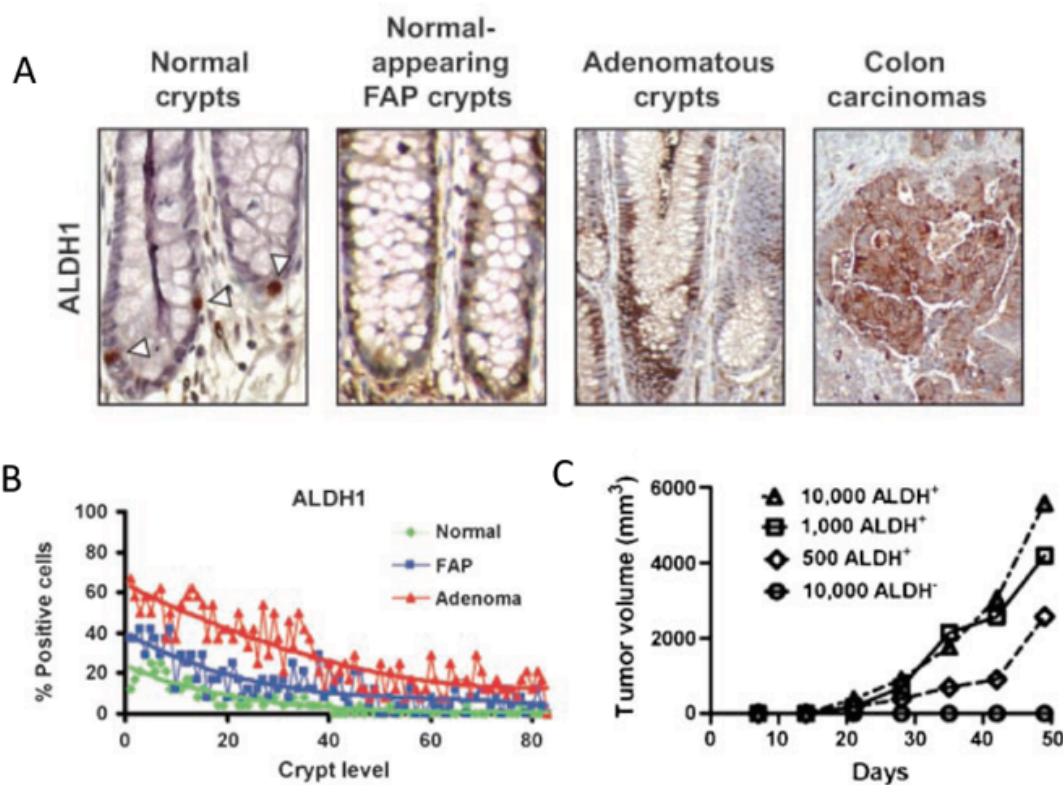


Figure 1.4: ALDH1 as a marker for colon cancer stem cells. A) ALDH1 staining in normal, FAP, adenoma and cancer tissue. B) Immunostaining analysis of ALDH1 at different positions of the crypt in Normal, FAP and adenoma. C) Tumor volumes at different days post inoculation of ALDH positive and negative cells. Reprinted from *Cancer Research*, 2009, 69, 8; 3382, Huang *et al.*, Aldehyde Dehydrogenase 1 Is a Marker for Normal and Malignant Human Colonic Stem Cells (SC) and Tracks SC Overpopulation during Colon Tumorigenesis, with permission from AACR.

1.9 Role of MicroRNAs in Colon Cancer:

As previously mentioned, the size of colonic crypts is maintained through tight regulation of proliferation, differentiation, migration and death of crypt cells. One of the major regulatory factors governing these processes is microRNAs (miRNAs). MiRNAs are short, non-coding RNA molecules (18-22 nucleotides) that play an important role in regulating gene expression post transcriptionally. They were first discovered in the early

1990's in *C. elegans* where the first miRNA, lin-4, was reported to down-regulate expression of the lin14 gene [39]. Subsequently, miRNA synthesis and function was well studied and has been reported by various groups.

1.9.1 Synthesis and Function:

MiRNAs are transcribed by RNA Polymerase II to form a primary transcript called the pri-miRNA, which has a cap structure at the 5' end and is poly-adenylated at the 3' end. This transcript bears stem loop structures that are identified and cleaved by a nuclear RNase III endonuclease, Drosha, and by DGCR8 (an RNA binding protein).

The cleavage results in a 70- nucleotide hairpin intermediate that is transported out of the nucleus by Exportin-5 and its co-factor Ran GTP. The pre-miRNA is further processed by an endonuclease, Dicer-1 in the cytoplasm to form an imperfect double

stranded miRNA duplex. This duplex is unwound by a helicase to form the mature miRNA. Transactivating response RNA binding protein (TRBP) recruits another protein, Agronaute, to the dicer complex, which holds the mature miRNA to form the RNA induced silencing complex (RISC). One of the mechanisms through which miRNAs cause translational repression is by binding to the 3' UTR of the target mRNA molecule via imperfect Watson Crick base pairing (**Figure 1.5**). The target mRNA can be sequestered by RNA degradation entities called P bodies [40] or can be degraded without them. Each miRNAs is predicted to target multiple genes because its nucleotide sequence has partial complementarity to the target 3' UTR of multiple mRNAs. Algorithms have been developed to generate tools such as *rna22*, TARGETSCAN and miRANDA to predict target mRNAs for a particular miRNA and vice versa [41-43].

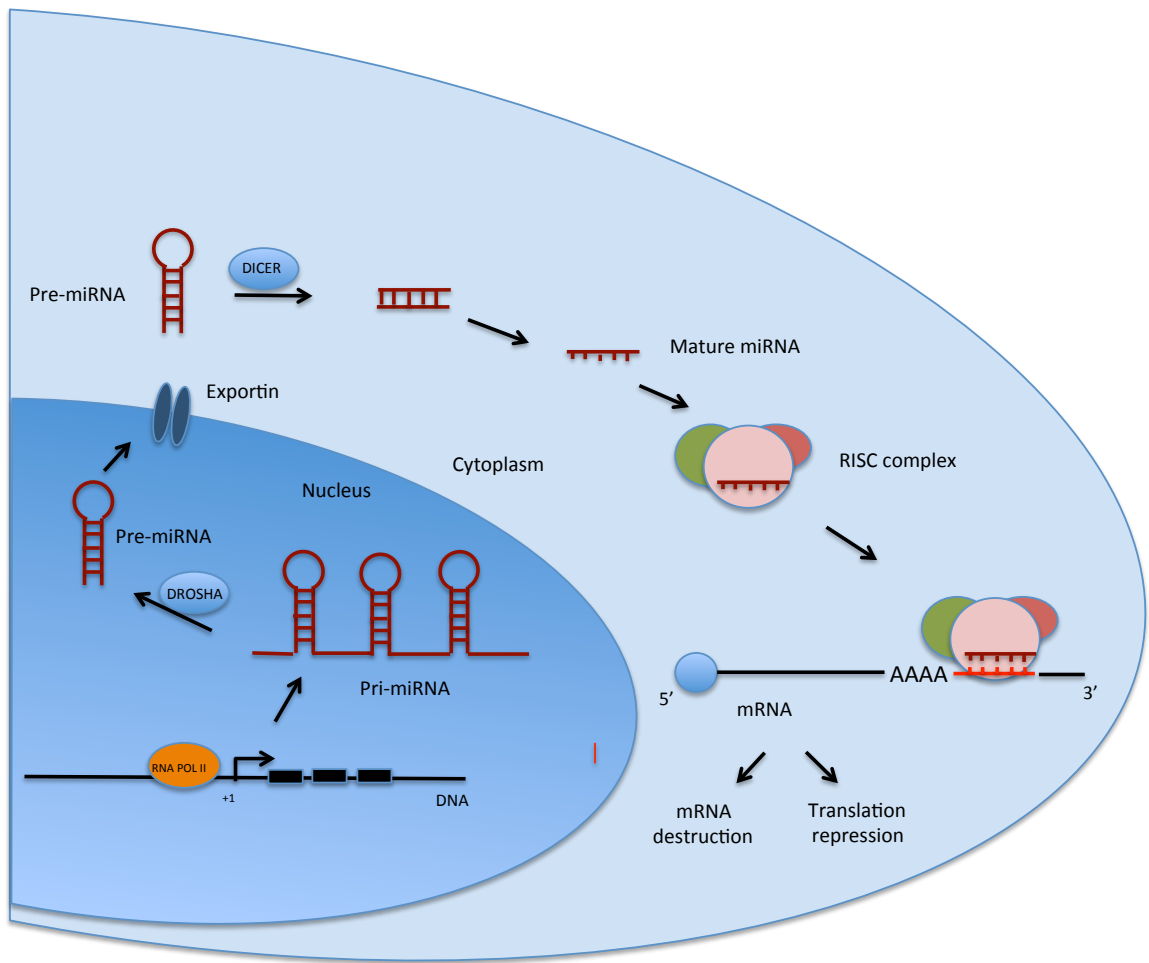


Figure 1.5: miRNA biosynthesis. The RNA polymerase II enzyme in the nucleus transcribes MicroRNA genes to form pri-miRNA. It undergoes multiple rounds of processing to become the mature miRNA strand, which associates with a group of proteins to form the RISC complex.

1.9.2 Deregulation of MiRNAs in Cancer:

MiRNAs has been shown to be involved in various aspects of cancer biology and they operate as oncogenic miRNAs or tumor suppressor miRNAs. For example, Let-7 was one of the first tumor suppressor miRNAs, which was identified to be downregulated in lung cancer and associated with elevated levels of RAS onco-protein [44]. Further studies identified multiple binding sites for Let-7 miR on the 3' UTR of RAS gene and other oncogenes such as MYC, CDK6, Cyclin D, CCND2 and HMGA2, which supported its role as a tumor suppressor miR in a wide range of tumors [45, 46]. On the other hand, there are miRNAs such as members of miR 17-92 cluster, which have been identified as oncomiRs. These miRNAs have been shown to target proteins, which promote apoptosis for example, BIM, PTEN and p21 [47, 48]. MiR21, a well studied member of that cluster has been targeted by knockdown approaches and resulted in inhibition of growth of cancer cells via the activation of apoptotic proteins, induction of TGF signaling and also cell cycle arrest in glioblastoma cells [49]. Perturbation of miRNAs affects other properties of cancer as well such as metastasis and drug resistance. MiRNA 10b is one of the well-identified miRNAs, which promotes metastasis by directly regulating Twist1, a facilitator protein involved in EMT [50].

1.9.3 Mechanism of Deregulation of MiRNAs:

Native miRNA expression is vital for the normal functioning of a cell, and disruption or induction of their expression could promote or maintain disease

conditions such as cancer. There are various mechanisms by which a miRNA expression could be altered:

1.9.3.1 Genomic Abnormalities:

Majority of the miRNA coding genes are found to be located at fragile sites in the genome. These sites are prone to chromosomal rearrangements such as amplification, translocation and deletion. The deletion of a segment of chromosome 13q14 responsible for expression of miR 15 and miR 16 in the case of B cell chronic lymphocytic leukemia (B-CLL) is a classic example of such abnormality[51].

1.9.3.2 Histone Modification and CpG Island methylation:

Hypermethylation of CpG islands located in the promoter regions leads to silencing of miRNA genes in cancer. For example, miR- 127, one of the common downregulated miRNAs in cancer, is silenced due to DNA methylation or histone modification, and inhibiting DNA methylation resulted in repressed levels of its target Bcl-6, an anti-apoptotic protein[52].

1.9.3.3 Regulation by Transcription Factors:

Some of the transcription factors such as p53 are down-regulated in a majority of cancers and regulate expression of various genes including miRNAs. P53 promotes transcription of miRNA 34a, which modulates various effects of this protein such cell cycle arrest and apoptosis [53].

1.9.3.4 Abnormal Maturation of MiRNAs:

MicroRNAs are processed in a RNase dependent fashion to give rise to a mature miRNA. Dysregulation of the expression involved in the maturation process could lead to the synthesis of faulty miRNAs, thus decreasing their expression. Lin28, which is overexpressed in human cancers, is a RNA binding protein, which is involved in the biogenesis of Let-7 miRNA. It inhibits DICER to proceed with its function and results in the accumulation of faulty Let-7 [54].

1.9.4 Differential Expression of MiRNAs in Colorectal Cancer:

MicroRNA profiling techniques have been used for identifying miRNAs that show a differential expression in CRC as compared to normal tissue. Multiple reports have confirmed that altered miRNA expression is associated with disease initiation and maintenance [55] (**Figure 1.6**). One of the recent studies identified a set of 23 microRNAs, which show a significant difference in their expression in cancer versus normal [55]. In CRC, the more number of miRNAs show an elevated level of expression which are due to the fact that there are more gain genomic copy number of miRNA coding region than loss. Michael *et al.* provided one of the first reports of differential miRNA expression, where they identified miR 143 and miR 145 as tumor suppressor miRNAs in CRC [56]. MiRNA 21 was identified as an oncogenic miRNA by various studies, which is overexpressed across various cancer types including CRC [57]. MiRNA signature could be further categorized based on the subgroups of CRC, which are MSI status, KRAS and P53 status. MiRNA 155 and miR 21 are

overexpressed associated with MSI phenotype [58]. MiRNAs are dysregulated at various stages of progression and can be represented in **Figure 1.6**. MiRNA 21, a well-studied oncogenic miRNA, is overexpressed in both colon adenomas as well as carcinomas, which reflects its role in tumor initiation, progression and metastasis. Increased miR21 expression leads to increased cell proliferation, decreased apoptosis and increased migration. This phenotype is achieved by the repression of its tumor suppressor gene targets including PTEN, PDCD4, CDC25a, TPMI and SPRY2 [59].

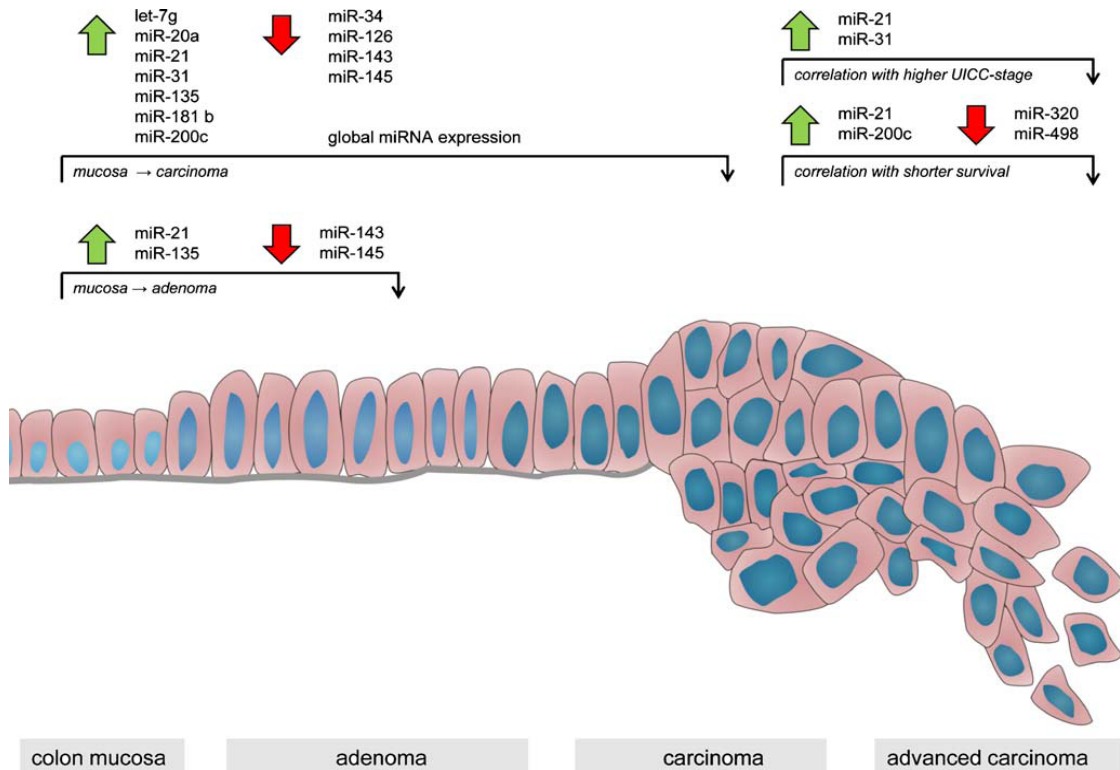


Figure 1.6: Differential expression of miRNAs at different stages of colorectal cancer. Image reproduced from Springer and Virchows Archive, 454, 2009, page, The impact of microRNAs on colorectal cancer, Claudius Faber, figure number 3, with kind permission from Springer Science and Business Media.

1.9.5 MiRNAs as Biomarkers in Colorectal Cancer:

Differential miRNA expression in CRC could be utilized as a tool to diagnose, prognose and predict survival. MiRNAs in serum and plasma have been newly identified as potential diagnostic tools for cancer. Ng *et al.*, compared the levels of circulating miRNAs in blood plasma of CRC and control samples and identified miR-92 to be overexpressed in the CRC samples [60]. The fact that levels of this miRNA are reduced following surgical removal of the tumor strengthens its identity as a possible diagnostic marker for CRC. Similarly, elevated levels of miRNA 141 in serum were strongly associated with metastatic CRC disease, which suggested that this miR could be used along with CEA to detect CRC with distant metastasis [61]. Another approach to use miRNAs as diagnostic markers involves studying their expression in stool samples in CRC and control patients. A pilot study of 29 cases identified elevated levels of miR 21 and miR 106a in the stool samples of CRC patients [62]. MicroRNA expression levels could also aid in the prognosis of the cancer disease, which is important for physicians who decide what kind of therapy would be appropriate for such a patient. There have been various reports confirming signature expression pattern of microRNAs associated with the prognosis and outcome of the disease. Four different studies have reported miRNA 21 as a robust marker, whose elevated levels in the cancer tissue has been associated with worse prognosis [40, 63-65]. There are other microRNAs such as miR 145, miR 125b and miR 106b,

which have been identified as independent prognostic markers for colorectal cancer [66-68].

1.9.6 MicroRNAs Target Signaling Pathways affected in Colorectal Cancer:

The initiation of the disease is strongly linked to the inactivation of the APC gene as discussed previously. Interestingly, miR 135 a/b levels are inversely correlated with the levels of its predicted target APC [69]. This results in uncontrolled proliferation (neoplasia), and further accumulation of somatic gene mutations including that of miRNAs. The inactivation of genes coding for miRNAs such as Let-7, miR-18a* and miR-143 are responsible for inhibiting their oncogenic target KRAS [70-72]. This leads to the activation of EGFR-MAPKinase pathway. Overexpressed miRNAs such as miR 21 inhibit the function of tumor suppressor gene PTEN, (an inhibitor of PI3K/AKT pathway), promoting proliferation of adenomatous cells [73]. The crucial step in the conversion of adenomas to carcinomas is the loss of p53, which as mentioned earlier, controls miR 34a expression, an important regulator of cell cycle [74]. The altered expression of miR 17-92 cluster also is responsible upregulates c-myc expression, which drives tumor progression from adenoma to adenocarcinoma [75]. An overview of differential miRNA expression affecting various signaling pathways in colon cancer is shown in **Figure 1.7**.

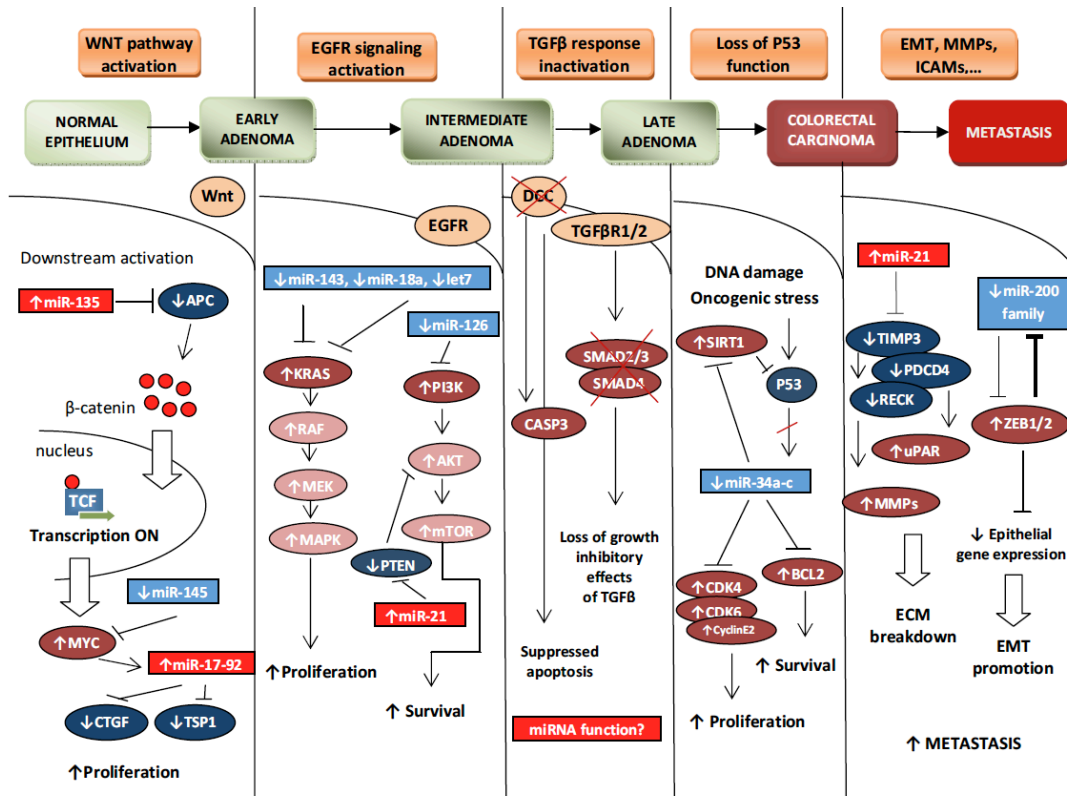


Figure 1.7: miRNA expression at various stages of colon cancer. Differential microRNA expression at various stages of colorectal cancer effects the expression of their target mRNAs involved in major signaling pathways promoting tumor growth. Image reproduced from the review article, MicroRNAs in colorectal cancer: translational of molecular biology into clinical application, Ondrej Slaby, Molecular Cancer 2009, 8:102.

1.10 MiRNAs in Cancer Stem Cells:

The dysregulation of self-renewal in CSCs allows them to surpass the restrictions of environmental cues and gives them unlimited self-renewal ability. One of the subcellular processes that might be responsible for the dysregulation of CSCs is aberrant miRNA activity [76]. MicroRNA 200c was the first miRNA to be identified as being differentially expressed in CSCs (of the breast). It was found to target the mRNA of BMI1, which codes for an important signaling molecule in pathways governing the self-renewal capacity of SCs. Another important self-renewal pathway regulator, RAS, is regulated by let-7 miRNA, which is down-regulated in breast CSCs. This miRNA also targets HMG2A mRNA and regulates characteristics of SCs such as multipotent differentiation and the ability to form tumors [77]. Similarly, miRNA 128 and miRNA 199-5p were found to be down-regulated in the CSC population of high-grade gliomas and medulloblastomas, respectively [78, 79].

For colon, there are published reports, mainly using cell lines, of the identification of many different miRNAs in the CSC population. The diversity of these findings might be due to the differences in the methods and markers used in the isolation of CSCs and/or due to differences in the cell lines. CSCs have been sorted from HT29 cells using CD133 as a marker. Researchers have identified a specific set of miRNAs that show differential expression in CSC (vs non-CSC) from this cell line. This set of miRNAs is thought to play a role in CSC function and maintenance [80]. Zhu *et al.*, also reported that a putative stem cell marker, ASCL2 (a transcription

factor), might regulate the expression of miRNA 302b, which affects SC-like characteristics in colon cancer cell lines [81]. In SW116 cells grown in a suspension culture to enrich for CSCs it was found that miRNA 93 was down-regulated significantly in this enriched population of cells as compared to the parental cell line [82]. There have been no reports yet of miRNAs that are differentially expressed in CSCs of freshly isolated colon tissue.

This leads to my research statement that there are candidate miRNAs, which are differentially expressed in the cancer stem cells versus the normal stem cells of the colon, which regulate proteins involved in self-renewal pathways and promote cancer initiation and maintenance.

Chapter 2

MiRNA23B REGULATES SELF-RENEWAL AND CHEMORESISTANCE PROPERTIES OF COLON CANCER STEM CELLS

2.1 Introduction:

The molecular mechanism through which the self-renewal function of the normal stem cell gets disrupted in cancer development is not yet clearly understood. The cancer stem cell model predicts that there is a dysregulation of self-renewal function in the stem cell compartment residing at the bottom of the colonic crypt, which could initiate and maintain tumorigenesis. The cancer stem cell model was first demonstrated for chronic myeloid leukemia [22], and has been subsequently extended to solid tumors as well [23-25]. We initially explained this event with the help of a mathematical model [27], and provided biological evidence by utilizing the stem cell marker, Aldehyde dehydrogenase 1 (ALDH1)[28].

One of the subcellular processes that might be responsible for the dysregulation of CSCs is aberrant miRNA activity [76]. Differential expression of miRNAs has been previously reported for various types of tissue specific cancers and has been correlated with prognosis and survival [83, 84]. In colon cancer, differential miRNAs signatures were related to stage and origin of the disease [40].

Mounting evidence has shown the role of miRNAs in the maintenance of the cancer stem cell phenotype. The first miRNA signature in HT29 cells positive for CD133 has been reported to play a role in CSC function [80]. Stem cell enrichment of the colon cancer cell line SW116 has identified miRNA 93, which acts as a tumor

suppressor gene [82]. Also, stem cell specific markers, like ASCL2, regulate the expression of miRNA302b, which, in turn affects the stem cell characteristics of colon cancer cells [81].

We looked the expression of microRNA in stem cell enriched sections of normal crypt and compared to rest of the crypt. We identified 4 microRNAs (has-mir-206, hsa-mir-7, hsa-mir-25 and hsa-mir-23b) to be differentially expressed in the crypt bottom (**Figure 2.1**). Their independent expression levels alone can differentiate normal tissue from colon cancer tissue. Out of the four miRNAs, miR23b was differentially expressed in cancer stem cells of the colon. I describe for the first time the role of miR23b in the regulation of cancer stem cells. The miR23b gene is located on chromosome 9 and is part of a cluster with mir-27b and mir24-1. Initially, miR23b was studied in fluid shear experiments, where it was elucidated that pulsatile shear in endothelial cells regulates its expression. This miRNA has been reported to play a role in cancer of prostate, breast, colon and gliomas. MiR23b has been shown to be important for metastasis of colon cancer cells via regulation of various important targets involved in metastasis such as TGFBR2, MAP3K1 and PAK2 [85]. On the basis of our preliminary profiling data and its already established role, I hypothesized that **differential expression of miR23b in colon CSCs is crucial for regulating their function and self-renewal abilities**. To test this hypothesis, I manipulated the levels of miR23b (transient and stable) and assessed its effect on the proliferation, cell cycle, EMT, invasion and ability to self-renew, as well as response to chemotherapy. My overall findings from my studies supported my hypothesis *in vitro* and bolster its role in CSC function as well as response to chemotherapy.

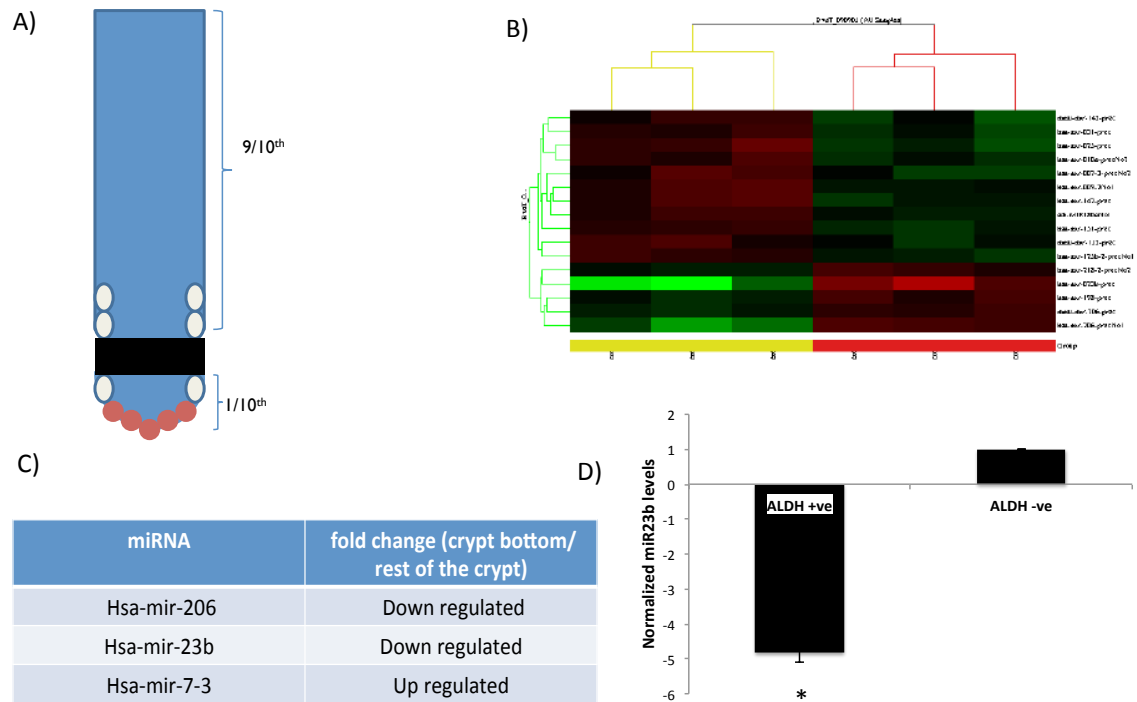


Figure 2.1: miRNA expression in stem cell enriched crypt bottom. A) Cartoon depicting micro-dissection of the normal colonic crypt to lower 1/10th and rest of the crypt used for miRNA profiling. B) Heat map showing differential expression of 16 miRNAs in bottom of the crypt (left panel) as compared to rest of the crypt (right panel). Red color represents overexpressed and green color represents down-regulated. C) Table showing the expression profile of 3 differentially expressed miRNAs. D) Expression levels of miR23b in normal ALDEFUOR positive stem cells as compared to the ALDEFUOR negative cells. Error bars represent standard error of the mean and * indicates a significant p value < 0.05.

2.2 Methods:

2.2.1 Cell Lines used:

HT29 and SW480 colon cancer cell lines were purchased from ATCC Inc., (Manassas, VA) and were used in this study. Cells were grown at 37 °C with 5% CO₂ and 95% air and were passaged regularly.

2.2.2 ALDEFUOR assay:

ALDEFUOR assay was performed according to manufacturer's protocol. ALDEFUOR assay (STEMCELL Technologies Inc., BC, Canada) was performed according to manufacturer's protocol. The cells were trypsinized using 0.25% Trypsin-EDTA followed by neutralizing the trypsin using media containing FBS. The cells were spun down at room temperature and resuspended in ALDEFUOR buffer. The cell suspension was divided into three tubes: ALDEFUOR only, ALDEFUOR + DEAB (inhibitor) and Blank. The tubes were incubated in the dark at 37 °C for 25 minutes. After incubation, the cells were spun down once and resuspended in ALDEFUOR buffer. The cells suspension was transferred to a FACS sample tube through a 70-micron filter. The samples were run in BD FACS ARIA II using the FACSDiva Software. The gates were drawn to weed out doublets and to include 0.1% in the positive gate of cells in the respective DEAB control and appropriate ALDEFUOR positive samples.

2.2.3 Cell Sorting by Flow Cytometry:

The BD FACS ARIAII flow cytometer was turned on 30 minutes prior to start of the experiment allowing the laser to warm up. The 85-micron or the 100-micron nozzle was used for the sorting experiment. The stream was turned ON and was

Cytometer setup and Tracking was done to calibrate the machine. The stream is left on for 20 minutes to let it stabilize. Accudrop experiment was carried out to determine the delay between the drop prior to any sorting. A test sort was done to ensure proper collection of sample in the collection tubes. The dot plots were created and the cell populations were appropriately chosen to eliminate doublets out of the analysis. The blank sample was run through FACS initially. Voltage of FSC and SSC were adjusted if needed to set the cell population in the center of the first dot plot. Appropriate regions within the plots were selected so that only single cells could sort. The sample with the DEAB control was run through FACS and data was recorded. Using the DEAB alone sample, the gates for the ALDEFUOR negative and ALDEFUOR positive were created in the dot plot for SSC vs FITC. The ALDEFUOR positive cells were identified and gates were readjusted so that top 15% of the ALDEFUOR positive and lowest 15% of the ALDEFUOR negative cells are sorted into sterile tubes containing media.

2.2.4 Taqman MiRNA Assay:

MicroRNA taqman assay for individual miRNAs were purchased from Life technologies Inc. Carlsbad, CA. The cDNA synthesis was performed following manufacturers instructions. Twenty nanograms of RNA were used in a final volume of 5 μ l. Primer for the miR or U6 Control (3 μ l), dNTPs (0.15 μ l), 10X PCR buffer (1.5 μ l), RNase Inhibitor (0.19 μ l), RT enzyme (1.0 μ l) and water was added to make a final volume of 15 μ l. The samples were mixed gently using a sterile pipette and spun down momentarily. The samples were placed in the thermocycler and cDNA was synthesized using the following temperature conditions: 16 °C for 30 min, 42 °C for 30 min, 85 °C for 5 min and 4 °C forever. The cDNA (1.33 μ l of RT product) was used

for preparing realtime reaction which also contained 10ul of 2X PCR master mix (Applied biosystems, no AmpErase UNG), the realtime provided in the kit and water to a final volume of 20 µl. The samples were prepared in triplicates and added to the 96 well thermocycler plate (VWR Inc., Radnor, PA). The realtime PCR was run using Applied Biosystems 7500 fast PCR machine for 95 °C for 10 min followed by 40 cycles of 95 °C for 15 sec and 60 °C for 1 min. The Ct value obtained was used to calculate the average Ct for each sample. The fold change in expression of miRNA in treatment versus control was calculated using the formula $2^{-(\Delta Ct (\text{treatment}) - \Delta Ct (\text{control}))}$. Any value greater than 2-fold change was regarded as significant.

2.2.5 Transient Transfection:

MiR23b antimir and precursor siRNA molecules were purchased from Ambion, Life technologies (Carlsbad, CA). The amount of siRNA and transfection reagent (Lipofectamine 2000, Invitrogen) was standardized for both the cell lines SW480 and HT29 using a GFP coupled scrambled siRNA from DHARMACON Inc. (Pittsburgh, PA). The cell lines were transfected in a 12 well or a 6 well format and media was changed 24 hours post transfection. The increase or decrease of the miRNA levels was tested by miRNA Taqman Assay. The cells were analyzed 24- 48 hours post transfection.

2.2.6 Proliferation Assay:

Cells were plated in triplicates per experiment condition in a 24 well plate and the initial count was regarded as day 0. The cells were then trypsinized 24, 48 or 72 hrs past the experiment, and were counted using trypan blue dye exclusion method and an Invitrogen cell counter. These numbers represented cell count for day 1, day 2

and/or day 3. Three independent sets of experiment were carried out for each condition.

2.2.7 Cell Cycle Analysis by PI Staining:

Cells are plated at equal density to make sure that they reach the same confluence at the day of the experiment. Cells are trypsinized using 0.5% trypsin in EDTA, and are washed twice with ice cold PBS. The cells are then fixed with 75% chilled ethanol and stored at 4 °C for 49 hours. The cells are washed once with ice cold PBS and replaced by fresh PBS. RNase A solution (final concentration: 1 µg/ml) is added to the PBS and the cells are incubated at 37 °C for 20 minutes. Then propidium iodide stain was added to the same solution and incubated for 20 min more. After the incubation time, transfer the tubes to ice under analysis for FACS. The FACS software, a histogram plot was created where the Y-axis represents the count of cells and the X-axis represents the PI staining intensity (a linear scale). The results were analyzed using ModFit software and the percentage of cells in each phase of the cell cycle was estimated.

2.2.8 Soft Agar Assay:

A base layer of 1.0% low melting agar in media was set in a 6 well plate format. A top layer of 0.3% agar in media containing cells was added carefully to the base layer, which was supplemented by 3 ml of appropriate growth media. The cells were grown for ten days with media changes every two days. The colonies were stained with crystal violet and observed under a bright field microscope (ZEISS). The colonies were counted using the software Image J with same threshold values for the treatment and the control.

2.2.9 Colonosphere Assay:

Cells were plated at a cell density of 200 cells per 100 μ l of stem cell media which composed of serum free DMEM/F12 (GIBCO Inc., Grand Island, NY) with Epidermal Growth Factor (EGF) and basic Fibroblast Growth Factor and B-27 complex without Vitamin A (Life technologies, Carlsbad, CA). Low attachment plates were used for this assay and colonospheres were analyzed for their size and count on day 8 using a 10x objective of a phase contrast microscope (Zeiss).

2.2.10 Protein Isolation:

Media was removed from the dish and the cells were washed twice with sterile PBS. Then RIPA buffer containing 1X protease inhibitor cocktail was added to the dish. Cells were treated with RIPA for 2-3 hours on ice before they were scraped off using a sterile cell scraper. The scraped off cells in RIPA buffer was transferred to a labeled sterile 1.5 ml microfuge tube. The tube was spun at 12000 rpm for 10 min at 4 $^{\circ}$ C to pellet all the cell debris. Clear supernatant containing the dissolved proteins were collected in a fresh sterile tube and stored in -80 $^{\circ}$ C.

2.2.11 BSA Colorimetric Protein Estimation Assay:

The BSA colorimetric assay was performed following manufacturers instructions provided in the kit. The samples were prepared in a clear bottom transparent 96 well plate (CORNING Inc., Corning, NY). Ten μ l of each standard protein sample (in duplicates) and the unknown protein (in triplicate) was pipetted into the 96 well plates. This was followed by adding 200 μ l of the working solution (Solution A + solution B in a ration of 1:50) to each of the well with the sample. The sample was placed in a plate shaker for few seconds to mix the contents thoroughly and was incubated at 37 $^{\circ}$ C for 30 minutes. After 30 minutes, the absorbance of the

samples at 550 nm were estimated using the TECAN plate reader. The data set was exported in form of an excel file. The average of each sample absorbance was calculated which was used to plot of graph of absorbance vs protein concentration in excel. The slope (m) of the line was calculated, which was used later to estimate the concentration of the unknown sample.

2.2.12 SDS PAGE Electrophoresis:

Precast gels (LONZA Inc., Rockland, ME) were used for this experiment. Approximately 30 micrograms of protein sample was used for each treatment and samples were made in RIPA (with protease inhibitor cocktail) and Lamelli buffer (with beta-mercaptoethanol) in a ratio of 1:1 to a total volume of 30 μ l. Sample were heated at 95 °C for 10 min and then loaded carefully into the well of SDS gel along with the ProSieve quad color protein ladder (LONZA Inc., Rockland, ME). The BIORAD setup was used to set up the gel and was filled up to the designated mark with Tris SDS running buffer. The lid with the external electrodes was carefully placed on the gel tank, which was eventually connected to a power supply. The gel was run under a constant voltage of 100 Volts for approximately 90-120 minutes depending upon the size of the protein to be detected.

2.2.13 Western Blot:

PVDF membrane (Thermo Scientific Inc., Waltham, MA) was used as a transfer membrane for western blotting. The membrane was dehydrated using 100% methanol for 30 seconds followed by quick rehydration by rinsing it in distilled water. It was soaked in transfer buffer (Tris Base, Glycine, 20% methanol in distilled water) until ready to use. Filter pads and filter paper needed for transfer were also soaked in

transfer buffer. The gel was carefully removed from the cast using surgical blade and transferred to a container holding transfer buffer in it. The whole sandwich was placed carefully into the western transfer tank (BIORAD Inc., Hercules, CA) containing transfer buffer and an ice pack. Lid was closed and electrodes were connected to an external power supply. The transfer was run for 1 hour at constant voltage of 100 volts. After one hour, the membrane was removed and blocked overnight in 3% BSA in TBS-T. Next day, primary antibody in blocking buffer was added on to the blot and incubated overnight at 4 °C. After 16 hours of incubation, the blot was washed thrice in TBS-T for 10 min each. SuperSignal West Dura Extended Duration Substrate (Thermo Scientific Inc., Waltham, MA) A and B (1:1) was added on to the blot and mixed well for 5 min.

2.2.14 RNA Isolation:

RNA isolation was done according to manufacturers protocol using Trizol Reagent (Life Technologies Inc., Carlsbad, CA). One ml of Trizol was added per million cells and incubated at 4 C for ten minutes. Chloroform (0.2ml per ml of Trizol used) was added to the cells and the solution was mixed vigorously for 15 seconds. The tubes were then allowed to sit in ice for two min and then they were spun at 12000 rpm at 4 °C for 15 minutes. Following centrifugation, the upper clear layer was carefully removed from each sample tube and transferred to a new tube. RNA was precipitated by adding Isopropanol (0.5 ml per 1 ml of trizol added) to the tube followed by incubation for 10 minutes in ice. Spinning down the solution at 12000 rpm for ten minutes at 4 °C pelleted the precipitated RNA. The supernatant was discarded and the RNA was washed twice with by spinning down the pellet in 1 ml of

ice cold 70% ethanol per ml of Trizol used. The pellet was allowed to air dry for removing left over ethanol and was dissolved in Nuclease free water.

2.2.15 RNA Quantification:

RNA quantification was done by looking at their absorbance at two wavelengths 260 and 280 nm, using the TECAN plate reader and Nanoquant plate. Two μl of sterile water was used for blanking the instrument, followed by 2 μl of the RNA sample. The concentration values provided by the instrument were taken in triplicates and averages were calculated for each RNA sample.

2.2.16 cDNA Synthesis:

cDNA synthesis was done using the manufacturers protocol for Super Script III reverse transcriptase enzyme (Life Technologies Inc., Carlsbad, CA). The Reaction for each sample was set up as follows:

dNTPS:	1 μl
Oligo dT primer:	1 μl
RNA:	(5 ug of RNA)
Water:	(rest of the volume)
Total:	13 μl

This was heated to 65 °C for 5 minutes and then cooled down in Ice for 1 min.

To each reaction tube, following constituents were added:

DTT:	1 μl
5X first strand Buffer:	4 μl
RNAse Inhibitor:	1 ul
SuperScript III enzyme:	1 μl

The samples were mixed thoroughly using a sterile pipette and were run in a Thermal Cycler using the following conditions: 50 °C for 60 min, 72 °C for 15 min, 4 °C for ever.

2.2.17 Realtime PCR:

Realtime PCR was done in triplicates for each sample. The amount of cDNA and the sequence of primers used for each realtime PCR reaction are summarized in Table. The PCR reaction was done in triplicates and was run using an Applied Biosystems 7500 Fast PCR machine. The cycling conditions for each of the primer sets are mentioned in Table 2 in Appendix 1. The reaction mixture comprised of:

Forward and Reverse Primer:

SYBR green PCR master mix: 41.25 µl

cDNA:

Water:

Total volume: 82.5 µl (for three sets of reactions)

The average Ct value obtained after the PCR was used to determine the fold change and was calculated by using the formula $2^{-(\Delta Ct(\text{treatment}) - \Delta Ct(\text{control}))}$. Any value greater than 2 fold change was regarded as significant.

2.2.18 Immunocytochemistry:

SW480 cells were grown in 4 well NUNC chamber slides. They were fixed in 4 % paraformaldehyde in PBS for 20 minutes and then blocked overnight in 10% BSA in PBS. The next day, primary antibodies of mouse anti-human E-Cadherin (ABCAM Inc., Cambridge, MA) and rabbit anti-human Vimentin (ABCAM Inc., Cambridge, MA) were added and incubated for 16 hours at 4°C. The cells were washed thrice in

PBS and incubated for 1 hour at RT in PBS containing anti-mouse Alexafluor 488 and anti-rabbit Alexafluor 594 (Life technologies Inc., Eugene, OR) at a concentration of 1:1000. Cells were washed again in PBS and incubated in Nuclei stain solution containing Hoescht for 30 minutes at RT. Cells were washed, allowed to dry partially and were covered with Anti FADE Gold reagent (Life Technologies Inc., Carlsbad, CA) and a coverslip. The cells were viewed using a ZEISS fluorescence microscope and 10 random fields of view were captured. The cells positive for both markers were counted in different field of views and noted.

2.2.19 Invasion Assay:

Cells were plated onto an 8-micron pore size 24-well insert containing Matrigel (300 µg/ml) in serum free DMEM media (GIBCO, Life Technologies Inc., Grand Island, NY). The insert was carefully placed in a 24 well plate with media containing 10% fetal bovine serum. Cells were incubated for 48 hours after which, the invasive cells were fixed in 4% paraformaldehyde and stained with crystal violet. The images were taken using a NIKON light microscope and the number of cells were counted for each replicated per treatment.

2.2.20 Transformation, Transfection and Transduction:

HEK 293 cells were transfected with miR23b precursor expressing lentiviral vector, miR23b miRZip lentiviral inhibition vector or the control vector (System Biosciences, Inc., Mountain View, CA) together with helper plasmid (pCMVΔR8.2) and envelope plasmid (pMD.G) in the ratio of 1:3:1. Five hundred thousand HEK293 cells were plated in day 0 of the experiment in a 6 well plate format. The transfection mixture was made from 500 µl of OptiMEM (Life Technologies Inc., Carlsbad, CA),

the three plasmids and 10 µl of Lipofectamine 2000 (Life Technologies Inc., Carlsbad, CA) was incubated for 25 minutes. Media was replaced by 3 ml of fresh DMEM media and the transfection mixture was added drop wise slowly on top of the cells. The plate was swirled gently to mix the solution uniformly and kept back in the incubator. Media was changed with fresh media 18 hours post transfection and the first viral collection was done 48 and 72 hours post transfection.

HT29 cells were plated a day before transduction at a cell density of 500,000 cells per well of a 6 well plate in complete McCOY media (GIBCO, Life Technologies, Grand Island, NY). On the day of the transduction, aspirate the media and add 3 ml of freshly collected viral media filtered through 0.22-micron sterile filter. Three µl (1000x concentration) of polybrene solution was added to the media, which enables cell membrane to lose charge and makes it easier for the virus to infect.

2.2.21 Luciferase Assay:

Plasmids expressing luciferase and the 3'UTR of the predicted target genes, LGR5 and LRIG1, were purchased from GeneCopoeia, Rockville, MD. Thirty thousand cells were plated in a 96 well plate and 24 hours later co-transfected with the luciferase vector and miR23b precursor (cat# AM17100, Life technologies Inc., Carlsbad, CA) and Precursor control molecules (Cat# AM17110, Life technologies Inc., Carlsbad, CA) using Lipofectamine 2000 as the transfection reagent. The media was changed 24 hours post-transfection and the cells were used for dual-color luciferase (Promega Inc., Madison, WI) and luminescence was recorded using the TECAN plate reader.

2.2.22 Determination of IC₅₀ for 5-FU for HT29:

The IC₅₀ was determined for 5 FU (SIGMA-ALDRICH Inc., St. Louis, MO) against HT29 cell lines using varying concentrations of the drug (20-60 μM). The drug at the IC₅₀ concentration was added to the cells and the cells were counted 24 hours post treatment.

2.2.23 RNA SEQ analysis:

HT29 cells transfected with miR23b antimirs, precursor and their respective controls were used for mRNA seq. The RNA was isolated 48 hours post transfection using Trizol LS reagent (Life Technologies Inc., Carlsbad, CA) according to the manufacturer's protocol. The RNA quality was determined and cDNA libraries were generated with pooled samples to give increased depths in the read out. Samples were sequenced using Illumina technology. The reads were then processed using TopHat, Bowtie and CuffDiff to narrow down the list of genes which show more than 2 fold change with a significant p value in the treated samples as compared to the control. The gene list was narrowed down further using GO term enrichment analysis tools like DAVID and results from miRNA target prediction tools like TARGETSCAN, miRANDA and *rna22*.

2.3 Results:

My results suggest that miR23b is important in regulation of the proportion of CSCs in colon cancer. Manipulation of miR23b levels affects various aspects of cell function such as proliferation, cell cycle and EMT. Decreasing miR23b levels also has a significant effect on ability of cancer cells to self-renew in low attachment conditions as well as on their chemo-resistive abilities. My findings are described as follows:

2.3.1 MiR23b is Upregulated in Colon Cancer Stem Cells and Has an Effect on Proliferation and Cell Cycle.

MicroRNA Taqman Assay for miR23b on the ALDEFUOR high and low sorted populations revealed that miR23b is significantly overexpressed (>2 fold) in the ALDEFUOR positive cells as compared to the ALDH- cell populations for the cell lines HT29 and SW480 (**Figure 2.2 A**). The importance of the high expression of miR23b in the ALDEFUOR positive population was tested by transient transfection of the cell lines with Antimir, precursor specific for miR23b, and their respective controls and looking at changes in proportion of ALDEFUOR positive cells 24 and 48 hours after transfection (**Figure 2.2 C**). The transient increase in miR23b significantly increased the proportion of ALDEFUOR positive cells and decrease of miR23b showed the opposite effect. This effect was seen in both cell lines SW480 and HT29. To confirm whether ALDEFUOR positive cells get transfected as well, I used TagRFP/miR23b double transfection. I identified the same trend of increase or decrease of proportion of ALDEFUORhigh/TagRFP+ve cells in response to miR23b modulation (**Figure 2.2 D**).

2.3.2 Mir23b Causes a G0/G1 Arrest In Cells and Decreases Proliferation:

An increase in miR23b levels resulted in a decrease in the proliferation rate of both SW480 and HT29 cells. Increasing the levels of miR23b transiently significantly decreased the proliferation of cells as compared to the control (**Figure 2.3A**). On the other hand, there was an increase in the proliferation rate when transfected with the

antimirs against miR23b (**Figure 2.3B**). The effect of miR23b manipulation on cell cycle was tested in the colon cancer cell lines 48 hours post transfection with the miR23b precursor. There was a significant increase in the number of cells in the G0/G1 phase with an increase in miR23b and a corresponding decrease in the proportion of cells in S phase with a decrease in miR23b (**Figure 2.3D**).

2.3.3 Mir23b is Important for Self-Renewal Function of Colon Cancer Stem

Cells:

To test anchorage independent growth that is reflective of self-renewal ability of cancer cells, I analyzed the growth of HT29 cells in soft agar. Forty-eight hours post-transfection with miR23b precursors and antimirs cells were grown in soft agar for ten days. The results showed that decreasing the levels of miR23b using the antimir significantly decreased colony formation of HT29 cells (**Figure 2.4A and 12.4B**). SW480 cells demonstrate poor colony formation in soft agar and were not used for this assay. HT29 cells transiently transfected with the mir23b antimir formed significantly smaller colonospheres after eight days compared to control cells. The opposite was seen in cells transfected with miR23b precursor, as these cells formed larger spheres than the control cells (**Figures 2.4C and 2.4D**).

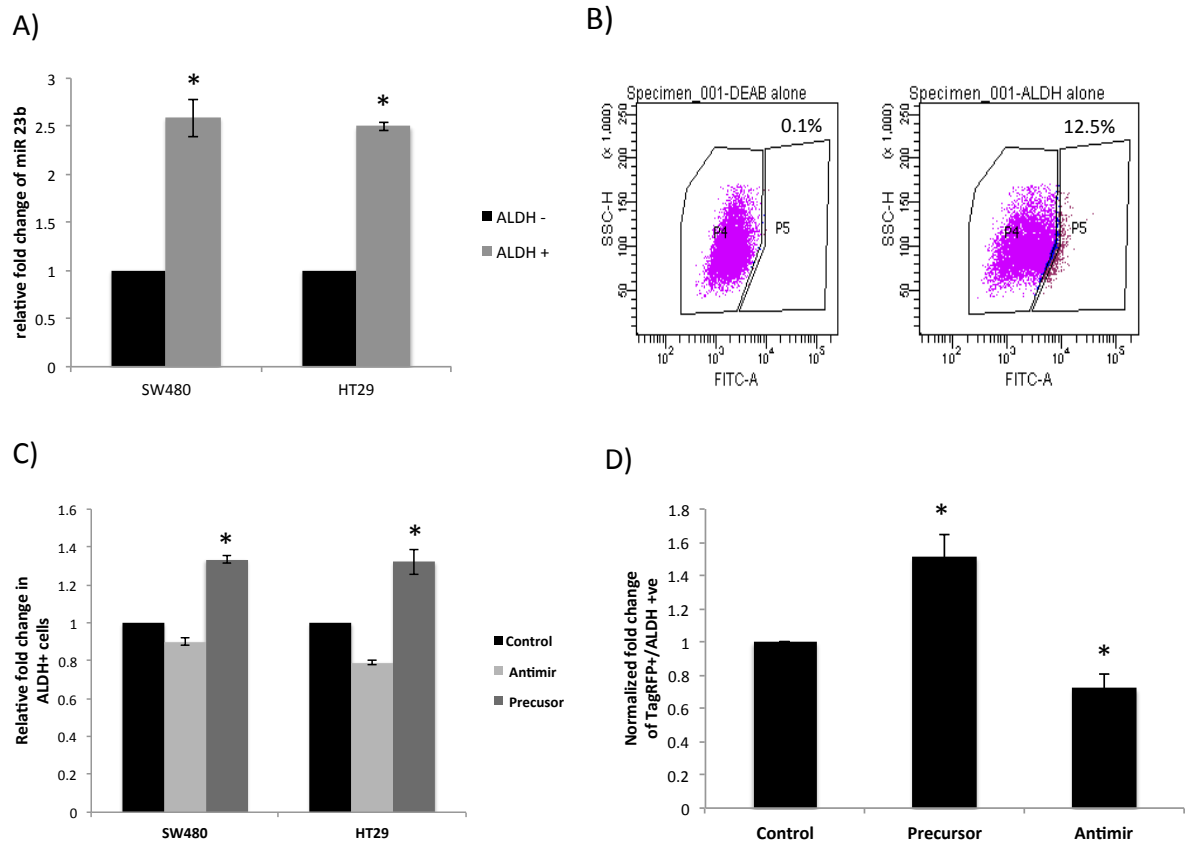


Figure 2.2: ALDEFUOR assay for HT29 and SW480 and miR23b expression in ALDEFUOR positive cells in HT29 and SW480 cells. . A) MicroRNA 23b expression in ALDEFUOR positive cells Vs. ALDEFUOR negative cells in colorectal cancer cell lines SW480 and HT29. B) ALDEFUOR assay on SW480 cells for ALDH activity showing two plots, one is the presence of the DEAB (left) and the other is the one with without DEAB (right) which identifies 12.5% ALDEFUOR positive cells. C) Fold changes in ALDEFUOR positive cells transfected with precursor or antimir of 23b with respect to their controls in the two cell lines SW480 and HT29. (*) represents significant difference between the treated and the control with a p value < 0.05 D) Fold changes in ALDEFUOR positive/Tag RFP co-positive cells transfected with precursor or antimir of 23b with respect to their controls in HT29 cell line. * represents significant difference between the treated and their respective controls with a p value < 0.05. Error bars represent the standard error of mean.

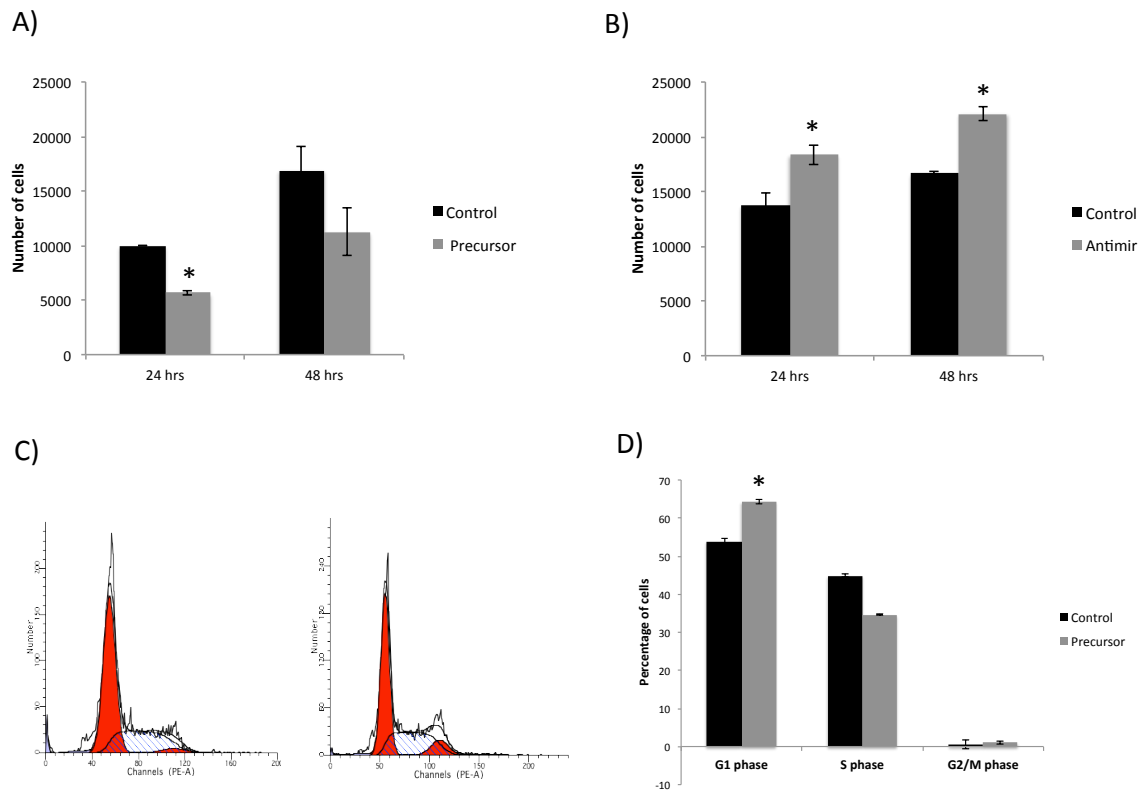


Figure 2.3: MiRNA23b inhibits proliferation via promoting G0/G1 cell cycle checkpoint. A and B) Proliferation Assay results shows number of cells 24 and 48 hours post transfection with miR 23b precursor, antimir and their controls. C) DNA content profile of cells 48 hours post transfection with precursor (left) and its control (right). The percentages of cells in the various phases of the cell cycle (D) were quantified by using ModFit software. Error bars represent standard error of the mean (SEM) and * represents significant difference between treated group and control with a p value < 0.05

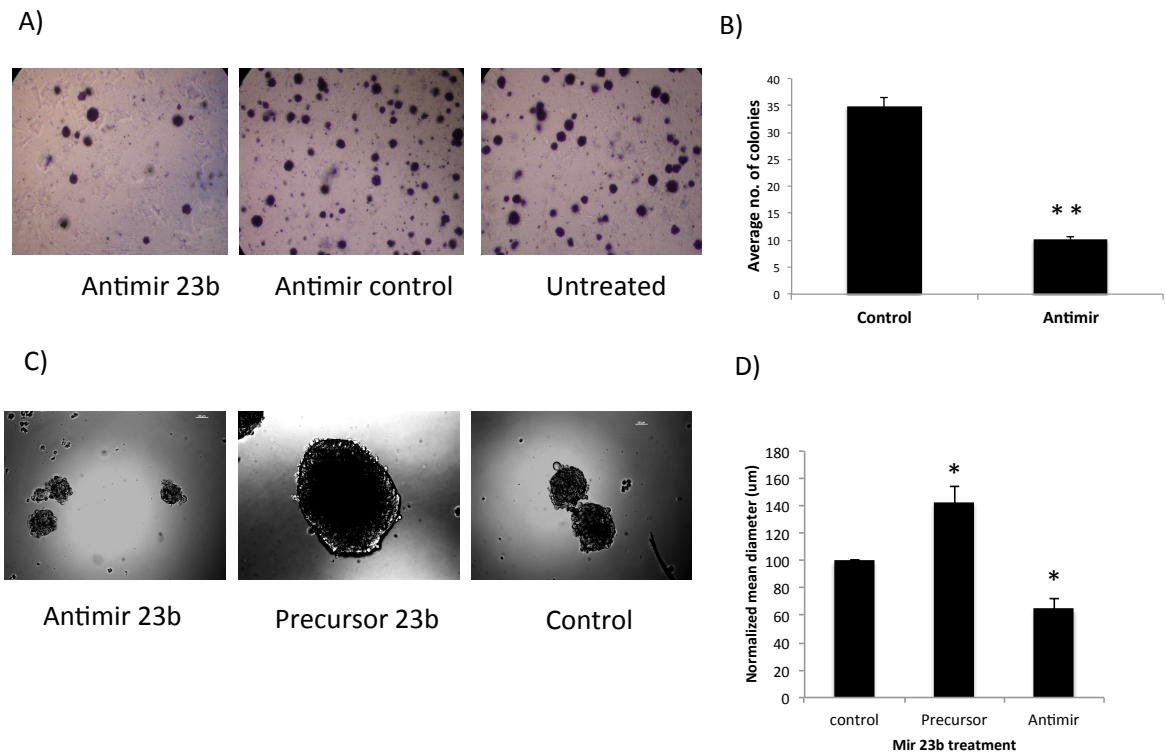


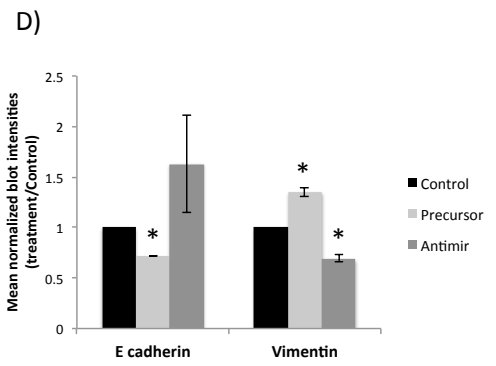
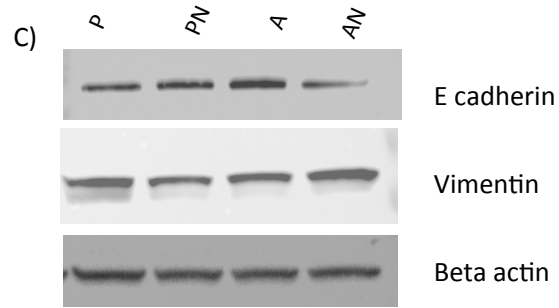
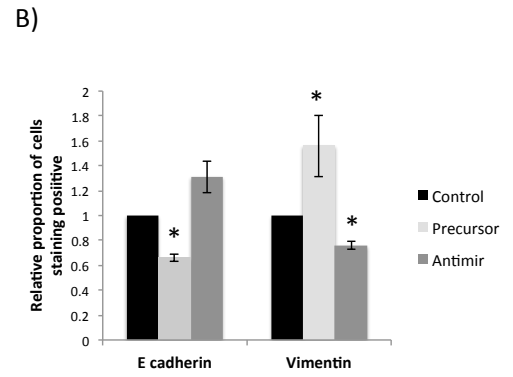
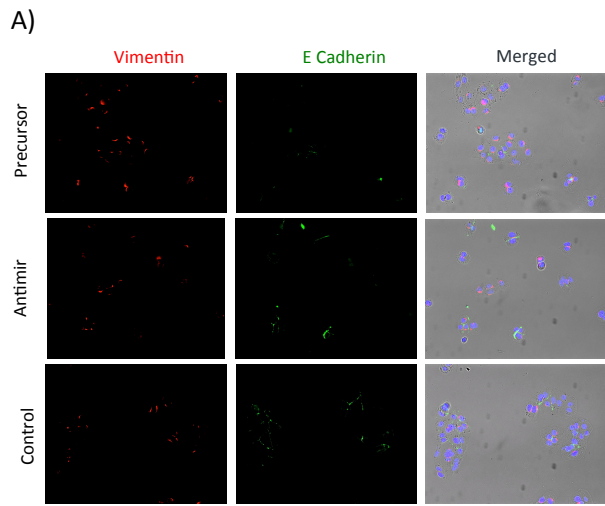
Figure 2.4: MiR23b promotes self-renewal. A) Soft Agar assay for HT29 cells post transfection with miR23b antimir, its control and untreated samples. The colonies were stained with crystal violet, counted and quantified in graph B. Colonosphere assay for HT29 (C) cells post transfection with miR 23b precursor, antimirs and their control samples. The colonospheres were quantified and shown in D. Error bars represent standard error of mean. * indicates significant difference between the treated and the control samples with a p value < 0.05 and ** represents significant difference with a p value < 0.01

2.3.4 MiR23b Promotes EMT and Invasion in Colon Cancer Cells:

I found that transient transfection of cells with antimirs and precursor of miR23b had an affect on EMT (Epithelial to Mesenchymal transition) in colon cancer cells. Specifically, immunocytochemistry for EMT markers Vimentin and E-Cadherin showed that transfection with the precursor promoted EMT as indicated by increased staining of Vimentin and decreased E-Cadherin staining in SW480 cells (**Figure 1.4A and B**). The opposite effect, a decrease in Vimentin and an increase in E-Cadherin, was observed in the cells treated with the antimir for miR23b. The immunostaining results were validated by Western Blotting (**Figure 2.5C and D**). HT29 cells did not express detectable amount of Vimentin so they were not used in this experiment. MiR23b overexpression in HT29 cells significantly promoted the invasion of cells compared to the control (**Figure 2.5E and F**) as shown by the Matrigel invasion assay.

2.3.5 Stable Expression and Knockdown of MiR23b Modulates Proliferation, Cell Cycle and Self-renewal Function:

Stable expression and knockdown of miR23b in the HT29 cell line had an effect on the cell proliferation and cell cycle as shown in Figure. Over four days, miR23b overexpressing clones grow significantly slower than the miR23b knockdown clone (**Figure 2.6A**). The colonosphere assay results confirmed the transient transfection results that miR23b promoted the self-renewal of cells. Mir23b overexpressing cell lines yielded much larger spheres compared to those formed by the control vector clones and the miR23b knockdown clones (**Figure 2.6C and D**).



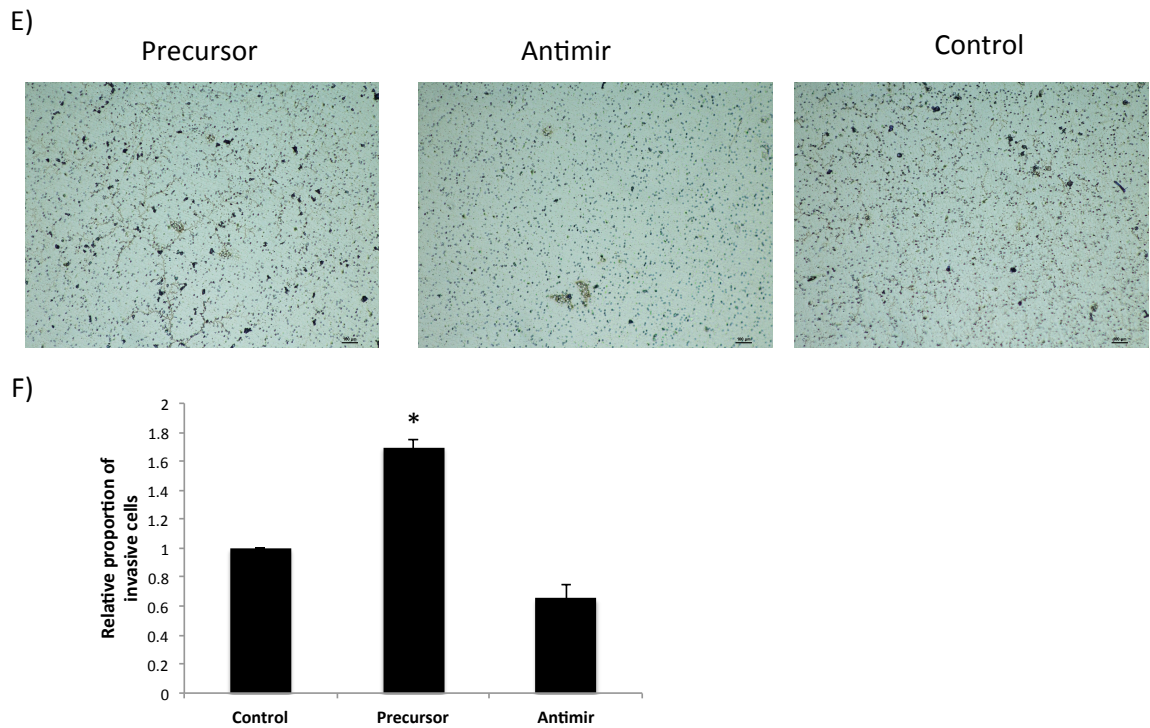


Figure 2.5: MiR23b promote Epithelial-Mesenchymal transition. A) Immunocytochemistry for E cadherin and Vimentin for SW480 cell lines 48 hours post transfection with mir 23b antimir and precursor. B) Quantification and representation of ICC results shown in A. Panel C shows Western Blot results for EMT marker E-Cadherin and Vimentin expression in cells 48 hours post transfection by miR 23b precursor (P), antimir (A) and their respective controls (PN and AN) which were quantified by densitometry and shown in Graph D. Invasion assay done on SW480 cells treated with miR 23b precursor, miR 23b antimir and control (E). Cells were stained with crystal violet and quantified and shown in graph above (F). Error bars represent standard error of mean. * indicates significant difference between the treated and the control samples with a p value < 0.05.

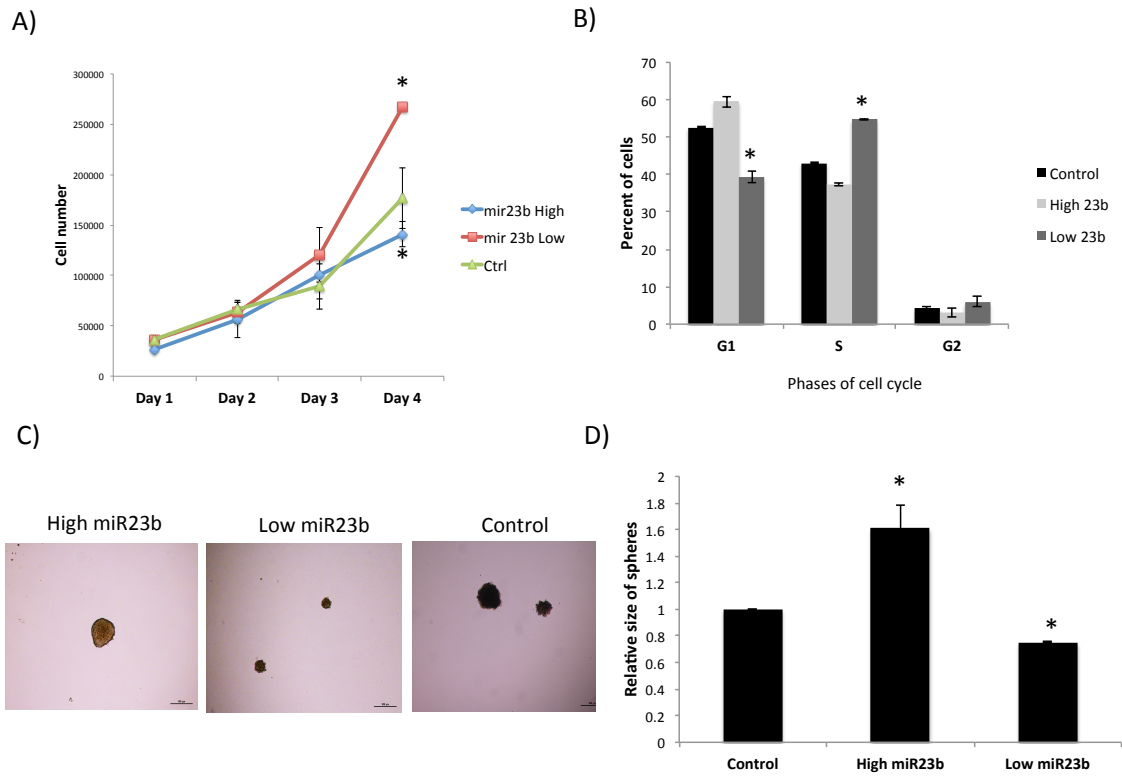


Figure 2.6: Effects of long-term manipulation of miR23b A) Proliferation assay results on the miR 23b overexpressing, knockdown and the Control clones. B) The bar graph represents percentage of cells in various phases of the cell cycle of the overexpressing and the knockdown clone as compared to the control. C) shows bright field images of colonospheres generated at day 8 from the miR 23b overexpressing, knockdown and the Control clone. The sizes of the colonospheres were estimated, which is represented in graph D. Error bars represent standard error of mean. * indicates significant difference between the treated and the control samples with a p value < 0.05.

2.3.6 MiR23b Knockdown Promotes Chemoresistant Properties in HT29 cells Against 5-FU Drug via the Up-regulation of LGR5:

The expression of miR23b in HT29 cells goes down in a dose dependent fashion when treated with the anti cancer 5-FU primarily around the IC₅₀ concentration (**Figure 2.7A**). This effect was further investigated by treating the drugs to the overexpressing and the knockdown clone of miR23b. The drug treatment on HT29 stable clones of miR23b knockdown had less cytotoxic effects on the proliferation of cells when compared to the control (**Figure 2.7B and C**). LGR5, a colon cancer stem cell marker, was identified as a predicted stem cell marker using TARGETSCAN, which was verified using luciferase assay. The miR23b precursor treated HT29 cells showed a significant 42% reduction in luciferase activity of vectors with LGR5 3'UTR as compared to the control (**Figure 2.8A**). The LGR5 mRNA levels were found in inverse relation to the levels of miR23b in the stable HT29 clones (**Figure 2.8C**).

2.3.7 LGR5 and ALDH Positive Cells are Two Different Sub-populations in Colon Cancer Cell Line HT29:

It was identified by mRNA analysis and FACS staining that LGR5 and ALDH1 identify different sub-populations in HT29 cells. LGR5 mRNA levels were significantly down regulated in ALDEFLUOR high cells as compared to the ALDEFLUOR low cells (**Figure 2.9C**) and FACS staining showed distinct populations of LGR5 positive and ALDH-high cells (**Figure 2.9A and B**).

2.3.8 RNA SEQ Analysis Identified Novel Targets of MiR23b:

RNAseq analysis across samples was done to identify genes that were differentially expressed with varying levels of miR23b in HT29 cells. Around 3000 genes were found to be upregulated (over 2 fold) in the antimir treated cells and down regulated in the precursor treated cells (**Figure 2.10A**). The Gene Ontology terms for this gene list identified broad categorical pathways such as cell cycle, apoptosis and DNA repair. Out of these 3000 genes, 72 gene transcripts were identified to be predicted targets of miR23b using multiple miRNA target prediction tools such as miRANDA, rna22 and TARGETSCAN (**Figure 2.10B**). Out of this 72, 11 genes were identified with a role in self-renewal pathways. This gene list is provided in **Figure 2.10C**. The raw and processed files of the RNA SEQ data have been submitted to NCBI and can be accessed using the GEO accession number **GSE59290**.

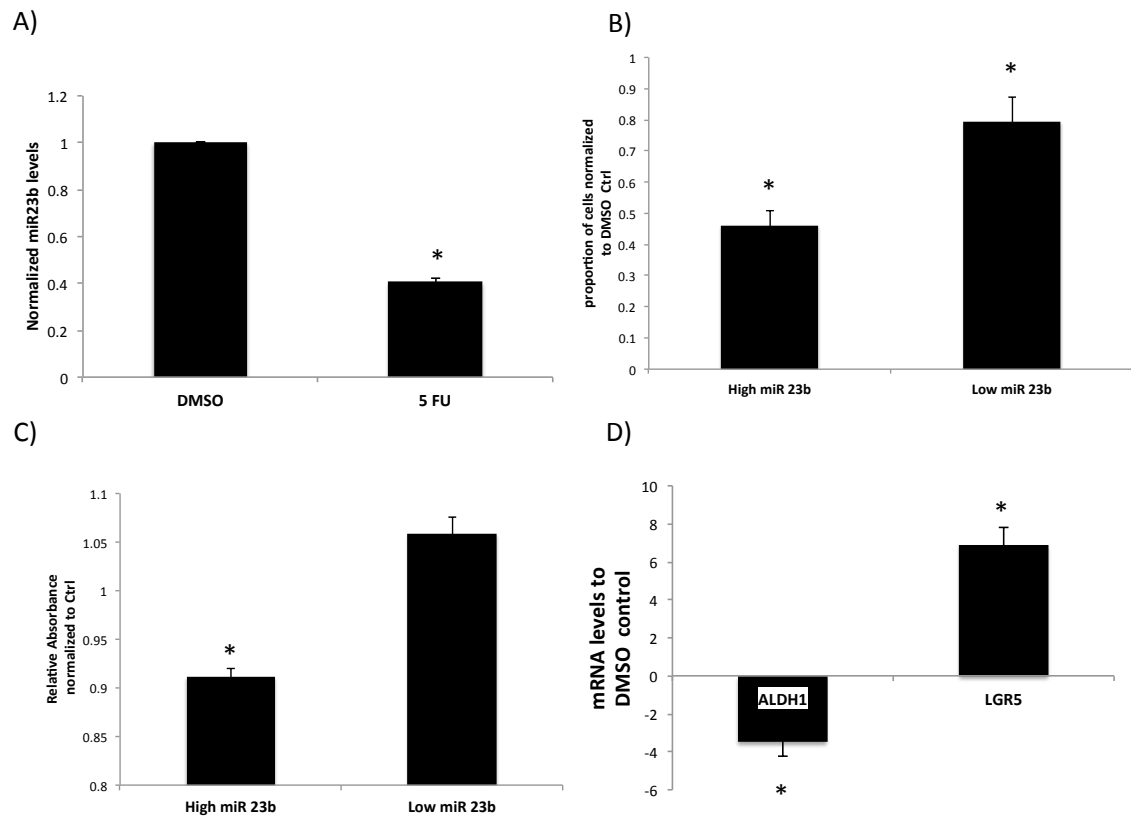


Figure 2.7: MiR23b inhibition promotes chemoresistance to 5-FU. A) Expression of miR23b in HT29 cells treated with 5-FU drug as compared to the DMSO control. B) Proliferation assay results post 24 hours of 5-FU treatment of the miR 23b clones. C) WST1 assay which was used to determine the viability of the miR23b overexpressing, knockdown and the Control clone 24 hours post 5-FU treatment. D) mRNA levels of ALDH1 and LGR5 in 5-FU treated HT29 cells compared to the DMSO control. Error bars represent standard error of mean. * indicates significant difference between the treated and the control samples with a p value < 0.05.

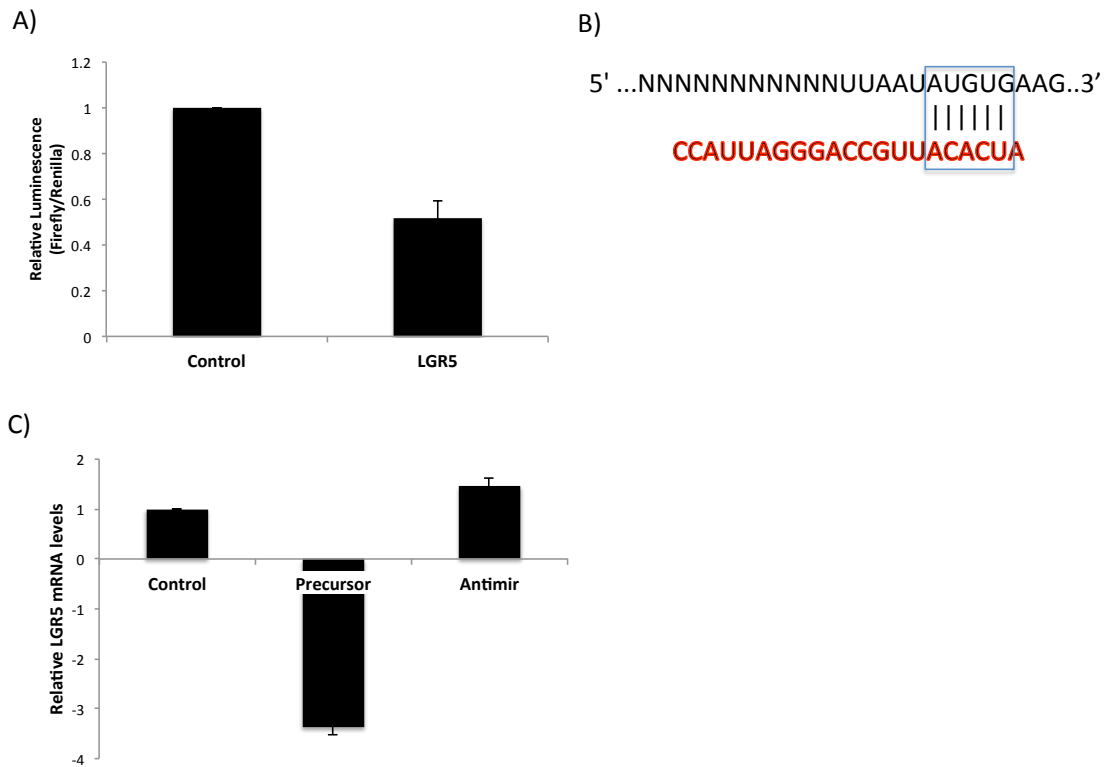


Figure 2.8: MiR23b targets 3' UTR of LGR5 mRNA. A) Luciferase assay results using HT29 cells showed that miR 23b has significant repression on luciferase activity of the vector with 3' UTR of the LGR5 mRNA as compared to the empty vector. Panel B is the representation of the predicted binding site at the 3' UTR of the LGR5 mRNA, the miRNA (in red) binds between position 6 and 12 of the UTR with a perfect 7mer-1A seed match (C) shows the relative mRNA levels of LGR5 in HT29 cells transfected with 23b precursor or antimir as compared to its control. Error bars represent standard error of mean across replicate samples. * indicates significant difference between the treated and the control samples with a p value < 0.05.

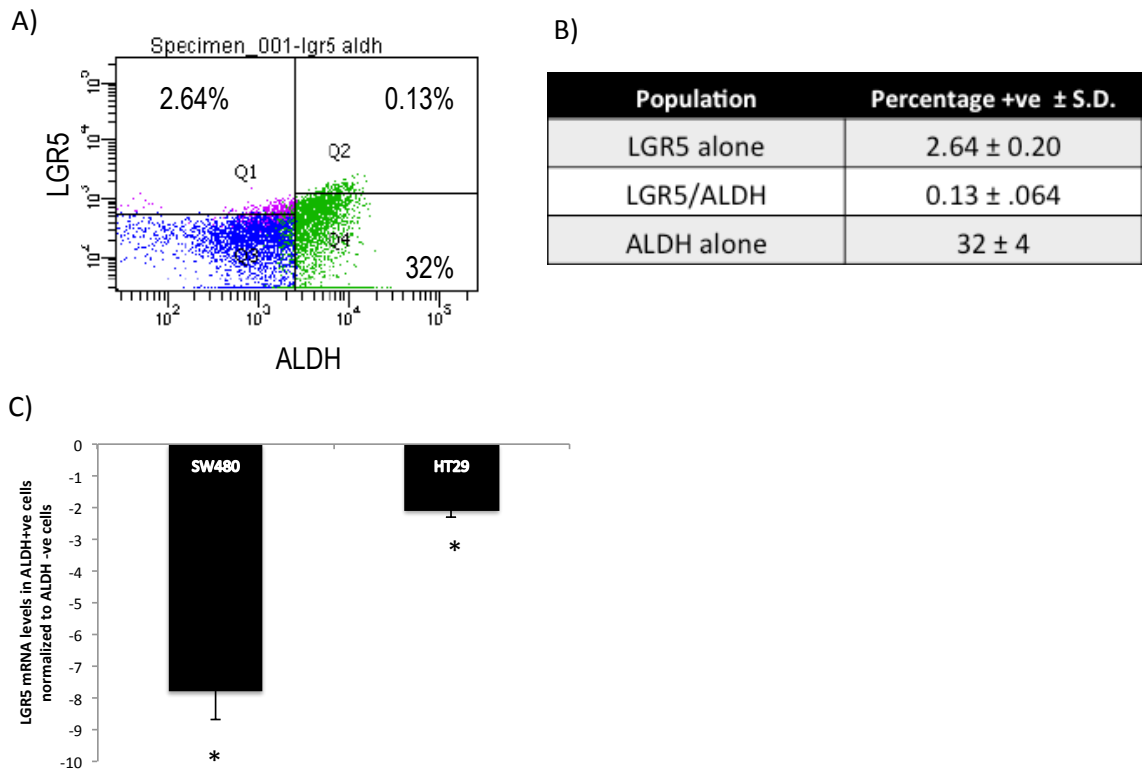


Figure 2.9: LGR5 and ALDH1 expression do not overlap in cancer cells. A) FACS staining results of HT29 cells for LGR5 and ALDELFLUOR (ALDEFUOR positive). The percent of cells positive for each or both markers are represented in Table B. Graph C shows the normalized mRNA levels of LGR5 in ALDH +ve cells as compared to the ALDH -ve cells of two cell lines SW480 and HT29. Error bars represent standard error of mean. * indicates significant difference between the treated and the control samples with a p value $<$ 0.05.

2.4 Discussion:

I hypothesized that miR23b regulates the proportion of ALDEFUOR high cells in colon cancer and response to chemotherapy. MiR23b has been studied extensively in prostate, renal, breast and colon cancer. Its various targets such as SMAD3, FZD7, PTEN, AKT, MAP3K and TGFbetaR2, belonging to vital signaling pathways, have been identified and validated [85-93].

Recently, the function of several miRNAs has been implicated in cancer stem cells in the breast, colon, prostate and brain [82, 87, 94, 95]. In the colon cancer cell lines HT29 and SW116, miRNAs have been identified to be involved in the maintenance of the CSC phenotype. It was shown earlier that ALDH1 is a good marker for stem cells in normal as well as cancerous colon [28]. The ALDEFUOR assay screens live cells for high ALDH activity and it can be employed to look at differential expression of candidate miRNAs in the ALDEFUOR positive vs the ALDH low populations. We observed that miR23b is overexpressed in the ALDEFUOR positive stem cell populations of two cancer cell lines tested. We found that modulation of miR23b levels significantly regulates the proportion of cells with high ALDH in the two cancer cell lines SW480 and HT29. This has not been reported before for miR23b and suggests its potential role in maintenance of the cancer stem cell phenotype. The negative effect of miR23b expression on proliferation was supported by the cell cycle analysis of cells with high miR23b expression. The reduction in the proliferation was caused due to the accumulation of cells in the G0/G1 phase of the cell cycle thus reducing the proportion of cells entering the cell cycle. This has already been reported for prostate and renal cancer as well as endothelial cells [89, 90, 96, 97]. We could extend this observation to the cancer stem cell model,

suggesting that the increase in the number of cells in the G0/G1 phase is reflective of an increase of relatively quiescent ALDEFUOR positive cells.

To test my hypothesis on the role of miR23b in regulating the ability of CSC to self-renew, it was pertinent to look at the effect of miRNA overexpression and knockdown on the self-renewal function of cancer stem cells. MiR23b promotes colony formation or sphere formation under low attachment conditions and reducing miR23b levels significantly inhibits the ability of HT29 cells to form colonies or spheres in vitro. The increase in the self-renewal ability could be due to the increase of ALDH-high cells with miR23b overexpression.

Cancer stem cells have been reported to be associated with increased EMT for breast cancer [98]. Our findings indicate that miR23b overexpression promotes EMT by decreasing E Cadherin and Vimentin in SW480 cells. This increase in EMT phenotype is suggestive of an increase in the cancer stem cell population due to miR23b overexpression. This finding could be cell line specific since conflicting reports have shown that miR23b actually promotes E-Cadherin expression [85, 99]. Recently, a study indicated that miR23b inhibition led to an increase in E-Cadherin expression in glioma cells [100]. Even in colon cancer, miR23b has already been shown to be an important negative modulator of cancer metastasis. It was shown that miR23b functions as a tumor suppressor in HCT116 cells and, when over expressed, significantly inhibits tumor growth in vivo [85]. MiR23b overexpression in breast cancer cells, on the contrary, showed no effect on the expression of E-Cadherin [88]. The varied results observed in our study might be due to the cell lines used. HCT116 has been shown to follow a stochastic model and not a cancer stem cell model. This means that the population in HCT116 line has been predicted to not follow a hierarchy

of stem cells, progenitor cells and differentiated cells [101]. It has also been reported to form spheres with a more differentiated phenotype and not enriched in stem cells. This could explain the discrepancy in the results obtained in our study.

Each miRNA in a cell is predicted to influence the expression of about 3000 mRNA targets, so it becomes essential to identify newer targets regulated by miR23b, which could possibly play a role in self-renewal mechanism of cancer stem cells. MRNA expression studies such as RNA SEQ analysis has already been done to identify global mRNA changes, caused due to miR23b for breast cancer cells [91]. Our RNA SEQ analysis of the colon cancer cell line HT29 with altered levels of miR23b revealed new gene targets such ATF2 and AKT2, which are important components of Wnt and AKT/PI3Kinase signaling pathway respectively. We predict that via the regulation of these candidate genes, miR23b plays an important role in driving tumor growth.

Recently, MiR23b was found to be crucial in chemoresistance for ovarian cancer stem cells where its expression was upregulated in the chemoresistant cells and tumor tissues as compared to the sensitive ones. Our results indicated that 5-FU treatment results in reduced miR23b expression in colon cancer cells, suggesting low levels of this miR probably have a role in chemoresistance. One of its predicted targets is LGR5 whose mRNA levels are inversely correlated with miR23a/b expression in colorectal cancer [102]. LGR5 levels have been shown to be a predictor of response to 5-FU treatment in cancer patients where high LGR5 expression is associated with poor outcomes post-chemotherapy with 5-FU [103]. We demonstrated using multiple functional assays that LGR5 expression is regulated by miR23b. An increase in the mir23b predicted target, LGR5, which marks the cycling stem cells, could explain the

increase in proliferation of cells with reduced miR23b levels. Various reports has identified transcription factors such as p53, AP-1 and Myc that regulates expression of this miR [104]. Myc expression can be upregulated by active Wnt signaling and is upregulated in 70% in colon cancer cases [105]. LGR5 protein has also been reported to enhance Wnt Signaling by associating with R-Spondins [106]. This mechanism suggests that LGR5 expression in turn regulates miR23b expression in a negative feedback loop mechanism mediated by Myc. Interestingly, LGR5 and ALDH-high populations are in HT29 cells, suggesting the co-existence of multiple populations with varying degrees of stemness. The ALDH-high cells have high miR23b levels and are slow cycling self renewing stem cells. The LGR5 positive cells have low levels of miR23b are rapidly cycling stem cells, with some degree of self-renewal and resistance to anticancer drugs. This model represented in **Figure 2.11** suggests that there is a hierarchy of cells with stemness within a tumor, which has also been indicated previously in normal intestine, where the BMI positive cells are capable of giving rise to LGR5 positive cells upon specific depletion of LGR5 cells in mice [107]. The LGR5 positive cells, when exposed to drug irinotecan undergo a transient conversion to LGR5 negative cells, which can revert back to LGR5 positive cells in the absence of the drug [108].

My study in particular established the role of miR23b in colon cancer stem cells in vitro, and has surfaced new avenues for the development of anti-cancer approaches. We also identified a hierarchy model of stem cells in tumor, which has been indicated before, and adds to the complexity of cancer growth and maintenance.

Colon Cancer Stem cells

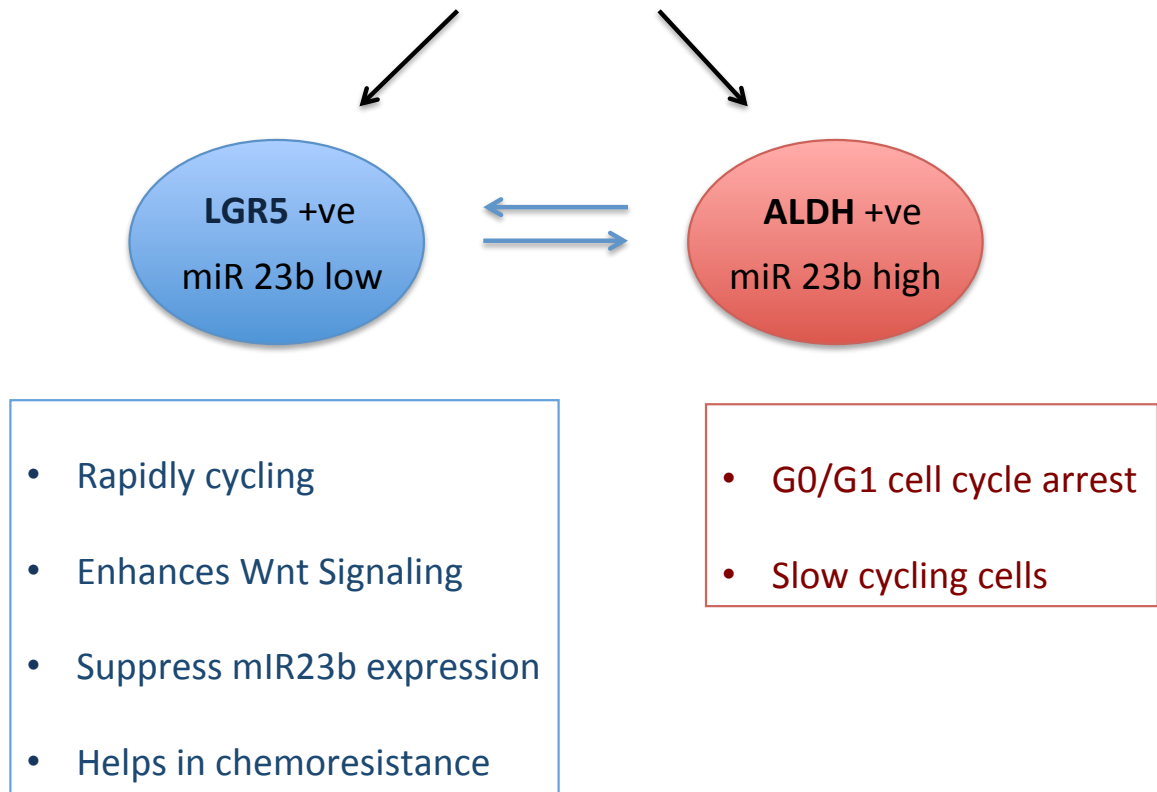


Figure 2.11: Proposed model of existence of hierarchy in colon CSCs. This model postulates that there are two exclusive CSCs in tumor population. One is driven by high LGR5 and low miR23b expression and are rapidly cycling chemoresistant SCs. The other population comprises of ALDH high and high miR23b expression, which are slow cycling SCs.

Chapter 3

IDENTIFICATION, ISOLATION AND MiRNA PROFILING OF COLON CANCER STEM CELLS

3.1 Introduction:

My project was based on the hypothesis that **there is a unique signature of miRNA expression that defines SCs in the normal colon; aberrant miRNA expression leads to the loss of control of SC self-renewal and to tumor initiation.**

Consequently, it is imperative that these normal and cancer stem cells can be identified and isolated from patient samples with the aid of a molecular marker. The advent of technology such as Flow Cytometry can aid in the identification of stem cells (SCs) using different molecular markers and in the isolation of SCs based on their protein expression or enzyme activity. This technology helped me contrast (profile) miRNAs in SCs versus non-SCs from both normal and CRC tissues. Colon cancer stem cell markers used to isolate and study SCs can be broadly categorized on the basis of their location and function in the cell. For example, Musashi 1, which was one of the first cancer stem cell markers to be identified in colon cancer, is a RNA binding protein present in the cytoplasm. ALDH1 is another prominent cancer stem cell marker, which functions as an enzyme that catalyzes the reaction of toxic aldehydes to alcohol. The number of stem cell markers, which have been identified so far in colon CSCs is a reflection of overlapping, complex signaling pathways that maintain stem cell homeostasis in the normal colonic crypt. The various colon stem cells markers can be described as:

3.1.1 Musashi 1:

Musashi-1, first identified in *Drosophila* [109], assists as a RNA binding protein during two rounds of asymmetric division. More specifically, it inhibits mRNA translation by competing with an initiation factor such as eIF4G [110, 111]. This protein is a highly conserved protein across species and was found to be prevalent in the neural progenitor cells of mammals [112]. Following its identification as a possible stem cell marker for mouse intestinal epithelium, Nishimura *et al.*, studied its expression pattern in normal human intestinal crypts. Musashi-1 staining was specific for the crypt bottom where the SCs reside [113]. They stated that Musashi-1 had already been identified to play a role in keeping stem cells in an ‘immature’ state by regulating the Notch pathway [110]. The expression of this protein is increased in APC min mice, indicative of its regulation by the Wnt pathway [114]. Indeed, when expression of Musashi-1 is induced in intestinal epithelial cells, it results in increased proliferation via the activation of Wnt and Notch pathways [115].

3.1.2 CD133:

It is a single chain five transmembrane glycosylated protein belonging to the Prominin family. The coding region of the gene consists of 27 exons which facilitates the synthesis of multiple isoforms by alternative splicing [116]. The expression of this protein is tissue specific and can be regulated by the stages of development [117]. The actual function of the protein depends upon its isoform and tissue. CD133 typically acts as a scaffolding protein with an array of functions including plasma membrane remodeling, migration and cell-cell interaction [118]. The reports of cell surface expression of CD133 on the stem or progenitor cells of different tissues such as hematopoietic [119], neural [120], prostate [121], liver [122], kidney [123], retina

[124] and also embryonic stem cells [125] strengthened its identity as a strong stem cell marker. Singh and his colleagues reported the first study where they used CD133 to isolate cancer stem cells in brain tumors [29]. Since then, many reports were published where they used CD133 as a marker for isolation of cancer stem cells from various tissues including colorectal cancer. The use of CD133 as a strong stem cell marker was challenged by frequent reports that suggest CD133 negative cells could give rise to a tumor. Three individual reports suggested something similar for colon cancer stem cells where they disregarded CD133 as a strong stem cell marker for colon [30, 126, 127]. Researchers suggested that the antibody used to detect CD133 protein might not work under all conditions due to variations in size and glycosylation patterns of the isoforms.

3.1.3 CD166:

Also known as *ALCAM* (Activated Leukocyte Cell Adhesion Molecule), CD166 is a cell membrane protein that was initially associated with the motility of leukocytes, especially macrophages, over endothelial cells through homophilic interactions [128]. It is also associated with other functions such as angiogenesis, capillary formation and has an anti-apoptotic role in cancer. The expression of CD166 is positively correlated with the aggressiveness of different cancer types including melanoma, prostate, breast, ovarian, bladder and colon [129]. CD166 expression has been correlated with poor prognosis in colorectal cancer. CD166, along with CD44, was initially recognized as a stem cell marker by Dalerba *et al.* [127], where they phenotypically characterized 'stem' cell fractions by looking at the expression of multiple stem cell markers such as ESA, CD44 and ALDH1. Cells that were co-positive for CD44/CD166 could give rise to new tumors in immunodeficient mice. Levin *et al.*,

demonstrated that CD166 cells stain the bottom of the crypt in both mice and humans, and enriches for stem-cell like cells (with high expression of stem cell markers such as CD44, LGR5 and ASCL2) and also committed progenitor cells [129].

3.1.4 ABCG2:

ATP Binding Cassette G2 protein is a member of a highly conserved ATP binding transmembrane group of proteins. ABCG2 expression has been seen in normal tissues such as in liver, breast, amnion, small intestine and colon [130]. In colon cancer, one study found the expression of this protein to be down regulated 6 fold as compared to the normal tissue [131]. A larger immunohistochemistry study actually disagreed with the previous finding and reported that ABCG2 expression was up-regulated in colorectal cancer tissue, specifically in invasive forms of cancer [132]. Their result was supported by the observation that ABCG2 expression is decreased in early cancer and then overexpressed in later stages of the disease. ABCG2 functions as a multidrug transporter and has been shown to efflux fluorescent dye out of cells, thus giving rise to population of unstained cells when performing a side population analysis. This property was used with the help of flow cytometry to identify and sort hematopoietic stem cells from murine bone marrow cells [133]. In multiple cancers for example anaplastic thyroid cancer, ABCG2 high expression was restricted to the side population, which conferred resistance to the anticancer drug doxorubicin [134]. In colon cancer, the role of ABCG2 in conferring resistance to drugs such as mitoxantrone, topotecan and anthracyclins was observed in the S1 cell line [135].

3.1.5 LGR5:

Barker and his colleagues recently discovered one of the very well studied stem cell markers, *LGR5*, by looking at small intestine and studying various Wnt target genes possibly expressed in intestinal stem cells. *LGR5* is a seven transmembrane protein which is highly hydrophobic and has small extracellular domains. The expression of *Lgr5* in the small intestine of mice was localized to cycling stem cells located next to the relatively quiescent paneth cells [136]. Through lineage tracing experiments, the same group also showed that APC mutations in the *LGR5* positive cells led to expansion of the stem cell compartment and eventually adenoma formation [137]. Yui *et. al.*, reported that colon organoids developed from single isolated *LGR5*+ cells in vitro, when grafted back into the mice intestine, could generate viable and functional crypts for at least 180 days [138]. Functionally, R-spondins (from paneth cells) mediate signaling via binding to *LGR5* and its homologs, which are associated with frizzled-Lrp5/6 complexes to activate downstream Wnt signaling in stem cells [106].

3.1.6 LRIG1:

Lucine rich repeats and immunoglobulin like domains (*LRIG1*) is a membrane protein, which is a negative regulator of ErBb signaling. It was first identified to regulate stem cell homeostasis in human epidermal stem cells [139]. It was shown in mice that *Lrig1* expression is restricted to relatively quiescent stem cells of the intestine, which are distinct from the *LGR5* positive cells. Loss of APC in *Lrig1* positive mice or ablation of *Lrig1* itself gave rise to adenomas and led to the increase of *Lgr5* positive cells, which suggests that it acts as a tumor suppressor and curbs the ErBb signaling in the crypt cells. *LRIG1* expressing crypt cells seem to be responsible

for immune regulation and protect the cells from oxidative damage. LRIG1 expression is lost in multiple cancers, including colorectal cancer. Immunostaining studies have shown that there is patient variability in the expression of LRIG1 in CRC [140].

3.1.7 BMI1:

B-cell specific Moloney murine leukemia virus integration site 1, or *BMI1*, belongs to the polycomb group of proteins. The protein harbors a N terminal ring finger domain and a central helix-turn-helix-turn-helix-turn motif which is responsible for its telomerase activity [141]. BMI1 expression was initially reported in leukemic stem and progenitor cells, as well as normal stem cells of the fetal liver [142]. Hematopoietic stem cells also demonstrate high expression of BMI1, which is lost upon differentiation [143]. In cancer, BMI1 expression has been shown to be up-regulated in multiple types of malignancies. Pertaining to cancer stem cells, BMI1 is co-expressed with other stem cell markers such as CD133 and CD44 in lung, liver and ovarian cancer stem cells [144-146]. In the intestinal epithelium, BMI1 and LGR5 were shown to identify two distinct populations of intestinal stem cells in the crypt base. BMI1 positive crypt cells are relatively quiescent and could proliferate when induced by injury or radiation, and give rise to LGR5 positive cells [147]. John Dick et al recently showed that BMI1 function is necessary for the self-renewal of colon cancer stem or initiating cells. By targeting BMI1 with siRNA or chemical inhibitors, the cancer stem cells failed to divide via self-renewal and resulted in termination of tumor growth [148].

3.1.8 Telomerase:

Telomere length maintenance is important for the replicative potential of adult stem cells. The enzyme telomerase is responsible for maintaining telomere length and is present in low levels in somatic stem cells. The hypothesis is that transient dysfunction of telomerase enzyme activity can cause telomere shortening in these stem cells, which could promote oncogenic mutations [149]. Cancer initiating cells of prostate, glioblastoma, breast and liver cancers have been shown to have telomerase activity and have been targeted by antagonists and inhibitors such as Imetelstat. Inhibition of telomerase in the enriched cancer stem cells have resulted in decreased proliferation and reduced tumor burden in mice [150-152]. With respect to CRC, telomerase activity was increased in colonospheres derived from the SW116 cell line as compared to the parental line and was used as a reference to study the proteome in the cancer stem cells [153].

3.1.9 ALDH1:

Aldehyde dehydrogenases are NAD(P)⁺ dependent enzymes that play a role in the metabolism of a wide spectrum of aliphatic and aromatic aldehydes. The isoform ALDH1 is involved in the two-step process of irreversible conversion of retinaldehyde to retinoic acid (RA). Retinoic acid is essential for many developmental processes, and it serves as a ligand for retinoid signaling pathways [33]. Hematopoietic stem cells are known to have high aldehyde dehydrogenase 1 (ALDH enzyme) activity, which confers on the cells protection against alkylating agents belonging to the oxazaphosphorines family [31, 32]. High ALDH1 expression was first reported in acute myeloid leukemia (AML) as a marker for leukemic SCs [34]. Wicha *et al.*, provided the first evidence of high ALDH1 expression in solid tumors.

Wicha studied breast cancer stem cells in which ALDH1 was found to be more specific than the CD44+/CD24low/ESA+ phenotype for determination of stem cells [23]. We also demonstrated the increase in ALDH1 expressing cells in the different stages of progression of the disease [28]. This biological evidence supported the mathematical model provided by Boman *et. al.*, which suggested that colon cancer is initiated due to dysregulation of self-renewal leading to the overpopulation of stem cells [27]. Similarly, ALDH1 has been reported as a promising marker for stem cells in normal and tumor tissue in the colon, as well as in other tissues such as lung, liver, prostate and ovary [35-38].

Multiple stem cell markers have been identified for colon cancer stem cells and yet there has been no study, which looks at their co-expression in normal and tumor colon tissue, which could possibly yield insight into better markers, used alone or in combination to isolate stem cells. To test my hypothesis, I proposed two aims:

Aim 1: To evaluate different SC markers for their ability to identify and successfully isolate normal and malignant colonic SCs.

Aim 2: To determine which microRNAs are differentially expressed in patient derived normal SCs versus the CSCs and identify their target genes.

3.2 Methods:

3.2.1 Immunofluorescence:

Paraffin embedded sections of matched normal and tumor samples of colon were used for all immunostaining studies. The slides were de-paraffanized by immersing them in Citra Solv reagent (Thermo Fisher Scientific Inc., Waltham, MA) three times for 10 minutes each. This was followed by treating the slides with two

100% and two 90% ethanol washes for three minutes each. Dipping them in distilled water for few seconds rehydrated the slides. Antigen retrieval was done by immersing the slides in microwave safe glassware containing 1X Antigen Retrieval Solution (DAKO, Thermo Fisher Scientific Inc., Waltham, MA). The slides were heated for 25 seconds on full power and then 12 minutes on the lowest power of the microwave. They were allowed to cool down to room temperature and subsequently washed in 1X Tris Buffered Saline (TBS) solution for 5 minutes (three times). Blocking reagent (10% Goat Serum and 1% Bovine Serum Albumin in PBS) was added to each of the sections and the blocking step was carried out overnight in 4°C. The next day, the blocking solution was removed from the slide by draining and blotting the excess. Then the primary antibody solution (list of primary antibodies and their concentration is provided in **Table 2.1**) was added to each of the tissue sections. Appropriate IgG solutions with the same concentration of the primary antibody were added to the control slides. The sections were incubated in the primary antibody overnight at 4°C. The following day, the primary solution was completely removed and the slides were washed with TBS three times for 5 minutes each. Secondary antibody solution (prepared by diluting the AlexaFluor Secondary (Life technologies Inc., Carlsbad, CA) in blocking solution at a 1:1000 concentration) was added to the slides, which were incubated for 2 hours at room temperature. Slides were washed three times in TBS again to get rid of the secondary solution. Sections were incubated with the counter stain, which also contained a nuclei stain for ten minutes. The slides were washed again two times in TBS. The slides were allowed to dry partially in the dark and then Gold Antifade reagent (Life technologies Inc., Carlsbad, CA) was added to each of the

section. Coverslips were placed carefully on each section. Images were taken using 20x objective of Zeiss Epi-fluorescence microscope.

Table 3.1: List of antibodies and their dilutions tested for expression in normal and tumor colonic tissue.

Antibody	Company	Dilution
<i>ALDH1</i>	BD Biosciences, Franklin Lakes, NJ	1:100
<i>CD166</i>	ABCAM, Cambridge, MA	1:100
<i>LRIG1</i>	Courtesy of Dr. Coffey	1:200
<i>BMI1</i>	ABCAM, Cambridge, MA	1:100
<i>LGR5</i>	Novus Biologicals	NA
<i>OLFM4</i>	ABCAM, Cambridge, MA	NA
<i>CD44</i>	SDiX	1: 200
<i>CD24</i>	ABCAM, Cambridge, MA	NA
<i>ABCG2</i>	ABCAM, Cambridge, MA	1:200
<i>hTERT</i>	ABCAM, Cambridge, MA	NA

3.2.2 Cell Lines:

HT29 and SW480 cell lines were purchased from ATCC Inc., (Manassas, VA). Cells were grown at 37°C with 5% CO₂ and 95% air and were passaged regularly.

3.2.3 Immunostaining and Flow Cytometry Analysis for CD166:

Cells were detached from a 100 mm dish using trypsin or EDTA based cell stripper. Cells were washed once with the blocking buffer (DMEM media with 5% heat inactivated FBS). Cells were incubated with the primary antibody for CD166,

(1:100, ABCAM Inc., Cambridge, MA) or IgG in blocking buffer on ice for 1 hour. Cells were washed thrice with the blocking buffer and incubated in the secondary antibody solution (1:200 dilution) for 1 hour in ice. After that, cells were washed again thrice in blocking buffer and resuspended in fresh blocking buffer. The samples were subjected to FACS analysis. The samples were run in FACS ARIALL using the FACS DIVA software. Plots were gated to eliminate cell doublets in the study. Appropriate gates were set using the control samples and the percent of positive cells for each marker was determined.

3.2.4 Tissue Microarray (TMA) Immunofluorescence Study:

The tissue microarray was purchased from Pantomics, Inc., (Richmond, CA). Each array was composed of two tissue cores from 75 patient tumor samples whose clinical features are presented in **Table 2.2**. Each array was used for immunofluorescence staining following the protocol mentioned above. There were three arrays that were co-stained for LRIG1/ALDH1, LRIG1/CD166 and ALDH1/CD166 (same antibodies and dilutions used earlier). Each array was analyzed using a Zeiss 780 confocal microscope using a 20X and 40X objective. The various patient sample cores were scored for the presence and intensity of expression of the markers. A chi square test was used to calculate the correlation of staining across the patient samples.

Table 3.2: Clinicopathological features of patient tissues used for the tissue microarray study.

<u>Variable</u>	<u>N</u>
Number of patients:	75
Mean age \pm SD:	59 \pm 14 years
Sex:	
Male:	64
Female:	11
Tumor Stage:	
T2N0M0	26
T2N1M0	1
T3N0M0	24
T3N1M0	18
T3N2M0	1

3.2.5 Isolation of Crypts and Dissociation of Normal and Tumor Tissue to Single Cells:

All patient samples were obtained after IRB approval. Normal and tumor tissue were washed three times in sterile PBS. The normal tissue was carefully cleaned of the muscle layer using clean forceps and surgical scissors. It was then placed in 3.0 mM solution of EDTA containing DTT and incubated on ice for 60-90 minutes. The crypts were separated from the submucosa by rigorous shaking of the tissue in solution for five minutes. The isolated crypts were washed with sterile PBS thrice. Single cell dissociation was achieved by treating the crypts with collagenase IV (Worthington Inc., Lakewood, NJ) solution in HBSS (10 mg/ml) and DNase I (Worthington Inc., Lakewood, NJ) for 60-90 minutes at 37°C. The tumor tissue was cut into small pieces using a sterile scalpel and incubated in collagenase/hyaluronidase and DNase I solution in HBSS to achieve enzymatic digestion of the tissue to single cells. Cells from both normal and tumor tissue were washed thrice with HBSS.

3.2.6 Aldefluor Assay, Propidium Iodide Staining and EpCAM Staining of Normal and Tumor cells:

The dissociated cells from both normal and tumor were washed thrice in sterile HBSS and then subjected to the ALDEFLUOR Assay following the manufacturer's protocol (STEMCELL Technologies Inc., BC, Canada). The cells were spun down at room temperature and resuspended in Aldefluor buffer. The cell suspension was divided into three tubes: ALDEFLUOR only, ALDEFLUOR + DEAB (inhibitor) and Blank. The tubes were incubated in the dark at 37°C for 25 minutes. After incubation, the cells were spun down once and resuspended in Aldefluor buffer. The cells

suspension was transferred to a FACS sample tube through a 50-micron filter. The samples were run on the BD FACSAria II using the FACSDiva Software. The gates were drawn to eliminate doublets and to include 0.1% in the positive gate of cells in the respective DEAB control and appropriate ALDEFUOR positive samples. Normal dissociated tissue was stained for propidium iodide to identify live cells following the Aldefluor staining. Cells were incubated in Aldefluor buffer containing PI stain at a concentration of 1 µg/ml for 20 minutes at RT in the dark. Cells were washed once with Aldefluor buffer and were stored on ice under further analysis. Tumor cells, after the Aldefluor assay, were incubated with an APC-labeled EpCAM antibody (1:100, BioLegend Inc., San Diego, CA) for 1 hour on ice in the dark. The cells were washed twice with Aldefluor buffer and were stored on ice until they were subjected to FACS analysis.

3.2.7 Cell Sorting by Flow Cytometry:

The 85-micron or the 100-micron nozzle was used for the sorting experiment. The stream was turned ON and was Cytometer setup and Tracking was done to calibrate the machine. Accudrop experiment was carried out to determine the delay between the drop prior to any sorting. A test sort was done to ensure proper collection of sample in the collection tubes. The dot plots were created and the cell populations were appropriately chosen to eliminate doublets out of the analysis. The blank sample was run through FACS initially. Voltage of FSC and SSC were adjusted if needed to set the cell population in the center of the first dot plot. Appropriate regions within the plots were selected so that only single cells could be sorted. The sample with the DEAB control was run through FACS and data was recorded. The ALDH alone (green only) and the PI alone (red only for normal) or EpCAM only (red only for tumor)

samples were run to calculate compensation between the two fluorophores to eliminate cross talk in the analysis. Using the DEAB alone sample, the gates for the ALDEFLUOR negative and ALDEFLUOR positive were created in the dot plot for SSC vs FITC. Similarly, gates for additional controls (PI and EpCAM) were also created using the blank sample. For normal tissue, PI negative samples were regarded as alive and were gated for Aldefluor positive or negative cells. For the tumor samples, EpCAM positive cells were selected and gated for ALDEFLUOR positive and ALDEFLUOR negative cells. At the end, we obtained four different sorted samples from each pair: PI-/ALDH+ and PI-/ALDH- from normal tissue and EPCAM+/ALDH+ and EPCAM+/ALDH- from tumor tissue.

3.2.8 RNA Isolation:

RNA isolations were performed according to the manufacturer's protocol using the Trizol Reagent (Life Technologies Inc., Carlsbad, CA). One ml of Trizol was added per million cells and incubated at 4°C for ten minutes. Chloroform (0.2ml per ml of Trizol used) was added to the cells and the solution was mixed vigorously for 15 seconds. The tubes were placed on ice for two min and then spun at 12000 rpm at 4°C for 15 minutes. Following centrifugation, the upper clear layer was carefully removed from each sample and transferred to a new tube. RNA was precipitated by adding isopropanol (0.5 ml per 1 ml of trizol added) to the tube, followed by incubation for 10 minutes on ice. Spinning down the solution at 12000 rpm for ten minutes at 4°C pelleted the precipitated RNA. The supernatant was discarded and the RNA was washed twice by spinning down the pellet in 1 ml of ice cold 70% ethanol per ml of Trizol used. The pellet was allowed to air dry and was dissolved in nuclease free water.

3.2.9 RNA Quantification:

RNA quantification was done by determining the absorbances of samples at two wavelengths (260 and 280 nm) using the plate reader (TECAN) and the Nanoquant plate. Two μl of sterile water was used for blanking the instrument, followed by 2 μl of the RNA sample. The concentration values provided by the instrument were taken in triplicates and averages were calculated for each RNA sample.

3.2.10 MiRNA Profiling:

The RNA samples were concentrated to get a minimum concentration of 33 ng/ μl by using 3.0 M Sodium acetate and glycogen as a carrier molecule. The samples were sent to Nanostring Technology Inc. (Seattle, WA) for profiling. Nanostring Technologies made use of a unique color-coded fluorescent probe, which is hybridized to mature miRNA with the help of a linker molecule. This array has the advantage of quantitation of miRNA levels in a cell population and requires as little as 150 ng of total RNA per sample. The results were presented as an excel spreadsheet with the raw counts for each of the miRNAs as well as negative and positive controls. This data was then imported to software NSolver. The software takes the average of the whole data set and ranks the miRNAs with the highest positive and negative values from the average. These values are then compared between samples to get fold changes between miRNAs expression. Candidate miRNAs, which showed differential expression in tumor ALDEFLUOR positive cells as compared to normal ALDEFLUOR positive cells, were selected for further analysis.

3.2.11 Taqman MiRNA Assay:

A microRNA taqman assay for miR92a and miR20a were purchased from Life Technologies Inc., (Carlsbad, CA). The cDNA synthesis was performed following the manufacturer's instructions. Twenty nanograms of RNA were used in a final volume of 5 ul. Primer for the miR or U6 Control (3 µl), dNTPs (0.15 µl), 10X PCR buffer (1.5 µl), RNase Inhibitor (0.19 µl), RT enzyme (1.0 µl) and water were added to make a final volume of 15 µl. The samples were mixed gently using a sterile pipette and spun down briefly. The samples were placed in the thermocycler and cDNA was synthesized using the following temperature conditions: 16 °C for 30 min, 42 °C for 30 min, 85 °C for 5 min and 4 °C for 1 hour. The cDNA (1.33 µl of RT product) was used to prepare the Real Time PCR reaction, which also contained 10ul of 2X PCR master mix (Applied biosystems, no AmpErase UNG), the primers provided in the kit and water to a final volume of 20 ul. The samples were prepared in triplicates and added to the 96 well thermocycler plate (VWR Inc., Radnor, PA). The realtime PCR was run using Applied Biosystems 7500 fast PCR machine for 95°C for 10 min followed by 40 cycles of 95 °C for 15 sec and 60 °C for 1 min. The Ct value obtained was used to calculate the average Ct for each sample. The fold change in expression of miRNA in treatment versus control samples was calculated using the formula $2^{-(\text{delta Ct (treatment)} - \text{delta Ct (control)})}$. Any value greater than 2-fold change was regarded as significant.

3.2.12 Transient Transfection:

MiRNA92a Antimir and Precursor siRNA molecules were purchased from Ambion, Life Technologies. The amount of siRNA and transfection reagent (Lipofectamine 2000, Invitrogen) was standardized for HT29 using a GFP coupled

scrambled siRNA from DHARMACON Inc., (Pittsburgh, PA). The cell lines were transfected in a 12 well or a 6 well plate and media was changed 24 hours post transfection. The increase or decrease of the miRNA levels was tested by the miRNA Taqman Assay. The cells were analyzed 24- 48 hours post transfection.

3.2.13 Proliferation Assay:

Cells were plated in triplicates per condition in a 24 well plate and the initial count was regarded as day 0. The cells were then trypsinized at 24, 48 or 72 hours and counted using trypan blue dye exclusion method and an Invitrogen cell counter. These numbers represented cell count for day 1, day 2 and/or day 3. Three independent sets of experiment were carried out for each condition.

3.3 Results:

3.3.1 Multiple Stem Cell Markers Stain Specific Cells in Normal Crypt Base as Well as in Tumor:

Immunostaining results showed that the ALDH1 antibody stains the cytoplasm of cells in the bottom of the crypt in normal colonic tissue (**Figure 3.1A**) and also stains small clusters of cells in the tumors (**Figure 3.1B**). The marker ABCG2 stained cells in the middle of the crypt including the region where proliferating cells reside (**Figure 3.2A**). There was also an increased staining for ABCG2 in colon tumor tissue (**Figure 3.2B**). CD166 showed specific membranous staining of the majority of cells in the bottom of normal colonic crypts on the apical surface of the cell (**Figure 3.3A**). It also stained small cells in the tumors in clusters, which were slightly larger than the ones identified by ALDH1 (**Figure 3.3B**). Staining for LRIG1 showed a similar staining pattern to ALDH1 at the bottom of the crypt, but a few cells at the top of the

crypt also were positive for LRIG1, which was consistent across patient samples (**Figure 3.4A**). LRIG1 expression in tumor tissues was patient specific ranging from no staining to staining majority of the cells (**Figure 3.4B**). Staining for nuclear protein BMI1 was found in specific cells at the bottom of the crypt (**Figure 3.5A**), but in colon tumor tissue, a majority of cells stained positive (**Figure 3.5 B**).

Costaining analysis of ALDH1 and CD166 in normal epithelium showed that most ALDH1 positive cells stain positive for CD166 at the base of the crypts (**Figure 3.6A**). Interestingly, in tumor tissues CD166 and ALDH1 did not co-stain cells but did stain different sub-population of cells (**Figure 3.6B**). In normal tissue, LRIG1 also showed co-staining with other markers such as CD166 and ALDH1 (**Figure 3.7A**, **Figure 3.8A**). In the tumor tissues, LRIG1 specifically stained cells that were different from cells that stained positive for ALDH1 or CD166 (**Figure 3.7B**, **Figure 3.8B**). BMI1 also identified cells, which were ALDH1 or CD166 positive in normal tissue (**Figure 3.9A**, **Figure 3.10A**). Other markers such as telomerase, CD24 and OLFM4 were also tested but failed to show specific staining of cells in colon tissue sections. The co-staining results from the tissue microarray confirmed that LRIG1 and ALDH1 preferentially stain different cells in the tumor (**Figure 3.11 A**, $p < 0.05$). There were some patient samples that showed either LRIG1 or ALDH1 staining alone. The LRIG1 expression was stronger in patients with Stage 3 diseases compared to patients with Stage 2 colon cancer ($p < 0.05$). LRIG1 and CD166 co-expression analysis in multiple patient samples also revealed that both markers do not co-stain in most of the tumor patient samples ($p < 0.05$) (**Figure 3.12**). Overall, results from my immunofluorescence study are summarized in **Table 3.3**.

To check whether, the costaining results of stem cell markers in tumor tissue could be extended to the colon cancer cell lines, I performed CD166 staining followed by ALDEFLUOR assay. Multiple marker expression analysis identified that subpopulations exist in SW480 and HT29 cell lines that stain positive for CD166 and have high ALDH enzyme activity (i.e. ALDEFLUOR+) (**Figure 3.13**). A different approach to validate tumor tissue immunostaining results was taken by staining freshly dissociated tumor tissue for ALDEFLUOR and CD166 and analyzing by flow cytometry. Results indicated minimal overlap between ALDH and CD166 expressing cells from freshly isolated tumor tissue (**Figure 3.14**).

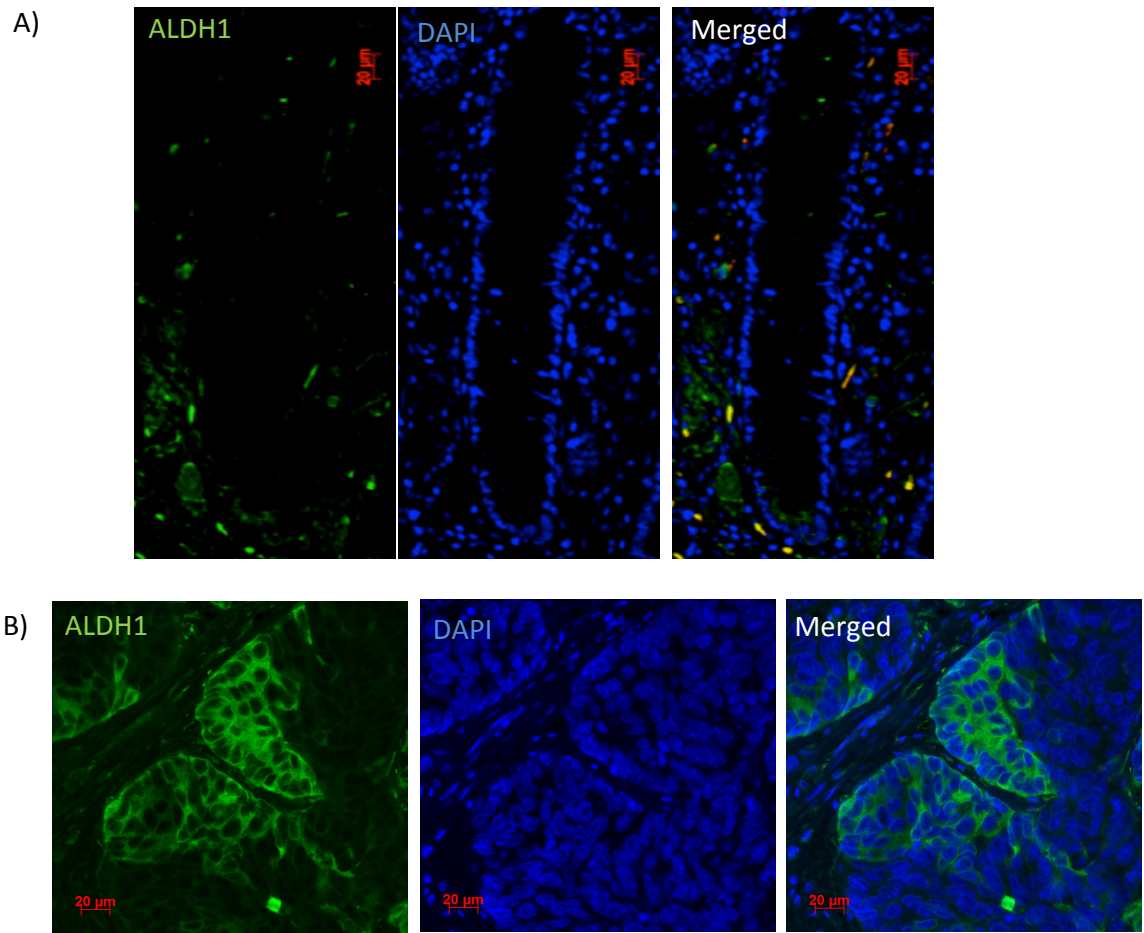


Figure 3.1: Expression of ALDH1 in normal colonic crypt and tumor tissue. ALDH1 stain cells at the base of the normal colonic crypt (A). It also stains specific populations of cells in the colonic tumor tissue (B). Blue represents nuclei stain.(3 matched normal and tumor sections).

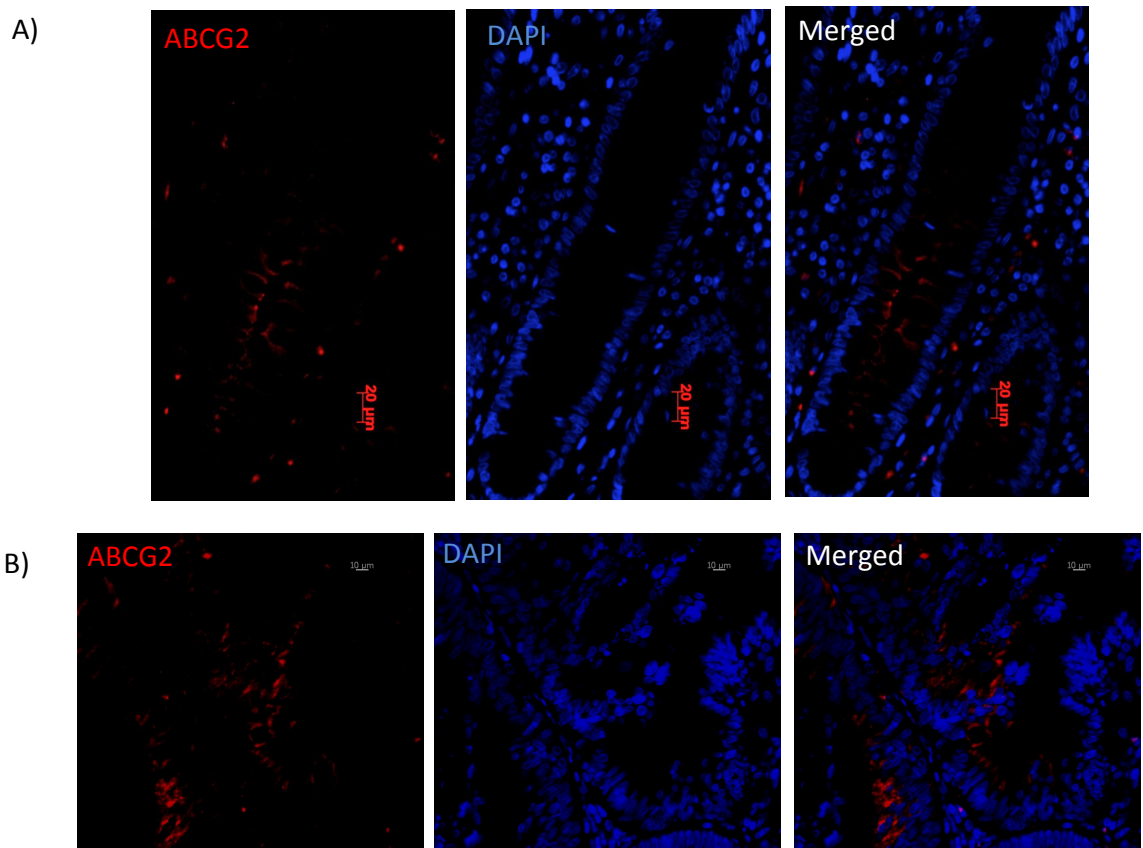


Figure 3.2: Expression of ABCG2 in normal colonic crypt and tumor tissue. ABCG2 stain cells at the base of the normal colonic crypt (A). It also stains specific populations of cells in the colonic tumor tissue (B). Blue represents nuclei stain. (3 matched normal and tumor sections).

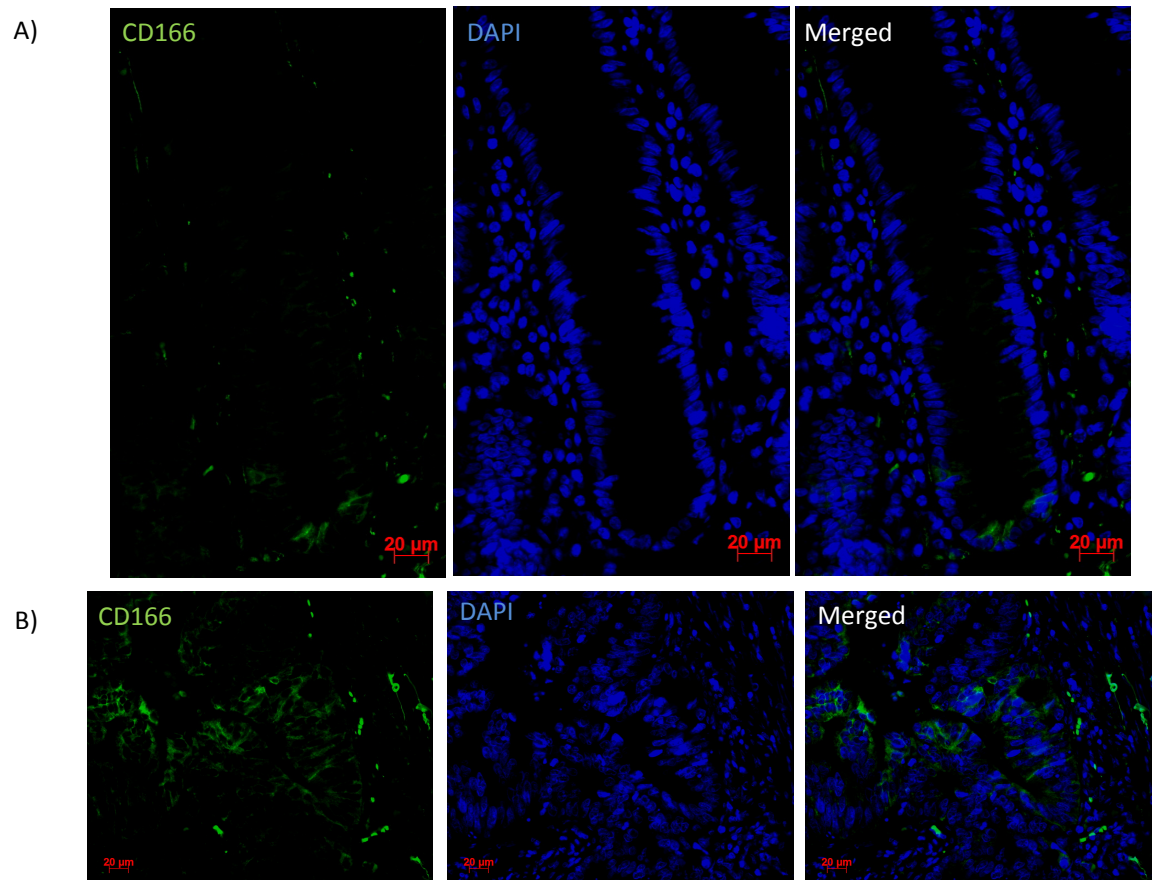


Figure 3.3: Expression of CD166 in normal colonic crypt and tumor tissue. CD166 stain cells at the base of the normal colonic crypt (A). It also stains specific populations of cells in the colonic tumor tissue (B). Blue represents nuclei stain. (3 matched normal and tumor sections).

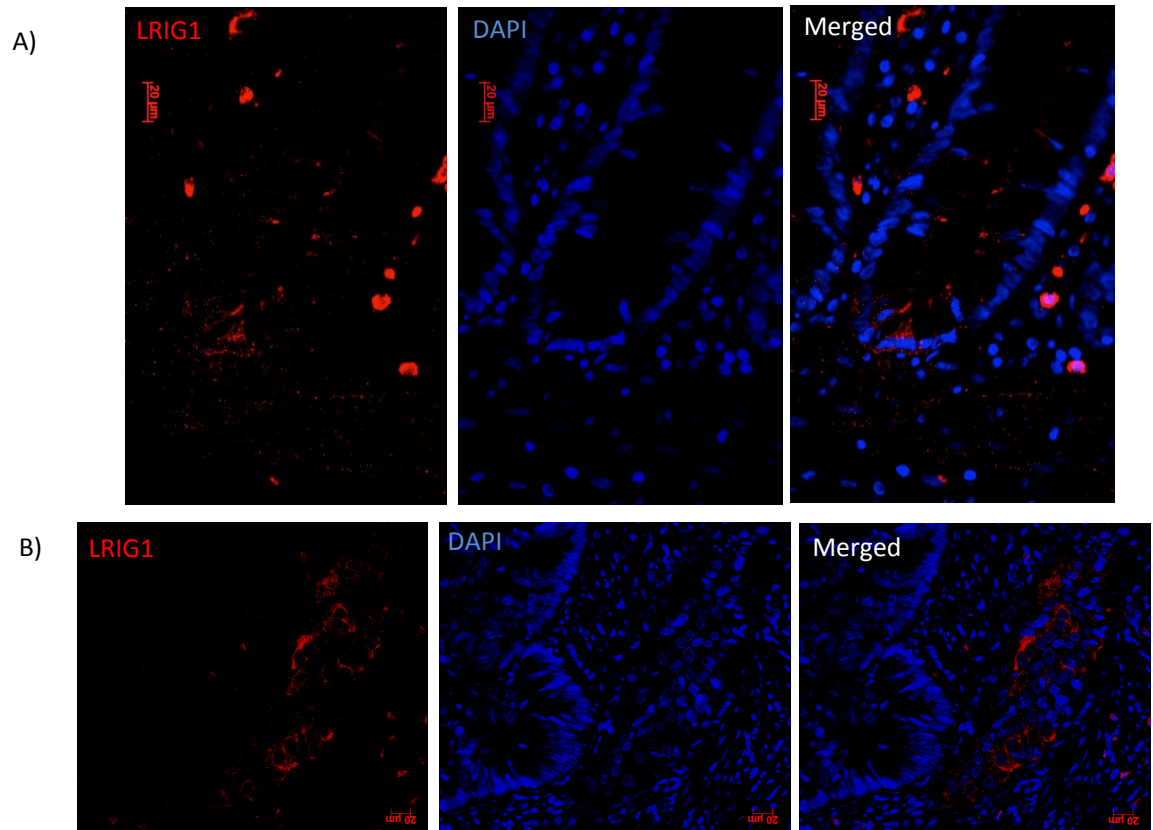


Figure 3.4: Expression of LRIG1 in normal colonic crypt and tumor tissue. LRIG1 stain cells at the base of the normal colonic crypt (A). It also stains specific populations of cells in the colonic tumor tissue (B). Blue represents nuclei stain. (3 matched normal and tumor sections).

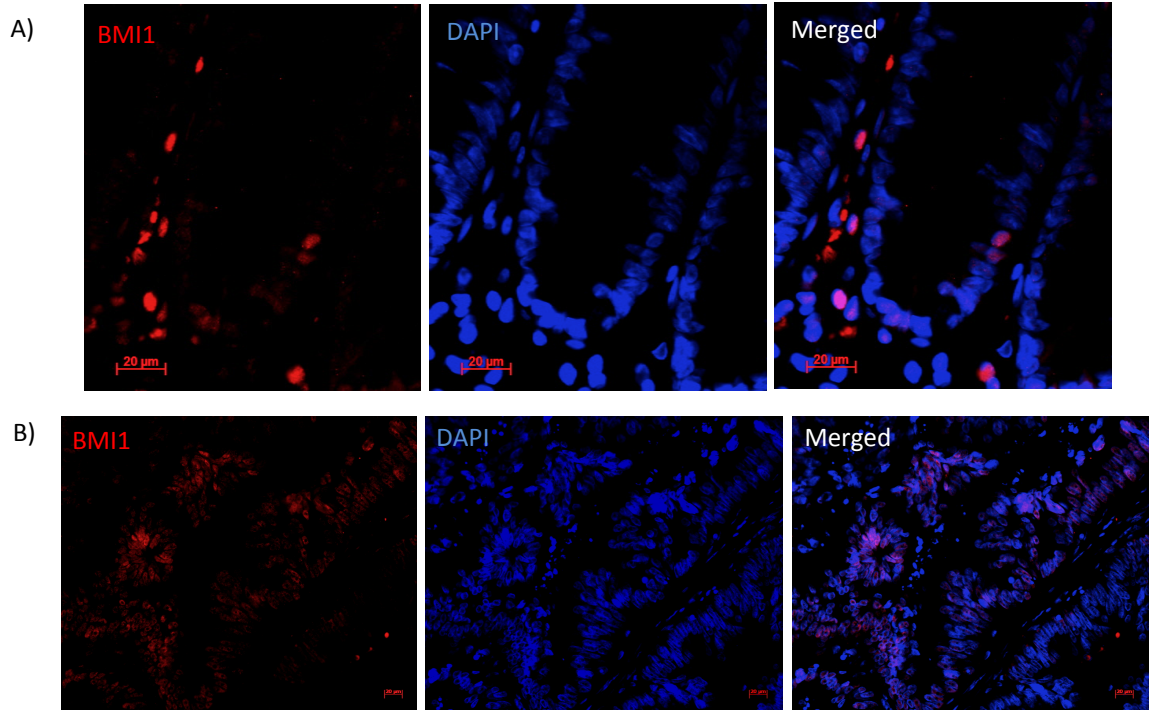


Figure 3.5: Expression of BMI1 in normal colonic crypt and tumor tissue. BMI1 stain cells at the base of the normal colonic crypt (A). It is found to be overexpressed in tumor tissue (B). Blue represents nuclei stain. (3 matched normal and tumor sections).

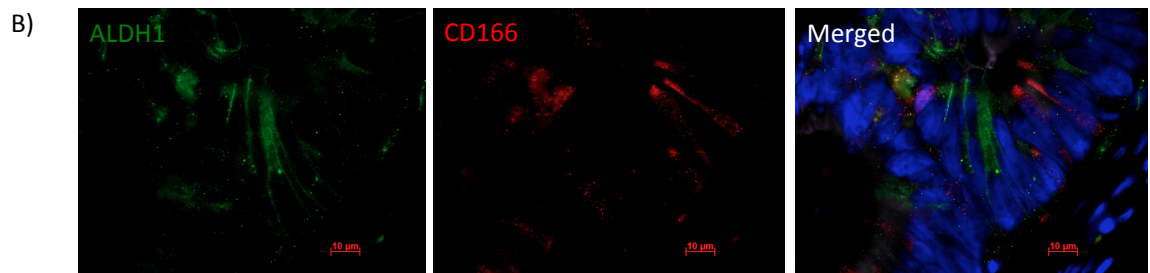
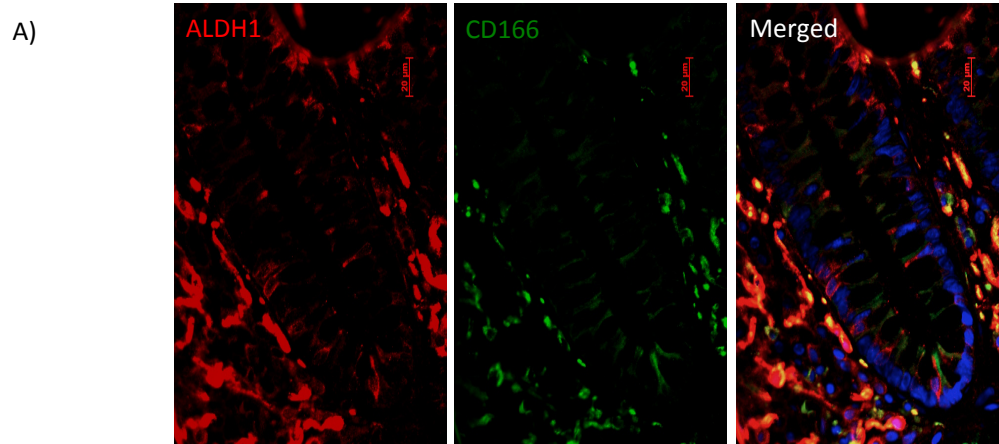


Figure 3.6: Co-staining of ALDH1 and CD166 in normal colonic crypt and tumor tissue. ALDH1 and CD166 identify co –populations in normal colon crypt (A), but identify different populations in tumor (B). Blue represents nuclei stain (3 matched normal and tumor sections).

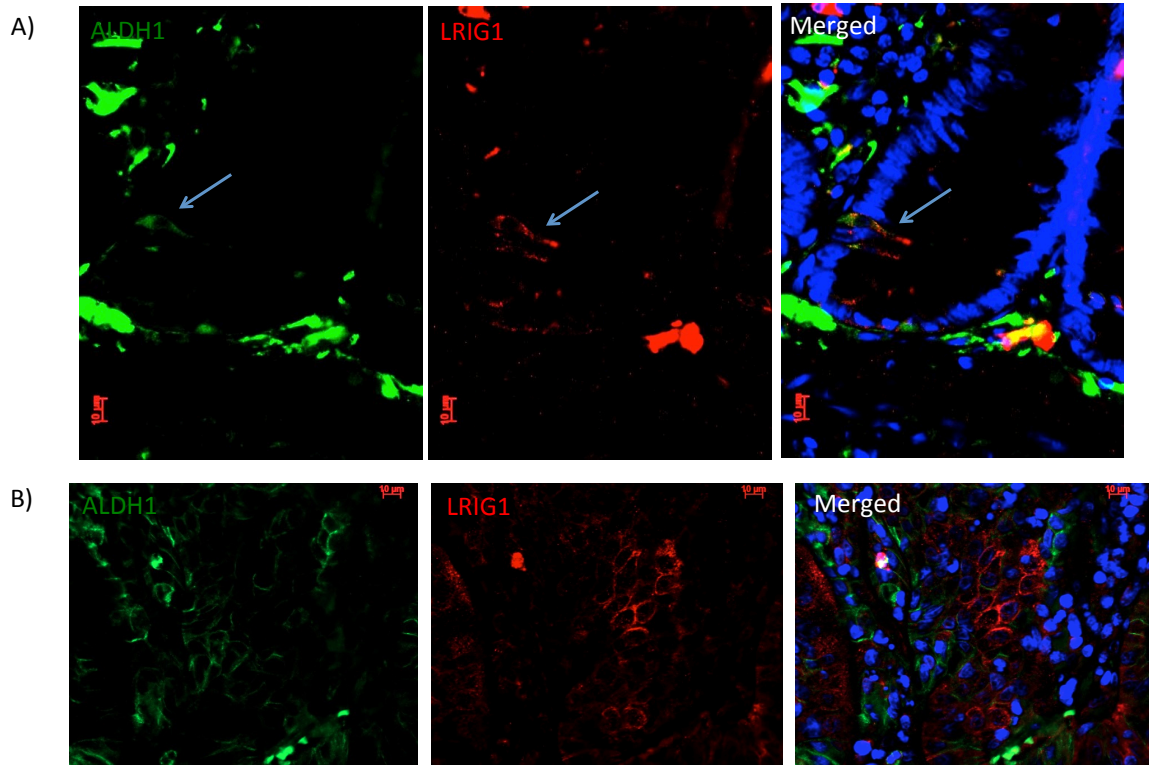


Figure 3.7: Co-staining of ALDH1 and LRIG1 in normal colonic crypt and tumor tissue. ALDH1 and LRIG1 identify co –populations in normal colon crypt (A), but identify different populations in tumor. Blue represents nuclei stain. (3 matched normal and tumor sections).

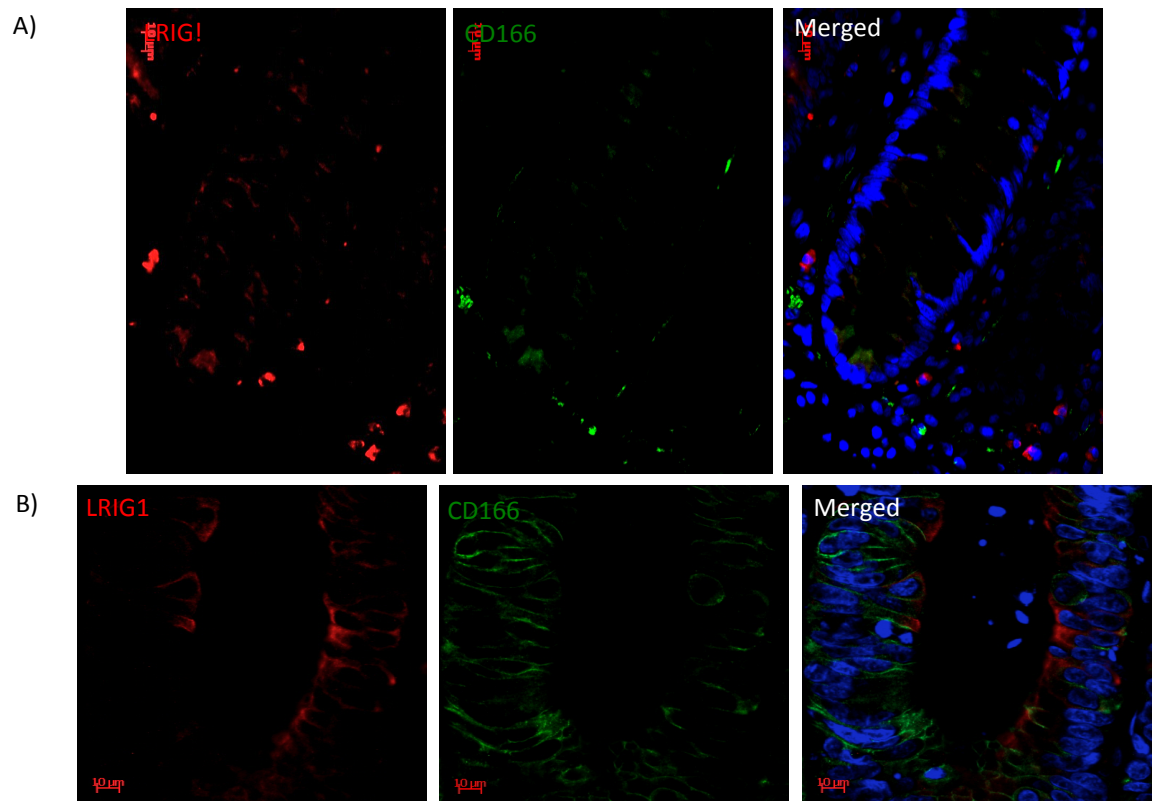


Figure 3.8: Co-staining of LRIG1 and CD166 in normal colonic crypt and tumor tissue. CD166 and LRIG1 identify co –populations in normal colon crypt (A), but identify different populations in tumor. Blue represents nuclei stain. (3 matched normal and tumor sections).

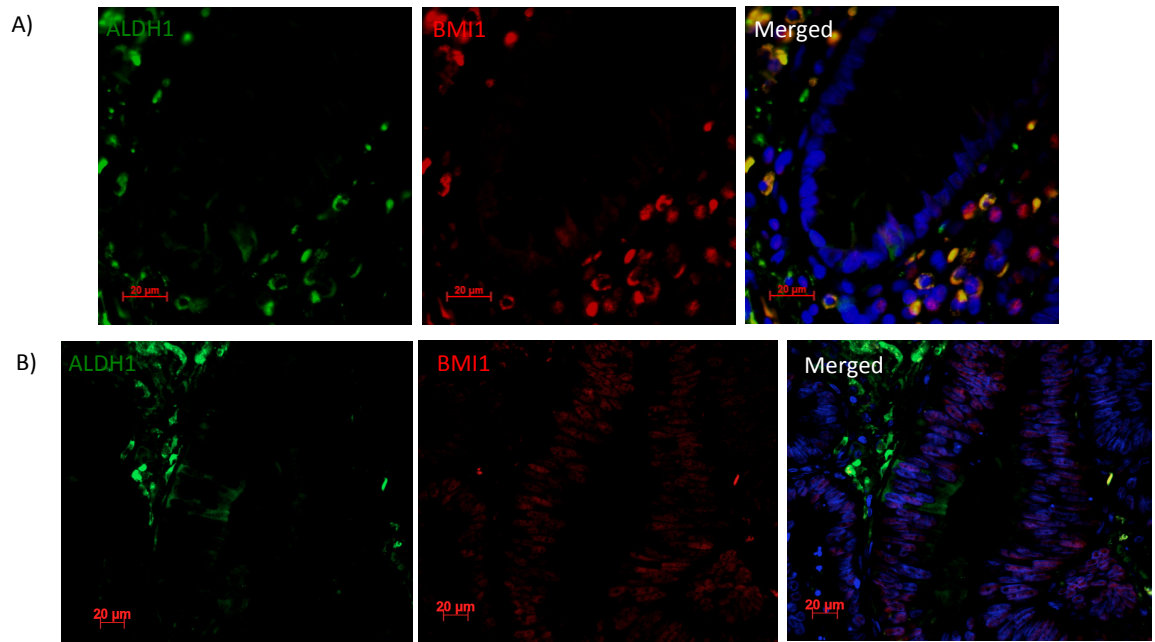


Figure 3.9: Co-staining of ALDH1 and BMI1 in normal colonic crypt and tumor tissue. ALDH1 and BMI1 identify co –populations in normal colon crypt (A), but in tumor BMI1 is overexpressed and loses its specificity to mark CSCs. Blue represents nuclei stain .(3 matched normal and tumor sections).

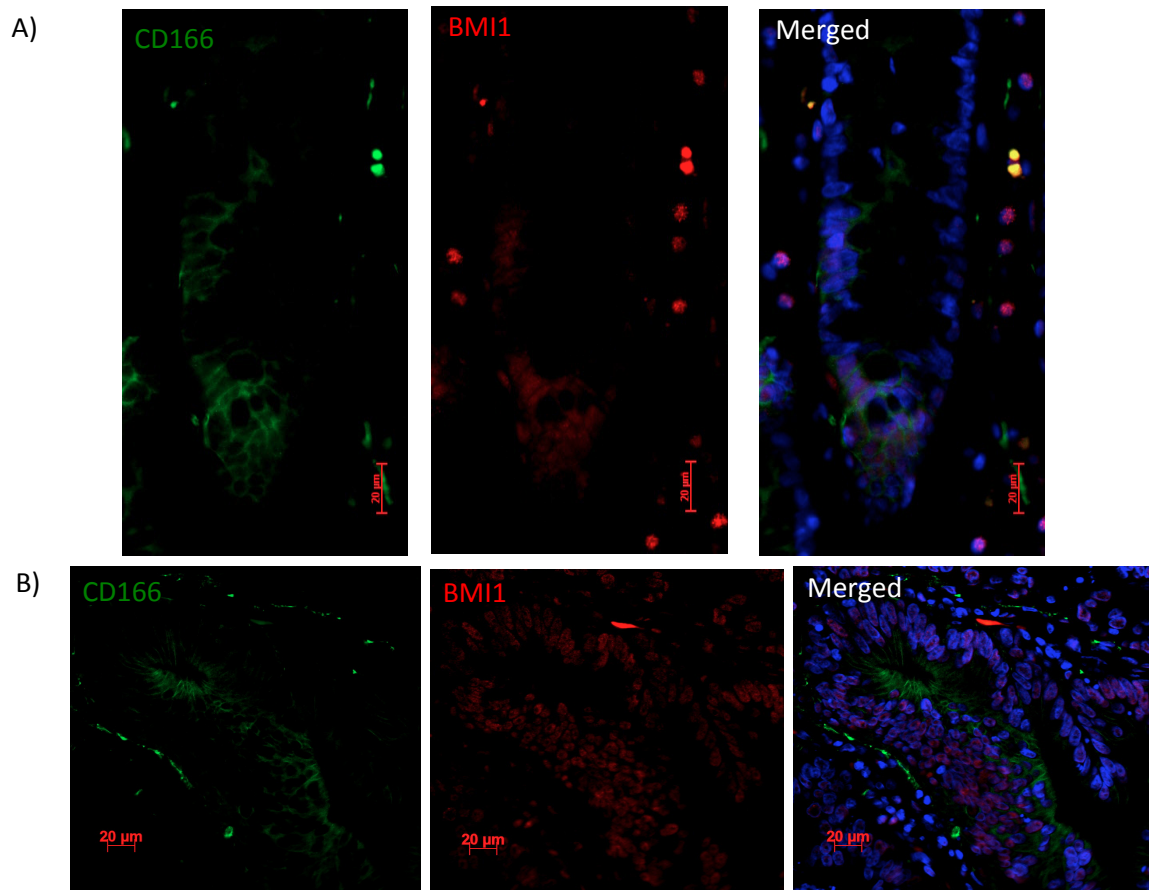


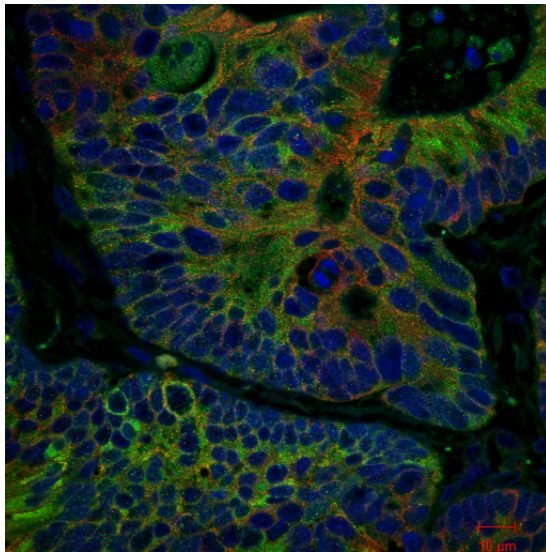
Figure 3.10: Co-staining of CD166 and BMI1 in normal colonic crypt and tumor tissue. CD166 and BMI1 identify co –populations in normal colon crypt (A), but in tumor BMI1 is overexpressed and loses its specificity to mark CSCs. Blue represents nuclei stain. (3 matched normal and tumor sections).

Table 3.3: Summary of expression pattern of different SC markers analyzed by immunofluorescence.

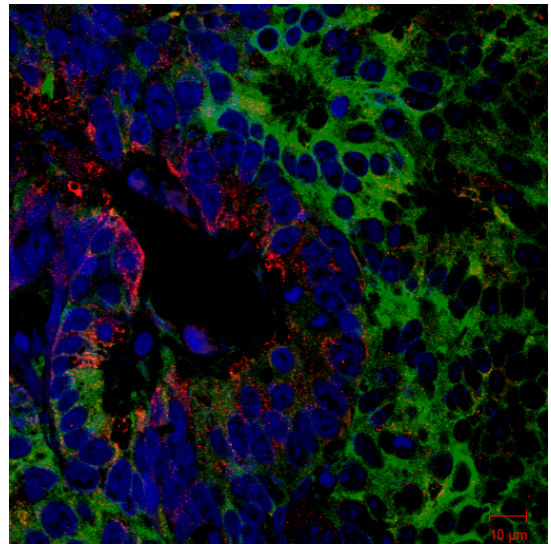
SC marker	Expression in Normal colon crypt	Expression in Tumor
ALDH1	Few cells in the bottom	Small clusters
CD166	1/3 rd of the bottom	Small clusters
LRIG1	Few cells in the bottom	Small clusters, overexpressed, no staining
BMI1	Few cells in the bottom	overexpressed
CD44	1/3 rd of the bottom, few cells at the top	Overexpression, no staining
LGR5	No staining	No staining
OLFM4	No staining	No staining
Telomerase	No staining	No staining

A)

LRIG1/ALDH1 costain



LRIG1/ALDH1 no costain



B)

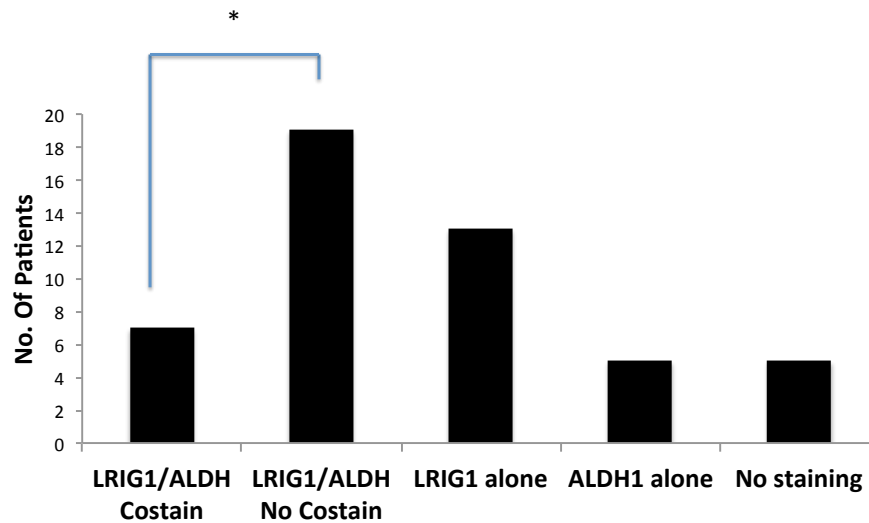
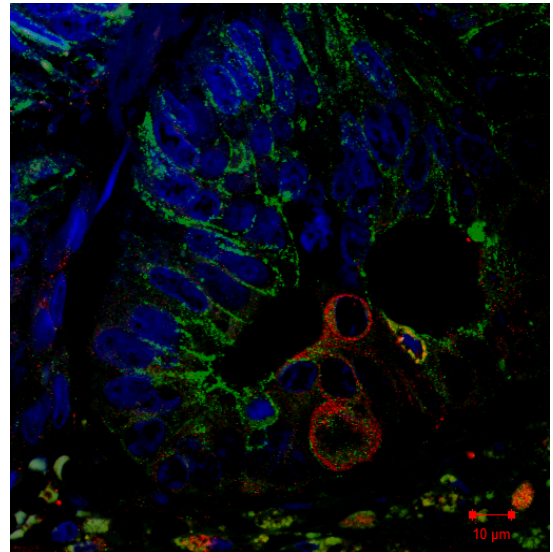
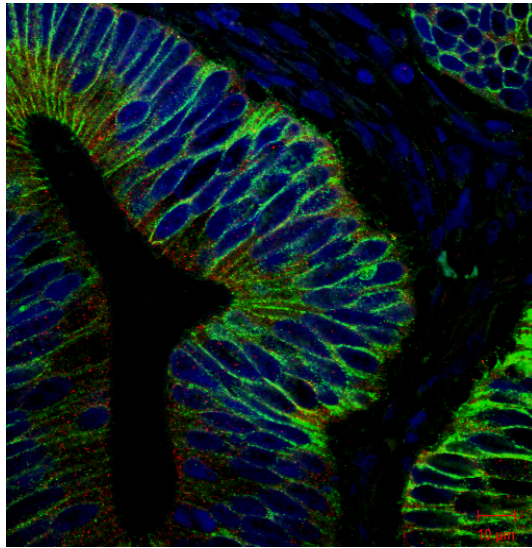


Figure 3.11: Staining patterns of ALDH1 and LRIG1 in colon tumors tissues from 75 patients. A) Immunostaining results shows that ALDH1 (in green) and LRIG1 (in red) either co-stain or do not co-stain cells in tumor. Nuclei stain is represented by the blue color. B) is a graph representing the number of patients with different staining pattern for the two markers ALDH1 and LRIG1. * represents significant p value < 0.05 determined by chi square analysis.

A)

LRIG1/ CD166 costain

LRIG1/ CD166 no costain



B)

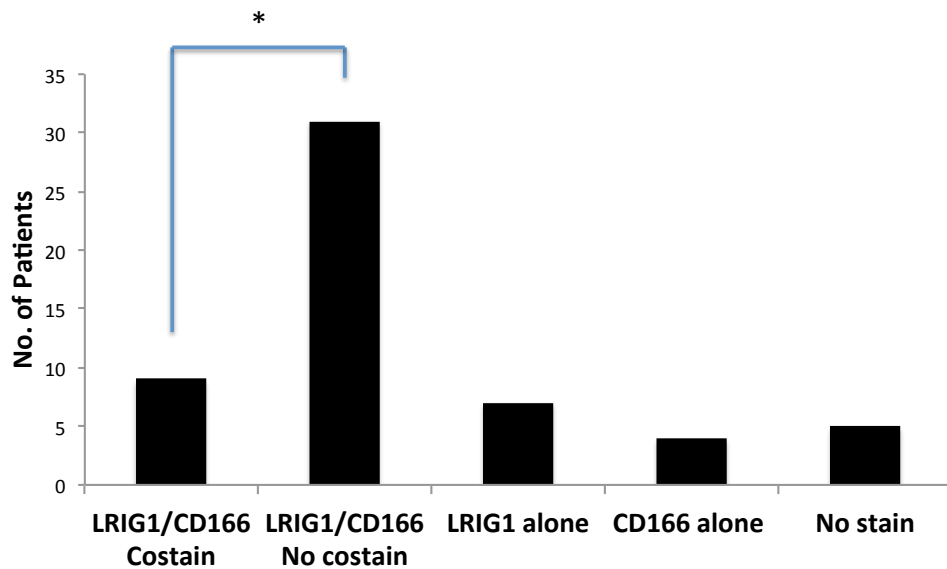


Figure 3.12: Staining pattern of ALDH1 and LRIG1 in colon tumors tissues from 75 patients. A) Immunostaining results show that CD166 and LRIG1 either co-stain or do not co-stain cells in tumor. Nuclei stain is represented by the blue color. B) is a graph representing the number of patients with different staining pattern for the two markers CD166 and LRIG1. * represents significant p value < 0.05 determined by chi square analysis.

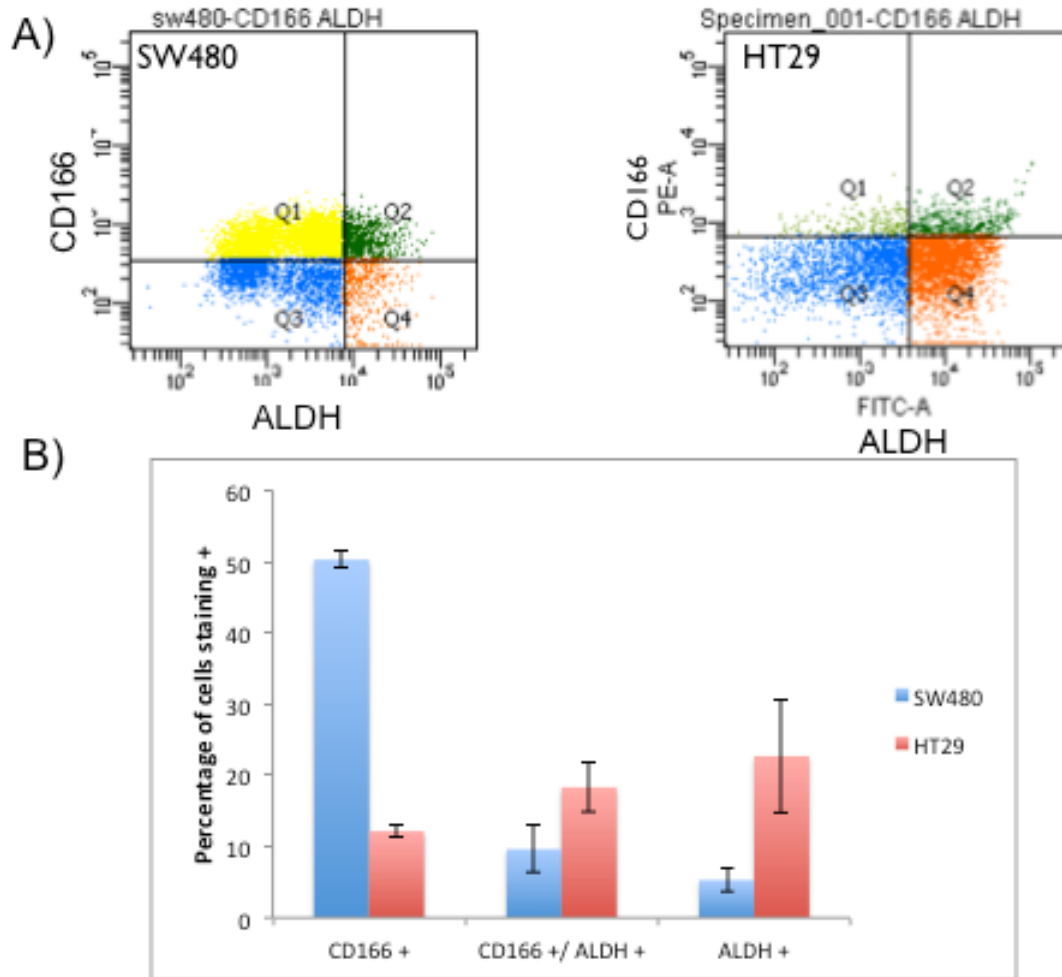
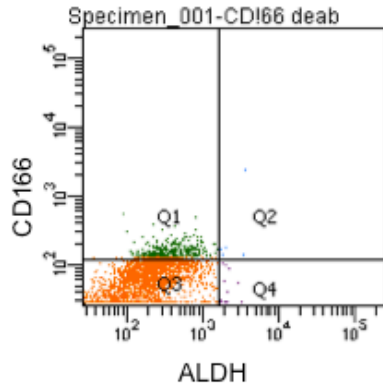


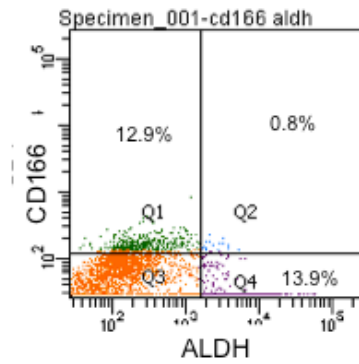
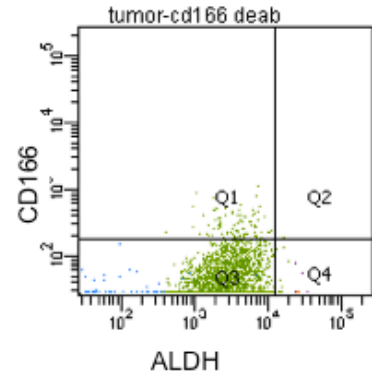
Figure 3.13: FACS analysis of multiple marker expression in colon cancer cell lines. Dot plots showing subpopulations of cells staining positive for ALDEFLUOR and CD166 as seen in the quadrant 2 of scatter plot in the colon cancer cell lines HT29 and SW480 (A). Percentage positive for CD166, ALDH1 and CD166/ALDH1 was quantified and plotted in graph (B). The experiments were performed in triplicate. Error bars represent standard error of the mean.

Normal colonic epithelial cells



Aldefluor
+DEAB

Dissociated tumor cells



Aldefluor

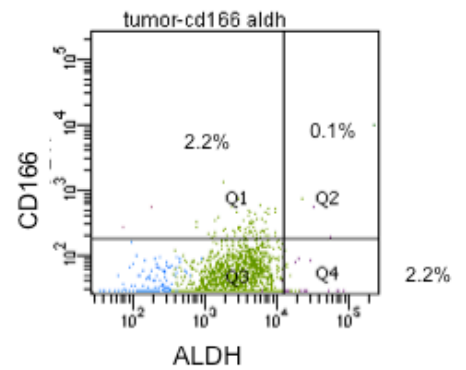


Figure 3.14: FACS analysis of multiple marker expression in colon normal and cancer cells from patients. Dot plots of isolated crypt cell from normal patients and epithelial cells from matched tumor tissues were stained for CD166 and assayed with the ALDEFLUOR assay. Cells in Q2 demonstrated high ALDH activity and CD166 expression. As indicated only a very small percentage of cells were positive for both markers (less than 1%) in tumor as compared to the normal.

3.3.2 Normal and Cancer Stem Cells were Identified and Sorted from Fresh

Tissue Samples:

Single dissociated crypts were obtained after 60 minutes of incubation in EDTA on ice. Cells at the bottom of the crypt, as well as dissociated tumor cells, stained green indicating high ALDH activity as shown in **Figure 3.15 and 3.16**. Cells that co-stained for both ALDEFLUOR and EpCAM were sorted, along with those that were EpCAM positive and ALDEFLUOR negative. ALDEFLUOR positive and negative cells from at least six pairs of matched normal and tumor tissue were sorted successfully (**Figure 3.17**). The percentages positive for different populations are represented in **Table 3.4**. Six pairs of sorted samples were used for isolation of RNA, which were sent for miRNA profiling.

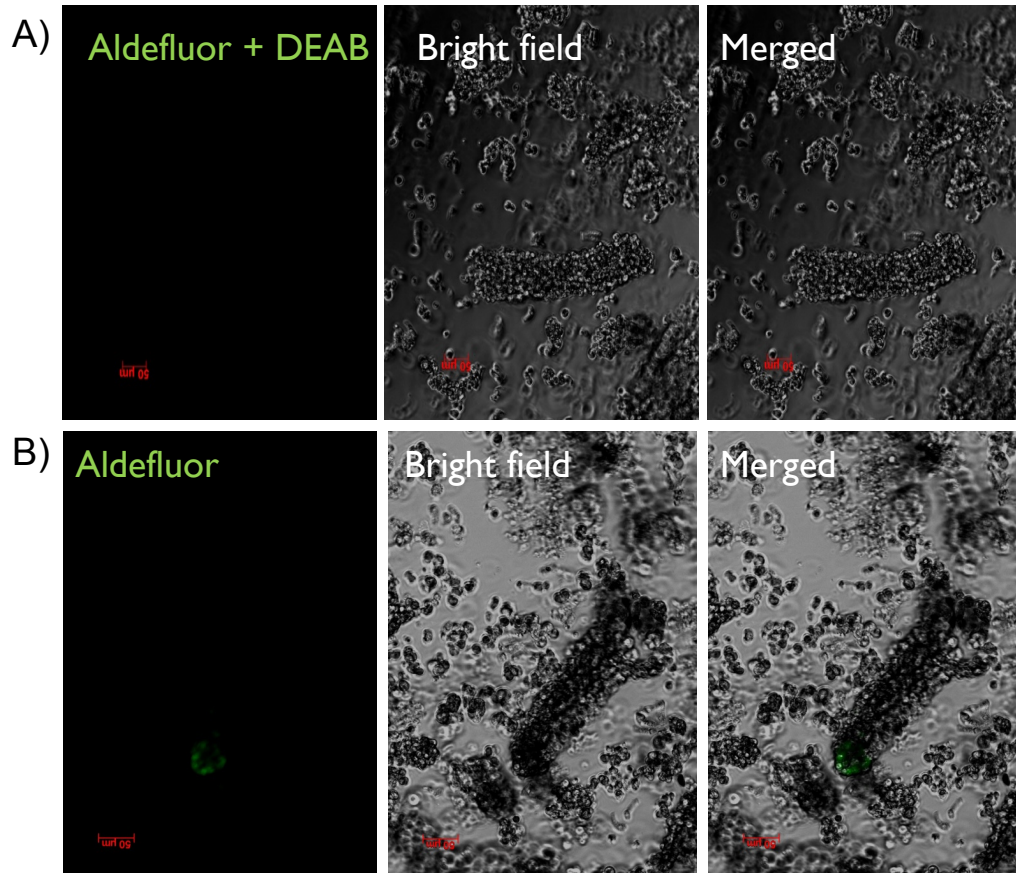


Figure 3.15: ALDH activity in the bottom of fresh normal isolated crypts. Normal isolated colonic crypts subjected to ALDEFLUOR assay in the presence (A) or absence of the inhibitor of ALDH activity (B). This image was taken using a Zeiss Epi-fluorescence microscope using the 10X objective.

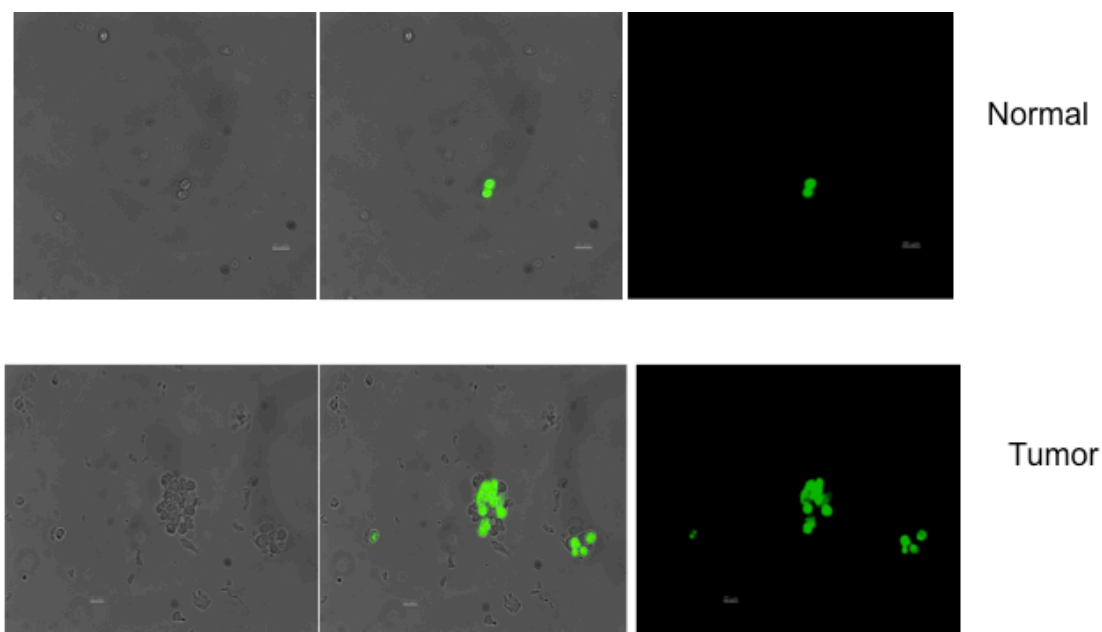


Figure 3.16: ALDH activity in fresh dissociated patient tumor cells. Dissociated cells from fresh normal and tumor tissue show small populations of ALDEFLUOR positive (green) cells. Image was taken using a Zeiss Epi-fluorescence microscope using the 10X objective.

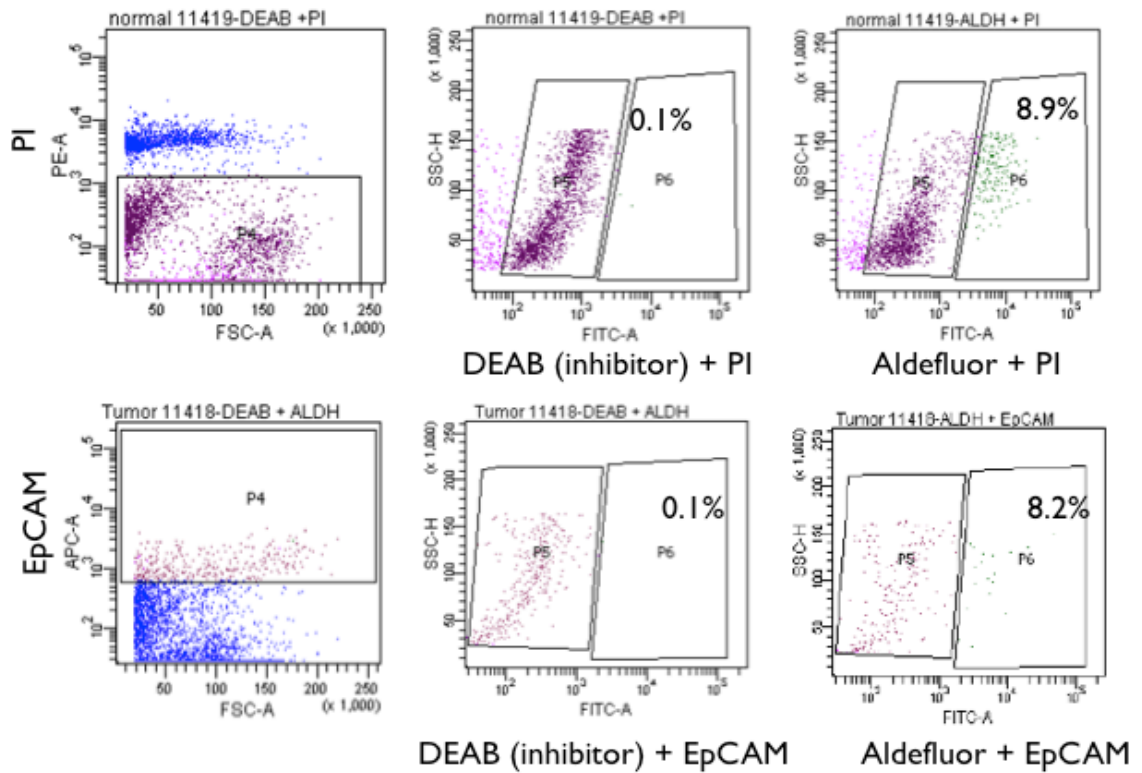


Figure 3.17: Isolation of stem cells from fresh patient normal and tumor samples. Dot plots showing percentages of isolated cells from fresh normal and tumor tissue positive for ALDH activity, when the DEAB control was set to 0.1%. Tumor cells were selected for EpCAM positivity and normal cells negative for Propidium iodide (viable) for ALDEFLUOR assay and sorting.

3.3.3 Cancer Stem Cells have Differential MiRNA Expression Pattern as Compared to the Normal Stem Cells:

MiRNA profiling for three out of six patients were unusable because of degraded or poor RNA quality in the isolated samples. Running samples in the Bioanalyzer assessed the quality of the RNA. The patient samples that yielded high quality samples were analyzed further to identify miRNAs, which were differentially expressed in normal ALDEFLUOR positive cells as compared to the tumor ALDEFLUOR positive cells. The counts were normalized to the mean and the relative fold change was calculated for each miRNA. This was achieved by dividing the normalized count for a microRNA in the ALDEFLUOR positive sample by the count in the ALDEFLUOR negative counterpart. The list of the top 25 miRNAs, which showed differential expression in the normal and cancer stem cells, are represented in **Table 3.5**. The heatmap, which represents each miRNA's relative log fold change from the mean of the sample across all four samples, is shown in **Figure 2.9**. Between the three samples, there were some candidate microRNAs that showed consistent differential expression in the tumor stem cells compared to the normal stem cells.

Table 3.4: List of patients matched normal and tumor colon samples with successful sorting of ALDEFLUOR positive cells.

Patient ID	Normal ALDH +	Tumor ALDH+
11201	4.0%	1.2%
12480	6.0%	1.9%
12457	2.8%	2.4%
12319	1.8%	1.2%
12293	4.2%	1.0%

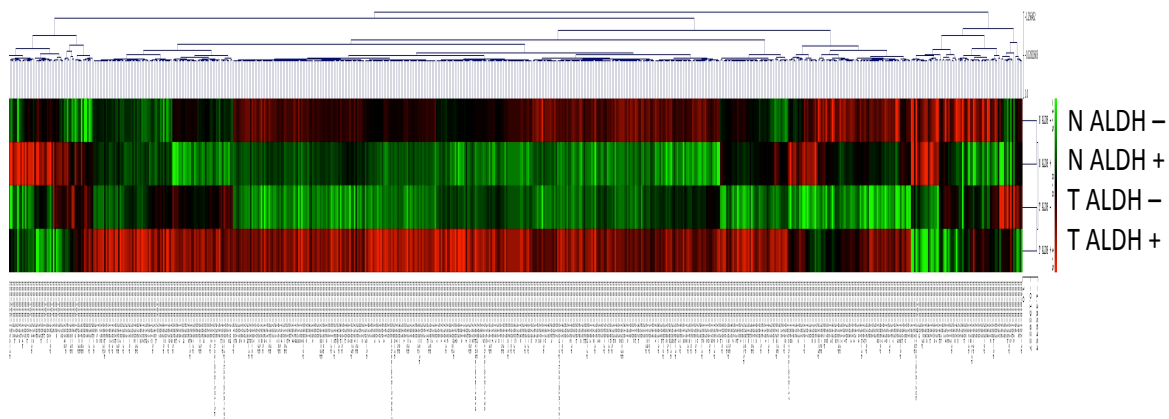


Figure 3.18: Differential expression of microRNAs in normal and tumor ALDEFLUOR positive and negative cells. The heat map represents the normalized log fold change from the mean across the four samples for each miRNA. Red represents up-regulation and green represents down-regulation.

Table 3.5: List of differentially expressed microRNAs in tumor ALDEFLUOR positive compared to normal ALDEFLUOR positive cells from one patient.

Normal patient 1		ALDH+/ALDH-		Tumor Patient 1		ALDH+/ALDH -	
miRNA	upregulated fold change	miRNA	downregulated fold change	miRNA	upregulated fold change	miRNA	down regulated fold change
hsa-miR-544	174.35	hsa-miR-494	-178.67				
hsa-let-7e	10.84	hsa-miR-142-3p	-26.58			hsa-miR-20a+hsa-miR-20b	-55.83
hsa-miR-125a-3p	6.9	hsa-miR-129-3p	-16.24	hsa-miR-1281	8.14	hsa-miR-192	-34.28
hsa-miR-296-5p	5.09	hsa-miR-451	-11.57	hsa-miR-586	7.9	hsa-miR-16	-9.98
hsa-miR-890	4.93	hsa-miR-144	-7.34	hsa-miR-1247	7.37	hsa-miR-1246	-8.04
hsa-miR-1274b	4.75	hsa-miR-337-3p	-6.09	hsa-miR-485-5p	7.37	hsa-miR-451	-6.86
hsa-miR-149	4.43	hsa-miR-549	-6.09	hsa-miR-138	7.02	hsa-miR-15a	-4.75
hsa-miR-602	4.19	hsa-miR-586	-5.41	hsa-miR-342-5p	6.91	hsa-miR-223	-4.65
hsa-miR-1979	4	hsa-miR-603	-5.18	hsa-miR-1179	6.58	hsa-miR-26a	-4.64
hsa-miR-20a+hsa-miR-20b	3.62	hsa-miR-610	-4.87	hsa-miR-1253	6.58	hsa-miR-630	-4.55
hsa-miR-374a	3.26	hsa-miR-622	-4.87	hsa-miR-139-5p	6.58	hsa-miR-1974	-4.48
hsa-miR-26a	3.24	hsa-miR-924	-4.47	hsa-miR-1469	6.58	hsa-miR-21	-4.26
hsa-miR-30c	3.1	hsa-miR-1285	-4.4	hsa-miR-921	6.58	hsa-miR-135b	-3.52
hsa-miR-665	2.96	hsa-miR-520d-3p	-4.4	hsa-miR-509-3-5p	6.14	hsa-miR-29a	-3.52
hsa-miR-887	2.96	hsa-miR-1275	-4.35	hsa-miR-337-3p	5.92	hsa-miR-382	-3.42
hsa-miR-361-5p	2.93	hsa-miR-630	-4.18	hsa-miR-762	5.92	hsa-miR-151-3p	-3.13
hsa-miR-1260	2.77	hsa-miR-133a	-4.06	hsa-miR-671-3p	5.87	hsa-miR-633	-3.12
hsa-miR-1274a	2.75	hsa-miR-153	-4.06	hsa-miR-608	5.79	hsa-miR-2116	-3.04
hsa-miR-203	2.69	hsa-miR-523	-4.06	hsa-miR-636	5.79	hsa-miR-1975	-2.55
hsa-let-7b	2.64	hsa-miR-541	-4.06	hsa-miR-449b	5.7	hsa-miR-30b	-2.46
hsa-miR-146a	2.54	hsa-miR-885-5p	-4.06	hsa-miR-495	5.64	hsa-let-7i	-2.45
hsa-miR-375	2.54	hsa-miR-939	-4.06	hsa-miR-498	5.64	hsa-miR-194	-2.43
hsa-miR-509-5p	2.46	hsa-miR-223	-4	hsa-miR-1228	5.6	hsa-miR-24	-2.32
hsa-miR-532-3p	2.46	hsa-miR-126	-3.98	hsa-miR-202	5.6	hsa-miR-602	-2.28
hsa-miR-543	2.46	hsa-miR-1538	-3.88	hsa-miR-591	5.47	hsa-miR-93	-2.28
				hsa-miR-548m	5.38	hsa-miR-200a	-2.2

3.3.4 MiR92a Show Differential Expression in ALDEFLUOR Positive Cancer Stem Cells and Target LRIG1 Gene:

MiR92a expression was up-regulated in tumor ALDEFLUOR positive cells compared to the normal ALDEFLUOR positive cells of the patient samples tested (**Figure 3.19 A**). To evaluate the role of this miRNA, the expression of miR92a was analyzed in ALDEFLUOR positive and negative populations of the HT29 cell line. I found that miR92a expression is significantly upregulated in the ALDEFLUOR fraction of cells as compared to ALDEFLUOR negative HT29 cells (**Figure 3.19 B**). A proliferation assay was done to assess the effect of this miR on the growth of cancer cells. Results showed that miR92a inhibition significantly reduced proliferation of cancer cells as shown in **Figure 3.19 C**. MiRNA target prediction tools *rna22* and TARGETSCAN revealed that miR92a targets the 3' UTR of the LRIG1 gene. To test this, a luciferase assay was performed that validated that miR92a targets LRIG1 3'UTR (**Figure 3.19 D**). However, manipulating miR92a levels did not have any significant effect on cell cycle, ALDEFLUOR positivity or colonosphere formation.

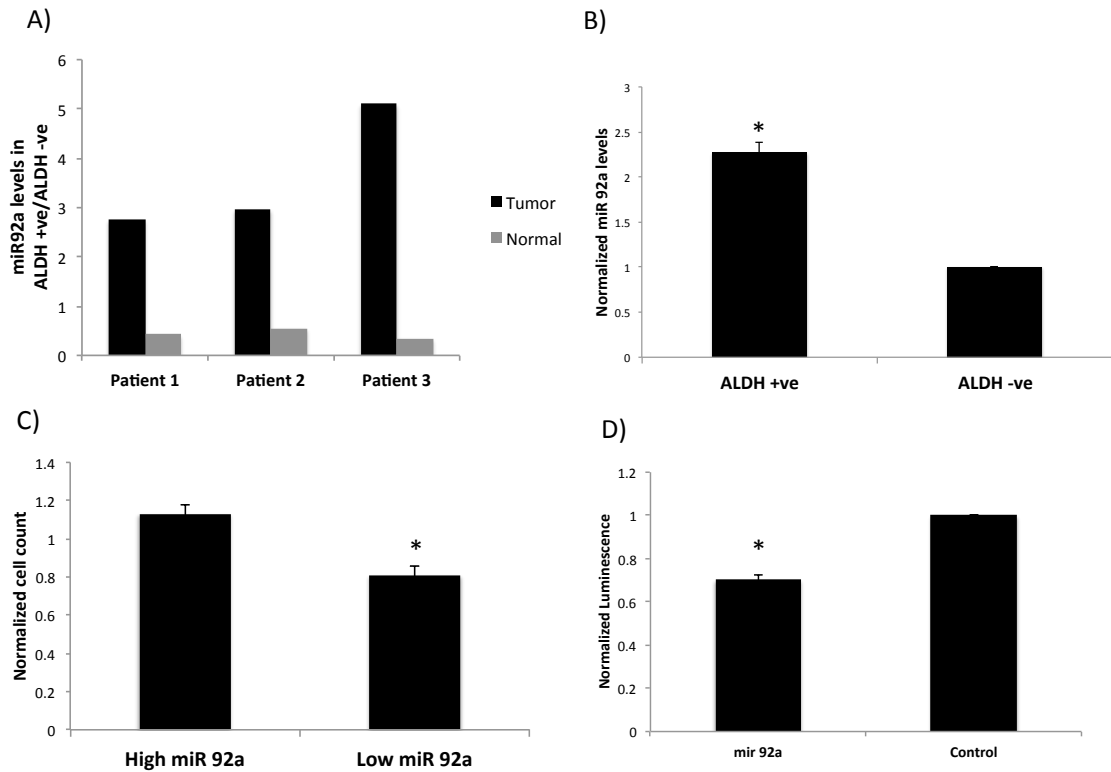


Figure 3.19: MiR92a is overexpressed in ALDEFLUOR positive cells and regulate the LRIG1 gene expression. A) MiR92a expression in tumor and normal ALDEFLUOR positive cells compared to ALDEFLUOR negative cells in patient samples. B) Normalized miRNA 92a expression levels in sorted ALDEFLUOR positive and negative HT29 cells. B) Normalized fold change in cell count of HT29 cells with increased and decreased levels of miR92a. C) Luciferase assay results showed that miR92a targets 3'UTR of LRIG1 gene indicated by the significant decrease in the relative luminescence intensity as compared to the control. Error bars represent standard error of mean and * represents a significant p value < 0.05.

3.4 Discussion:

The elaborate role of candidate miRNAs in regulating colon CSCs function such as maintenance of self-renewal ability and tumor initiation, are yet to be studied. To address this problem, I hypothesized that specific miRNAs are differentially expressed in colon CSCs as compared to normal SCs. Performing miRNA profiling of SCs and non-SCs from both normal and cancer tissue tested the hypothesis. Various investigators have identified different cancer stem cell markers, which aid in the isolation of cancer stem cells from rest of the tumor population. Our lab established ALDH1 as a stem cell marker, which has been used to trace the overpopulation of stem cells as we progress from normal, FAP, adenoma to carcinoma [28]. The ability to isolate cancer stem cells from colon tumors based on high ALDH activity has enabled us to work and manipulate them. ALDEFLUOR positive cells alone are capable of giving rise to tumors when introduced in the flanks of NOD-SCID mice, which is an indication of their tumor initiation capability. Other proteins such as CD166, LRIG1, LGR5 and BMI1 also were established as cancer stem cell markers for colon tumors. The existence of multiple markers raises the question whether they identify the same cells in the tumor or do they enrich the proportion of 'stem' cells when used together for isolation. Immunofluorescence co-staining studies demonstrated that stem cell markers do identify common population of cells in the bottom of the normal colonic crypt. However, in tumor, it was identified for the first time that different stem cell markers mark different population of cells. My co-staining results from the TMA study established that three cancer stem cell markers ALDH1, LRIG1 and CD166 preferentially identify different population of cells. These results were confirmed for ALDH1 and CD166 using fresh isolated patient normal and tumor samples as well. These novel findings are suggestive of subpopulations of CSCs, with

varying ability to self-renew and generate tumors. This has not been reported before, but reports have provided evidences supporting my hypothesis. One study showed that BMI positive cells in the colon are relatively quiescent and maintain the reserve ‘pool’ of stem cells. These cells are responsible for giving rise to LGR5 positive stem cells in the colon of mice, which are more rapidly cycling [107]. Even the LGR5 positive cells inter-convert to LGR5 negative cells in response to irinotecan drug treatment and these LGR5 negative cells still possess tumor initiating ability [108]. Another independent study suggested that LGR5 positive cells have an exclusive gene expression as compared to the LRIG1 positive cells.[140]. These reports are in coherence with my results indicative of an existence of sub-populations within cancer stem cells of the tumor. Such architecture in the tumor-initiating compartment presents a bigger challenge for the development of targets against CSCs to eradicate cancer. Further studies are required to elaborate the exact role of different SC markers in tumor cells and how they contribute towards providing stemness to the bulk of the population.

Our lab has established ALDH1 as a successful marker for the identification and isolation of stem cells from fresh normal and tumor tissue from patients [28]. The discrepancies in the expression pattern of other stem cell markers LRIG1, CD166 and BMI1 tested bolstered the idea of choosing ALDH1 for further analysis. MicroRNA profiling of the sorted ALDEFLUOR positive and negative samples from normal and tumor tissue of multiple patients identified differential microRNA expression in tumor ALDEFLUOR positive compared to normal ALDEFLUOR positive cells. This study is the first to report distinct microRNAs signature patterns in colon cancer stem cells isolated from patients. MicroRNA signatures have already been indicated in cancer

stem cells of the breast where they identified miR200c to be an important regulator of self-renewal [95]. MicroRNAs such as miR93, miR200abc and miR92a, that have already been reported to be associated with tumor initiating cells, also were identified in our study. MiR92a was one such candidate, which showed differential expression in tumor stem cells from patients. It belongs to the well-studied oncomirs cluster miR-17-92 and is overexpressed in medulloblastoma [154] and hepatocellular cancer [155]. It plays a role in gastric cancer stem cells [156] and for the first time it has been shown to be differentially expressed in the cancer stem cells of the colon. The expression of miR92a was found to be upregulated in the ALDH high cells of HT29 colon cancer cells, suggestive of its possible role in these cancer stem cells. Manipulating levels of miR92a decreased growth of colon cancer cells but had no effect on colonospheres formation ability or cell cycle distribution. Colonosphere formation assay provides an index of self-renewal under low attachment conditions. Kanwar *et al.*, demonstrated for the first time using this method, that enriched CSCs have the ability to give rise to colonospheres in culture [157]. The observed effect of miR92a on the ability of the HT29 CSCs to self-renew cannot be limited to one cell line tested, and have to be tested using other colon cancer cell lines such as SW480 and LOVO. On the other hand, the effect of miR92a on cell cycle and apoptosis has been studied before in a leukemic cell line, where they promoted cell death by inducing apoptosis via its inhibition [158]. More work has to be done to discern the mechanisms by which miR92a potentially regulates cancer stem cell phenotype in colon cancer. Future investigations pertaining to the function of miR 92a in the stem cell compartment might unravel new mechanisms of regulating self-renewal function of cancer stem cells and impacting tumor initiation and maintenance.

Chapter 4

DISCUSSION

Since the first microRNA profile of breast CSCs, there have been multiple reports with similar results [95]. However, in studying colon CSCs, all the reports of aberrant miRNA expression come from analysis of cell lines, which have been enriched in CSCs using anchorage independent growth assays or involved in isolation of CSCs using specific markers [80, 82, 159]. There have been no reports yet about miRNA expression profiling of colon CSCs derived from patient samples. I hypothesized that there is a distinct miRNA signature, which defines the SCs in the normal colon, and aberrant expression of miRNAs in CSCs leads to disruption of self-renewal function contributing to colon tumorigenesis. I had three main objectives to address my hypothesis: i) to identify SC markers for isolation of CSC and normal SC from fresh colon tissue ii) to do miRNA profiling to identify differentially expressed miRs in CSCs as compared to normal SCs and iii) to investigate the effect of manipulation of candidate miRs on cancer stem cell phenotype *in vitro* and *in vivo*.

MicroRNAs have been associated with an array of cell functions such as proliferation, differentiation, self-renewal and apoptosis [160-162]. Specific microRNAs are differentially expressed in cancer tissues compared to the normal counterpart belonging to wide variety of tissues [44, 47, 49]. Over the last two decades, the cancer stem cell (CSC) theory has emerged as a mechanism that explains the development and maintenance of cancer. Unlike the ‘stochastic’ or random theory, the CSC theory states that the cells in the tumor are maintained by a small group of

cells called the cancer ‘stem’ cells or cancer ‘initiating’ cells. It was first described in leukemia and then extended to solid tumors as well [22]. Over the years, this theory provided more and more evidence, explaining the mechanisms by which tumors arise from breast, prostate, gliomas, ovarian and also colon [23-25, 28]. For colon cancer, specifically, our lab provided some of the first evidence supporting this theory with the help of a mathematical model. The model suggested that overpopulation of the stem cell compartment at the base of the colonic crypt initiates colon cancer [27]. This model was strengthened by reports stating that as the transition happens from normal to FAP to adenomatous crypts, the number of SCs (marked by ALDH1) progressively increases [28]. ALDH1, or Aldehyde dehydrogenase, plays an important role in cell differentiation by converting retinol to retinoic acid in the cell [33]. It has been established as a successful marker for isolation of normal and tumor SCs based on ALDH activity using an assay called ALDEFLUOR. My results showed that ALDEFLUOR positive cells exist in a small proportion in both colon cancer cell lines as well as in cells from fresh tumor and normal tissue of patients. This assay has aided in the isolation of viable SCs using flow cytometry, which can be used for a number of downstream applications.

Our lab developed an innovative way to look at distinct miRNA expression patterns in the stem cell compartment of normal colonic crypts. Performing microdissection of the bottom 1/10th of the colonic crypt enables us to look at the microRNA signatures of the stem cell enriched region compared to the rest of the crypt. Preliminary miRNA profiling studies on normal colonic crypt subsections helped us to identify key miRNAs candidates that are differentially expressed in the stem cell enriched region. One of the candidates identified, miR23b, was significantly

downregulated in the crypt bottom compared to rest of the crypt. Mir23b has been studied in a variety of cancers and has been reported to act both as a tumor suppressor, as well as an oncogene [85, 86, 92, 93, 96, 163]. For colon cancer, reports suggest that miR23b is downregulated in tumors compared to normal [85]. In colon CSCs from the cancer cell lines HT29 and SW480, this miR was overexpressed. Differential expression of miR23b in CSCs compared to normal SCs suggested a possible role of miR23b in colon tumorigenesis. Perturbing miR23b levels changed the proportion of ALDEFLUOR positive cells in colon cancer cell lines, which was also reported for ALDEFLUOR positive cells from ovarian cancer. The transient and stable manipulation of miR23b levels affected proliferation rates because miR23b expression promoted accumulation of cells in the G0/G1 phase of the cell cycle. These findings were consistent with reports showing an effect of miR23b on cell cycle [89, 96, 97, 99]. Nonetheless, I speculated that an increase in the quiescent ALDH high stem cell fraction due to increased miR23b was probably due to its effect on cell cycle mechanisms. Other properties associated with CSCs are increases EMT and self-renewal. EMT enables the cancer cells to leave their microenvironment, enter the circulation and invade nearby lymph nodes and tissues. Published reports suggested that circulating CSCs in the blood stream are responsible for metastasizes- a mechanism that gives rise to secondary tumors [164]. Wicha and his colleagues reported that breast CSCs possess plasticity to interconvert between EMT and MET characteristics [165]. In addition, increased expression of EMT markers, such as Snail and Twist, increases the mammosphere formation of breast CSC [98]. Based on the results of miR23b on the ALDH high subpopulation of cells, I hypothesized that miR23b might promote stemness by increasing EMT characteristics in colon cancer

cells. Looking at the expression of common EMT markers, E-Cadherin and Vimentin, after manipulating miR23b levels, validated this hypothesis. The increase in EMT due to high miR23b levels also correlates with the known increased invasive properties of cancer cells.

Self-renewal is the mechanism by which SCs divide asymmetrically or symmetrically to give rise to more SCs, thus maintaining the SCs pool in the tissue [166]. Assays, such as the colonosphere formation assay, allows us to determine an index of the ability of CSCs to self-renew under low attachment conditions [157]. ALDEFLUOR positive cells from multiple tumor tissues have already been reported to generate larger spheres in such conditions as compared to the ALDEFLUOR negative cells [167, 168]. High miR23b levels increased the proportion of ALDEFLUOR positive cells and also increased their self-renewal as indicated by the increased formation of colonospheres. This is one of the first reports indicating possible role of miR23b in regulating self-renewal of colon CSCs. These findings in-turn open new avenues for investigating the underlying mechanisms by which miR23b is involved in self-renewal pathways. Multiple key signaling pathways such as WNT, TGF-beta, PI3K/AKT, Hedgehog and NOTCH are responsible for maintenance of self-renewal of SCs. Proteins belonging to these pathways such as NOTCH1, PTEN, TGFbetaR2, AKT and FZD7 have already been reported to be functional targets of miR23b, indicating its strong position in regulating in CSCs pathways [85, 93, 169].

Resistance to chemotherapy is one of the hallmarks of CSCs. There are different ways by which a CSC can resist the action of an anticancer drug. High ALDH activity in CSCs can convert the toxic aldehyde-based drugs to alcohol. Also, high expressions of multidrug resistance genes belonging to the ABC family of

proteins can efflux the drug out of the CSCs. Some drugs tend to target proliferating tumor cells, leaving behind the relatively quiescent CSCs, which leads to tumor recurrence. MiRNAs have been implicated as playing a role in chemoresistance as well. For example, miR451 was shown to be downregulated in colon spheres and it was predicted to target ABCB1 (MDR gene). Ectopic expression of miR451 made the cancer cells more sensitive to irinotecan treatment [170]. Similarly, another group of investigators identified that miR328 targets ABCG2 and increased mitoxantrone sensitivity in breast cancer cells [171]. Likewise, my results showed that miR23b expression is important for sensitivity to the anticancer drug 5-fluoro-uracil. An increase in miR23b levels increased the sensitivity to the drug by decreasing expression of its target LGR5. LGR5 expression has been reported to correlate with response in colon cancer patients to the 5-FU [103]. LGR5 functions to enhance Wnt signaling, which leads to the downstream expression of Myc that can repress miR23b expression [172]. This is suggestive of a negative regulatory mechanism that is responsible for maintaining the LGR5 positive cell population in colon cancer cells. LGR5 positive SCs are regarded as cycling SCs, which is a population exclusive from the slow cycling ALDH positive SCs. These findings, together with my immunostaining profiling data, strengthens that there exists a hierarchy of stemness in tumor CSCs. This makes it more challenging to target multiple populations of SCs with a single anti-cancer agent. MiR23b could potentially be used in the form of an adjuvant therapy with 5-FU to increase sensitivity to the drug and deplete the number of cycling SCs. Still, there is a need to decipher ways to target the quiescent SCs that are capable of giving rise to tumors. BMI1 is important for self-renewal and has recently been shown to be crucial for the function of colon CSCs that are slow cycling

[147]. This is consistent with the concept that drugs have to be developed against multiple SC markers and have to be used simultaneously to completely eradicate the source of tumor growth.

LGR5 is one of the gene targets influenced by miR23b. MiR23b also influences the expression of a number of targets implicated in various forms of cancer (Table 4.1). This implies that miR23b operates on multiple signaling pathways simultaneously which can be represented in Figure 4.1. To identify novel gene targets affected by altered miR23b expression, we conducted an RNA-SEQ analysis. We identified novel gene targets such as *AKT2*, *ATF2*, *ATF3* that appear to be regulated by miR23b levels and these targets have also been reported to be involved in self-renewal pathways [173]. For example, ATF2 is one of proteins that play a role in the downstream activation of the Wnt signaling pathway without the involvement of beta catenin [174]. ATF3, on the other hand, enhances stem cell properties of breast cancer initiating cells [175]. A similar study reported a RNA-SEQ analysis for breast cancer cells where they identified multiple genes involved in cytoskeleton function that were altered by miR23b levels. The pitfall of this latter study was the fact they compared data from two different breast cancer cell lines to identify differentially expressed genes [91].

Table 4.1: miR23b expression and its targets in cancer. This table represents the change in expression levels of miRNA 23b in various human malignancies compared to normal tissue. The list of candidate genes, which are differentially expressed in such malignancies, are functional targets of miR23b.

Cancer type	Level of miR 23b compared to normal	Functional target of miR 23b
Uterine	Upregulated	---
Prostate	Downregulated	Peroxiredoxin III, Src Kinase, Akt, PTEN, ATG12
Breast	Upregulated	Nischarin, PAK2, ANXA2, ARHGEF6, CFL2, LIMK2, PIK3R3 and PLAU
Gliomas	Upregulated/Downregulated	VHL, Pyk2
Colon	Downregulated	FZD7, MAP3K1, PAK2, TGFbR2, uPA
Renal	Upregulated	PTEN
Bladder	Downregulated	ZEB1
Cervical	Downregulated	uPA
Liver	Downregulated	uPA, c-met
Melanoma	Upregulated/Downregulated	MITF

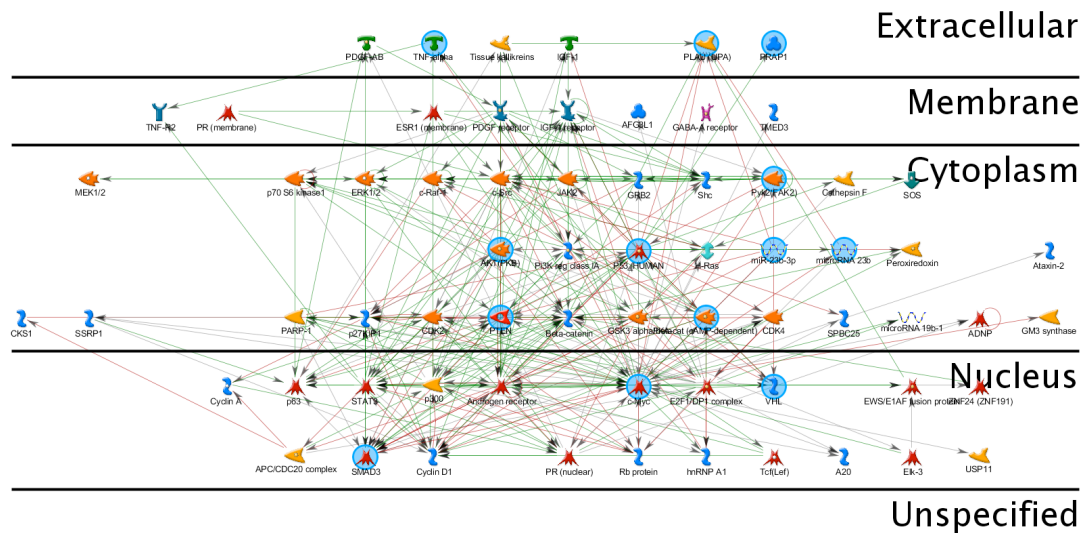


Figure 4.1: Network map of miR23b and its targets. This network map was generated using the tool MetaCORE by choosing miR23b and some of its validated targets such as SMAD3, MYC, and SRC as primary nodes. The network shown in the diagram is a representation of the magnitude of direct and indirect effects of the activity of miR23b. MiR23b directly binds to and inhibits the translation of some mRNA molecules (represented by red arrows). The mRNA targets, in turn, positively or negatively regulate the expression or activation of a range of molecules ranging from transcription factors, membrane receptors and their ligands and cytosolic enzymes involved in key signaling pathways (represented by red and green arrows).

The newly identified role of miR23b in colon CSCs shown by our *in vitro* studies sheds some light on the requisite to identify miRs that plays a vital role in colon CSCs derived from patient samples. To address this need, requires a tool that can be employed to effectively isolate and characterize CSCs from patient samples. The ALDEFLUOR assay, as discussed previously, is based on ALDH1 activity and is a widely accepted technique to serve this purpose, but it raises a few concerns. There are reports suggesting that ALDH1A1 (stem cell marker) is not the only isoform responsible for the ALDH activity in the ALDEFLUOR assay. ALDH has 19 isoforms in humans and investigators have identified other isoforms that contribute to ALDEFLUOR activity in cancer cells. For example, Levi et al identified ALDH2, ALDH3A1 and ALDH9A1 isoforms as contributing to ALDEFLUOR activity in hematopoietic cells with ALDH1A1 deficiency [176]. In prostate cancer cell, ALDH activity in this assay was predominantly due to the ALDH7A1 isoform [37]. In multiple cancers, studies have identified ALDH3B1 and ALDH1B1 to be expressed higher than ALDH1A1 [177, 178]. These findings, in addition to the existence of other stem cell markers for colon SCs, requires further study, which looks at their expression in both normal and tumor tissue of the colon.

Markers such as ABCG2, CD166, LRIG1, LGR5 and BMI1 have been reported as reliable stem cell markers for the colon. However, there have been no studies, which have looked at their co-expression in normal and colon tumor tissues. My immunostaining results for all markers indicated that expression of these markers was restricted to the bottom of the cells except ABCG2 that tends to stain the middle part of the colonic crypt, which constitutes the proliferative cells. There have been similar reports where ABCG2 expression was restricted to the proliferative cells and

not the stem cells [179]. LGR5 protein, due to its native structure (G-protein coupled receptor) and minimal extra protein domains not embedded in the membrane, has proven to be difficult for antibody generation. Multiple antibodies were tested in my study, but all failed to show any positive staining in normal, as well colonic tumor tissue. The co-expression of stem cell markers ALDH1, LRIG1 and CD166 in multiple patients (N=75) identified a novel expression pattern whereby they all tend to stain different cells in tumor. This is a very important finding because it suggests the existence of a hierarchy of stemness within the colon tumor population. For markers such as LRIG1 and LGR5, Powell *et al.*, stated that there are two different populations in normal colon tissue, which supports my findings [140]. For CD166, it is already known that a large number of cells are stained in the normal colonic crypt and I found that ALDH1 positive cells form a subset of CD166 positive cells. CD166 stains the neuroendocrine cells in the normal crypt too, which are partially differentiated [129]. LRIG1 is a well-studied marker in mice and has been shown to identify slow-cycling cells in the mouse colonic epithelium. Reports of tissue microarray analysis, which were done on 100 cancer patient samples, showed that LRIG1 had variable expression in colon cancer cases [140]. Similarly, my tissue microarray data suggested that LRIG1 expression varied from strong to moderate to no expression in the cancer tissues. These results are in agreement with the previous study, as same antibody against LRIG1 was used in both microarray analyses.

The expression profile analysis of colon stem cell markers revealed that stem cell markers also exist in different subpopulation of tumor cells, making it difficult to select the right combination of markers to isolate SCs. There have been conflicting reports about the authenticity of markers to enrich for CSCs. For example, one group

showed that both CD133 positive and negative cells in colon cancer cells from tissues possess tumor-initiating ability [30]. Recently, John Dick *et al.*, in their elegant study of targeting self-renewal in colon CSCs, suggested that different cancer stem cell markers such as CD44, CD29 and CD133 do not enrich for CSCs [148]. However, they did not look at ALDH activity as a marker for stemness in their study. ALDH or ALDEFLUOR positive cells have proven to be very successful for studying CSCs in breast, prostate, ovaries and colon [32]. Our lab was part of the investigation where ALDEFLUOR positive cells from patients were identified as possessing tumor - initiating abilities in NOD-SCID mice. The success of high ALDH activity as a marker for colon CSCs in our previous studies, reinforced by the fact that multiple markers tend to identify different subpopulation of cells, led me to choose the ALDEFLUOR assay for the isolation of normal and CSCs.

We were successful in sorting of ALDEFLUOR positive and negative cells from both fresh normal and tumor cells of patients, but also faced some pitfalls. Most of the time, the availability of the adequate size tumor with a matched normal tissue posed a problem for successful isolation of SCs. There were cases where tumor tissues presented with a necrotic center, which resulted in limited number of viable cells. Successful isolation of cells, achieved by good protocol for efficient RNA isolation, is mandatory. The quality, amount and concentration of the RNAs, particularly for the small RNA species, are crucial for miRNA profiling studies. The estimation of quality and concentration could be made by the absorbance ratio or by running it in the Bioanalyzer. Out of the six pairs of samples sent for profiling, only two of them had high quality RNA and yielded usable results. The absorbance values used for calculating RNA concentration could be a false read-out, as small levels of phenol in

the RNA collected could interfere with the readings. Nevertheless, the miRNA profile from three pairs of patient samples gave us promising results. There were miRNAs who showed a differential expression in ALDH positive cells of the tumor compared to the ALDH positive cells of matching normal tissue. These findings bolstered our hypothesis, that there is a dysregulation of expression of miRNAs, which results in conversion of normal SCs to tumor SCs. Our profiling results identified members of the mir-200 family members, which have also been reported in breast CSCs by Wicha *et al.*, [95]. Let-7 family members were also differentially expressed in tumor ALDH positive cells. Let-7 was one of the first miRs identified to play a role in breast cancer initiating cells. It was downregulated in breast CSCs and induction of let-7 expression inhibited their self-renewal [77]. MiRNA93 was another interesting candidate, which was downregulated in tumor SCs compared to normal SCs in my study. MiR93 expression is significantly decreased in colon tumors compared to the normal counterpart and has been associated with stage and outcome of the disease [180]. Increased expression of miR93 in breast cancer cells induced MET (reverse of EMT), downregulated multiple stem cell associated genes and depleted CSC populations [181]. Also, in the colon cancer cell line SW116, miR93 was found to be downregulated and when upregulated, was shown to suppress proliferation and colony formation [82]. This suggests a need to perform future functional studies to identify and elucidate the exact role of miR93 in colon CSCs. In the future, more extensive profiling studies with high quality RNA isolated from patients are pre-requisites for the successful identification of miRs that are differentially expressed in the colon CSCs.

We identified that MiR92a and miR20a are differentially expressed in the patient-derived CSCs. Both the miRs are a part of the oncogenic miR 17-92 cluster, which is upregulated in various forms of cancers such as medulloblastoma and gastric cancer [155, 156]. MiR20a was recently identified as to be overexpressed in prostate cancer and to be involved in metastasis and invasion [182]. However, my data suggested that only miR92a was differentially expressed in the ALDELFUOR high cells in colon cancer cell lines, suggesting that long passaged immortalized cell lines do not always give results that replicate what is found in patient-derived tumors. This challenge can be met by studying the expression of miRNAs in cells from patient-derived xenografts. I decided to pursue miR92a and found that increasing levels of miR92a promoted proliferation of cancer cells in vitro. This observation has been reported for glioblastomas and lymphoma models in which miR92a was found to have anti-apoptotic activity via inhibition of the pro-apoptotic protein BIM, and inhibition of miR92a can lead to the induction of cell death [183, 184]. Nonetheless, I found that manipulating miR92a levels had no effect on the colonosphere formation of colon cancer cells, suggesting that it might not play a role in their self-renewal. These findings can be explained based on the tissue specific origin of cancer, as there have been reports of the role of members of this cluster in maintaining self-renewal of gastric CSCs by modulating levels of inhibitors of the Wnt signaling pathway [156]. The function of miR92a in colon cancer ALDH high SCs is not very well understood, but my luciferase studies identified that it targets *LRIG1* mRNA. *LRIG1*, as stated above, is a colon stem cell marker and a tumor suppressor gene, which is involved in the inhibition of EGFR signaling. In concordance with my immunofluorescence study of the expression of CSC markers, increasing levels of miR92a can curb the tumor

suppressive role of LRIG1 in the ALDEFLUOR positive stem cell population. More functional studies are required to assess the various possibilities by which miR92a might be important for the function of the ALDH high fraction of colon CSCs.

Overall, my results provides evidence supporting the hypothesis that miRNAs are differentially expressed in colon CSCs and they play a role in regulating their self-renewal and represented in **Figure 4.2**. The hierarchy of stemness, represented by the expression of different SC markers (ALDH1, LRIG1, CD166 and LGR5) within colon tumor tissue, imposes new challenges related to which stem cell marker may to be used to characterize colon CSCs. MicroRNA expression profile across the population of CSCs marked by various markers might be characteristic and unique to that population as compared to the Normal stem cells. MicroRNAs, which are down-regulated are basically involved in regulating proliferation and self-renewal via targeting protein such as Wnt, LGR5 and BMI1. On the other hand, increased expression of miRNAs that inhibit cell death or differentiation will promote tumorigenesis as well. Thus, the differential expression of candidate miRNAs contributes to CSC phenotype in colon cancer. With the example of miR23b in my study, these candidate miRs can be also targeted using RNAi approaches, which ultimately results in suppression of tumor growth. The question that remains to be answered is which miRNAs have a primary role in regulating SC function. More studies have to be done to pursue this goal, with the underlying motive to develop new therapeutic intervention for treatment of colorectal cancer

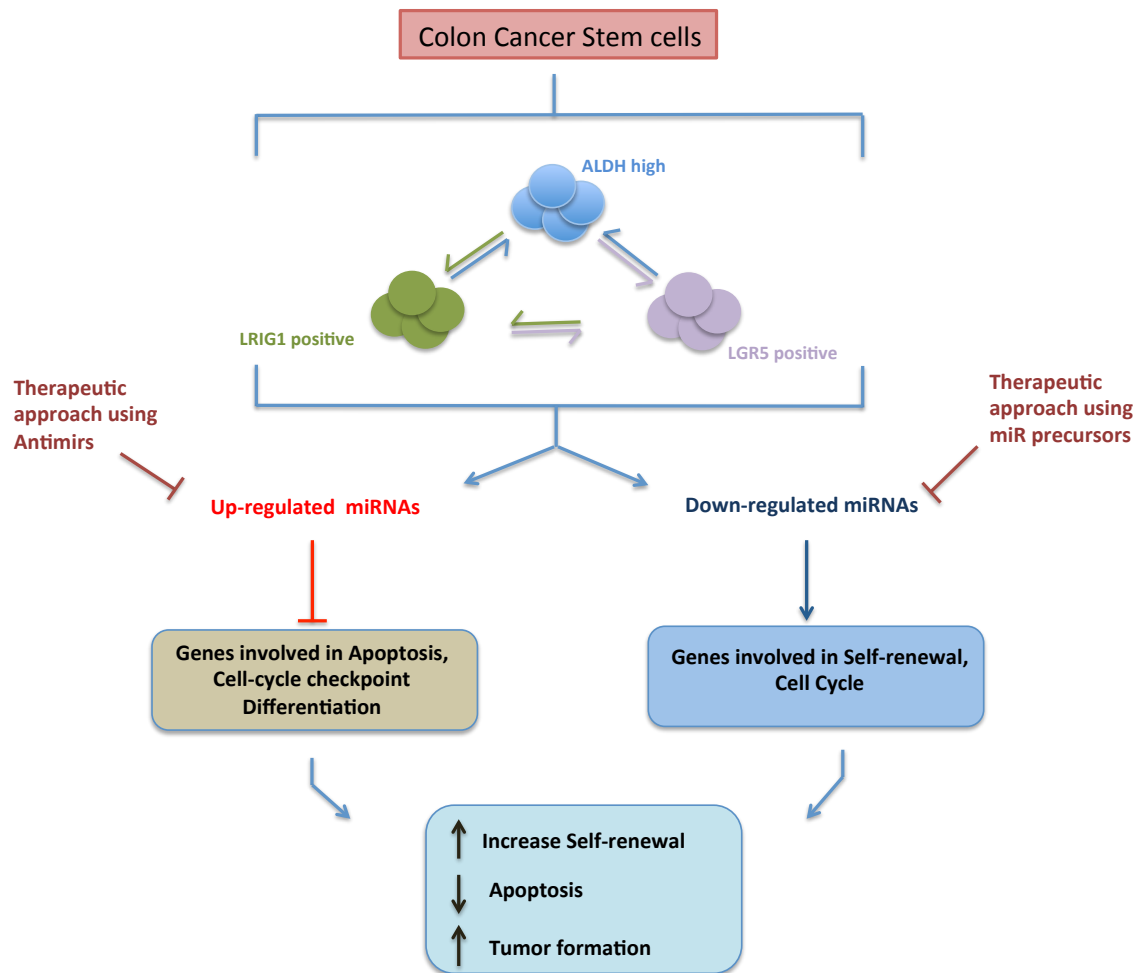


Figure 4.2: Role of microRNAs in colon cancer stem cells. The model represented above depicts the importance of miRNAs in regulating CSC function in colon cancer. Different populations of CSCs co-exist and regulate each other within the tumor population. The CSCs also have characteristic differential expression of miRs, which influence multiple signaling pathways effecting self-renewal, proliferation and apoptosis. These candidate miRs identified to be crucial for the CSC phenotype can serve as important targets for therapeutic intervention to curb tumor growth.

Chapter 5

FUTURE WORK

Our data supported the hypothesis that MiRs are differentially expressed in colon CSCs as compared to the normal SCs located at the base of the crypt. MiRNA profiling of ALDEFLUOR positive and negative cells from isolated tumor and normal tissue from patients have provided an elaborate list of candidate miRNAs that can be investigated further. MiRs such as miR200 family members and miR93 that are differentially expressed in the CSCs from patients have already been identified in breast cancer stem cells [95, 181]. MiR93 as discussed in the previous chapter could be an interesting candidate for investigation. Studying the effect of miR93 manipulation in proliferation, cell cycle, EMT, invasion and self-renewal ability of established colon cancer cells could provide data bolstering its role in CSC function. However, It would also be interesting to compare the miRNA profiles of ALDELFUOR positive and negative of established colon cancer cell lines (HT29 and SW480) with that of the primary tumor cells from patients. This comparison will enable us to look at the common differentially expressed miRs in cell lines compared to primary cells that can be studied further *in vitro* and *in vivo*.

In vivo studies with immunocompromised mouse models are a widely accepted way to look at the effect of manipulation of miRs on tumor growth. The inhibitory effect of miR23b overexpression on proliferation rate and cell cycle could be utilized as a way to keep a check on cycling tumor cells. Experiments can be designed where immunocompromised mice with developed tumors (from HT29 cells) can be administered with miR23b precursor or antimir molecules. The tumor growth

of the treated group can be monitored over time and compared to the control. A different approach to study *in vivo* effects of miR23b on colon cancer cells is via Chick embryo model which was described by Galileo *et al.*, [185]. This model is much simpler because the cells with altered levels of miR23b are injected into the optic tectum of 5 day-old chick embryos. The brains would be dissected out at day nine and gene expression analysis for human specific Alu repeats sequences would be done to provide an index of tumor growth as reported before for glioma cells [186].

Mir23b expression was shown to increase sensitivity of HT29 cells to the drug 5 FU *in vitro*. We speculate that miR23b decreases LGR5 levels, which have been associated with chemo-resistance to 5-FU. This can also be proved by designing a rescue experiment where the HT29 cells with high miR23b can be transfected with a vector expressing LGR5 protein. This would negate the effect miR23b have on endogenous LGR5 expression and increase resistance to the drug 5 FU as compared to the control cells. Testing this effect in mice models for tumor initiating ability could inspect our *in vitro* findings further. The use of nanoparticles to deliver miRs precursor or antimirs in conjunction with anti cancer drugs has already been reported in the case miR200c and Docetaxel that were used to target gastric cancer cells *in vivo* [187]. Use of similar technology will help us look at the effect of combined treatment involving miR23b precursor and 5-FU drug on colon cancer cells growth as compared to treating with 5-FU alone. We hypothesize that increasing miR23b levels will reduce LGR5 levels in these cells, and will increase their sensitivity to the anticancer drug. These experiments will help validate the essential role of miR23b in regulating chemo-resistive properties in colon cancer cells.

Differential expression of miRs in colon CSCs marked by different markers have been reported by various investigators. One study showed that ALDEFLUOR positive/ CD133 positive/ CD44 positive colon cancer cells from patients express low miR 34a and regulates asymmetric division via NOTCH pathway [188]. Similarly another study profiled CD133 positive and negative HT29 cells for miRNA expression and identified 11 overexpressed and 8 under expressed miRs speculated to have a role in stem cell differentiation [80]. Overall, different studies reported so far suggest that miRs identified to regulate CSCs in colon might be specific to the cells positive for the marker used for isolation. Based on the immunostaining profile of various SC markers from my study, it is evident that one single marker for colon CSC does not exist and multiple subpopulations co-exist within the CSCs. It is pertinent to investigate the expression of miRs in tumor cells isolated by using multiple SC markers in combination. For example, one could sort tumor cells for ALDH activity first, fix them and enrich them sub sequentially for expression of CD166, LGR5, CD44 and LRIG1 and use the subpopulation for miRNA profiling. Single cell profiling technology [189] can be employed to avoid possible pitfalls caused by availability of number of cells. Such a study would enable us to identify miRs, which show differential expression in highly enriched population of SCs in tumor. An alternative approach could be to work in collaboration with multiple investigators working in this field to possibly identify common miRs, which are differentially expressed across all the studies irrespective of the marker used for isolation and enrichment of CSCs. Candidate miRs identified can be further investigated by manipulating their levels and evaluating for an effect in well established colon cancer cell lines or in primary cells derived from patients. Use of multiple miRNA prediction tools would help us identify

candidate gene targets influenced by any given miR under investigation. Target validation with luciferase assays and RNAi approaches (*in vitro* and *in vivo*) will provide an insight on signaling pathways influenced by candidate miRs in the tumor cells. This would help us advance towards accomplishing the ultimate goal to decipher the role of miRs in regulating gene targets and the function of CSCs in colon tumors.

REFERENCES

1. Sleisenger, M.H., et al., Sleisenger & Fordtran's gastrointestinal and liver disease: pathophysiology, diagnosis, management. 6th ed1998, Philadelphia: W.B. Saunders.
2. Cheng, H. and C.P. Leblond, Origin, differentiation and renewal of the four main epithelial cell types in the mouse small intestine. V. Unitarian Theory of the origin of the four epithelial cell types. *Am J Anat*, 1974. **141**(4): p. 537-61.
3. Beck, D.E., et al., *The ASCRS Textbook of Colon and Rectal Surgery Second Edition*, 2011, Springer Science+Business Media, LLC: New York, NY.
4. American Cancer Society. What are the risk factors for colorectal cancer? 2014 [cited 2014 April 10]; Available from: <http://www.cancer.org/cancer/colonandrectumcancer/detailedguide/colorectal-cancer-risk-factors>.
5. American Cancer Society. WHAT IS COLON/RECTUM CANCER. 2014 01/31/2014 [cited 2014 April 10th]; Available from: <http://www.cancer.org/cancer/colonandrectumcancer/detailedguide/colorectal-cancer-what-is-colorectal-cancer>.
6. National Cancer Institute. Stages of Colon Cancer. 2013 [cited 2014 15th March]; Available from: <http://www.cancer.gov/cancertopics/pdq/treatment/colon/Patient/page2>.
7. Kelsen, D., *Principles and practice of gastrointestinal oncology*. 2nd ed2008, Philadelphia, PA: Wolters Kluwer/Lippincott, Williams & Wilkins. xv, 749 p., 16 p. of plates.
8. Leach, F.S., et al., Mutations of a mutS homolog in hereditary nonpolyposis colorectal cancer. *Cell*, 1993. **75**(6): p. 1215-25.
9. Bronner, C.E., et al., Mutation in the DNA mismatch repair gene homologue hMLH1 is associated with hereditary non-polyposis colon cancer. *Nature*, 1994. **368**(6468): p. 258-61.
10. Kane, M.F., et al., Methylation of the hMLH1 promoter correlates with lack of expression of hMLH1 in sporadic colon tumors and mismatch repair-defective human tumor cell lines. *Cancer Res*, 1997. **57**(5): p. 808-11.
11. Kastrinos, F. and S. Syngal, Recently identified colon cancer predispositions: MYH and MSH6 mutations. *Semin Oncol*, 2007. **34**(5): p. 418-24.

12. Issa, J.P., CpG island methylator phenotype in cancer. *Nat Rev Cancer*, 2004. **4**(12): p. 988-93.
13. Bos, J.L., et al., Prevalence of ras gene mutations in human colorectal cancers. *Nature*, 1987. **327**(6120): p. 293-7.
14. Davies, H., et al., Mutations of the BRAF gene in human cancer. *Nature*, 2002. **417**(6892): p. 949-54.
15. Parsons, D.W., et al., Colorectal cancer: mutations in a signalling pathway. *Nature*, 2005. **436**(7052): p. 792.
16. Goss, K.H. and J. Groden, Biology of the adenomatous polyposis coli tumor suppressor. *J Clin Oncol*, 2000. **18**(9): p. 1967-79.
17. Baker, S.J., et al., Chromosome 17 deletions and p53 gene mutations in colorectal carcinomas. *Science*, 1989. **244**(4901): p. 217-21.
18. Markowitz, S., et al., Inactivation of the type II TGF-beta receptor in colon cancer cells with microsatellite instability. *Science*, 1995. **268**(5215): p. 1336-8.
19. Yan, M., et al., 15-Hydroxyprostaglandin dehydrogenase, a COX-2 oncogene antagonist, is a TGF-beta-induced suppressor of human gastrointestinal cancers. *Proc Natl Acad Sci U S A*, 2004. **101**(50): p. 17468-73.
20. Dick, J.E., Stem cell concepts renew cancer research. *Blood*, 2008. **112**(13): p. 4793-807.
21. Clarke, M.F., et al., Cancer stem cells--perspectives on current status and future directions: AACR Workshop on cancer stem cells. *Cancer Res*, 2006. **66**(19): p. 9339-44.
22. Bonnet, D. and J.E. Dick, Human acute myeloid leukemia is organized as a hierarchy that originates from a primitive hematopoietic cell. *Nat Med*, 1997. **3**(7): p. 730-7.
23. Al-Hajj, M., et al., Prospective identification of tumorigenic breast cancer cells. *Proc Natl Acad Sci U S A*, 2003. **100**(7): p. 3983-8.
24. O'Brien, C.A., et al., A human colon cancer cell capable of initiating tumour growth in immunodeficient mice. *Nature*, 2007. **445**(7123): p. 106-10.
25. Ricci-Vitiani, L., et al., Identification and expansion of human colon-cancer-initiating cells. *Nature*, 2007. **445**(7123): p. 111-5.

26. American Institute for Cancer Research. and SpringerLink (Online service), Colon Cancer Prevention Dietary Modulation of Cellular and Molecular Mechanisms, in *Advances in Experimental Medicine and Biology*, 1999, Springer US : Imprint: Springer: Boston, MA.
27. Boman, B.M., et al., Computer modeling implicates stem cell overproduction in colon cancer initiation. *Cancer Res*, 2001. **61**(23): p. 8408-11.
28. Huang, E.H., et al., Aldehyde dehydrogenase 1 is a marker for normal and malignant human colonic stem cells (SC) and tracks SC overpopulation during colon tumorigenesis. *Cancer Res*, 2009. **69**(8): p. 3382-9.
29. Singh, S.K., et al., Identification of a cancer stem cell in human brain tumors. *Cancer Res*, 2003. **63**(18): p. 5821-8.
30. Shmelkov, S.V., et al., CD133 expression is not restricted to stem cells, and both CD133+ and CD133- metastatic colon cancer cells initiate tumors. *J Clin Invest*, 2008. **118**(6): p. 2111-20.
31. Kastan, M.B., et al., Direct demonstration of elevated aldehyde dehydrogenase in human hematopoietic progenitor cells. *Blood*, 1990. **75**(10): p. 1947-50.
32. Moreb, J.S., Aldehyde dehydrogenase as a marker for stem cells. *Curr Stem Cell Res Ther*, 2008. **3**(4): p. 237-46.
33. Vasiliou, V., A. Pappa, and T. Estey, Role of human aldehyde dehydrogenases in endobiotic and xenobiotic metabolism. *Drug Metab Rev*, 2004. **36**(2): p. 279-99.
34. Pearce, D.J., et al., Characterization of cells with a high aldehyde dehydrogenase activity from cord blood and acute myeloid leukemia samples. *Stem Cells*, 2005. **23**(6): p. 752-60.
35. Chang, B., et al., ALDH1 expression correlates with favorable prognosis in ovarian cancers. *Mod Pathol*, 2009. **22**(6): p. 817-23.
36. Ma, S., et al., Aldehyde dehydrogenase discriminates the CD133 liver cancer stem cell populations. *Mol Cancer Res*, 2008. **6**(7): p. 1146-53.
37. van den Hoogen, C., et al., High aldehyde dehydrogenase activity identifies tumor-initiating and metastasis-initiating cells in human prostate cancer. *Cancer Res*, 2010. **70**(12): p. 5163-73.

38. Wakamatsu, Y., et al., Expression of cancer stem cell markers ALDH1, CD44 and CD133 in primary tumor and lymph node metastasis of gastric cancer. *Pathol Int*, 2012. **62**(2): p. 112-9.
39. Lee, R.C., R.L. Feinbaum, and V. Ambros, The *C. elegans* heterochronic gene *lin-4* encodes small RNAs with antisense complementarity to *lin-14*. *Cell*, 1993. **75**(5): p. 843-54.
40. Schetter, A.J., et al., MicroRNA expression profiles associated with prognosis and therapeutic outcome in colon adenocarcinoma. *JAMA*, 2008. **299**(4): p. 425-36.
41. Lewis, B.P., et al., Prediction of mammalian microRNA targets. *Cell*, 2003. **115**(7): p. 787-98.
42. Miranda, K.C., et al., A pattern-based method for the identification of MicroRNA binding sites and their corresponding heteroduplexes. *Cell*, 2006. **126**(6): p. 1203-17.
43. Stark, A., et al., Identification of *Drosophila* MicroRNA targets. *PLoS Biol*, 2003. **1**(3): p. E60.
44. Johnson, S.M., et al., RAS is regulated by the let-7 microRNA family. *Cell*, 2005. **120**(5): p. 635-47.
45. Kumar, M.S., et al., Suppression of non-small cell lung tumor development by the let-7 microRNA family. *Proc Natl Acad Sci U S A*, 2008. **105**(10): p. 3903-8.
46. Mayr, C., M.T. Hemann, and D.P. Bartel, Disrupting the pairing between let-7 and *Hmga2* enhances oncogenic transformation. *Science*, 2007. **315**(5818): p. 1576-9.
47. Olive, V., et al., miR-19 is a key oncogenic component of mir-17-92. *Genes Dev*, 2009. **23**(24): p. 2839-49.
48. Hong, L., et al., The miR-17-92 cluster of microRNAs confers tumorigenicity by inhibiting oncogene-induced senescence. *Cancer Res*, 2010. **70**(21): p. 8547-57.
49. Papagiannakopoulos, T., A. Shapiro, and K.S. Kosik, MicroRNA-21 targets a network of key tumor-suppressive pathways in glioblastoma cells. *Cancer Res*, 2008. **68**(19): p. 8164-72.

50. Ma, L., J. Teruya-Feldstein, and R.A. Weinberg, Tumour invasion and metastasis initiated by microRNA-10b in breast cancer. *Nature*, 2007. **449**(7163): p. 682-8.
51. Calin, G.A., et al., Frequent deletions and down-regulation of micro- RNA genes miR15 and miR16 at 13q14 in chronic lymphocytic leukemia. *Proc Natl Acad Sci U S A*, 2002. **99**(24): p. 15524-9.
52. Saito, Y., et al., Specific activation of microRNA-127 with downregulation of the proto-oncogene BCL6 by chromatin-modifying drugs in human cancer cells. *Cancer Cell*, 2006. **9**(6): p. 435-43.
53. Raver-Shapira, N., et al., Transcriptional activation of miR-34a contributes to p53-mediated apoptosis. *Mol Cell*, 2007. **26**(5): p. 731-43.
54. Hagan, J.P., E. Piskounova, and R.I. Gregory, Lin28 recruits the TUTase Zcchc11 to inhibit let-7 maturation in mouse embryonic stem cells. *Nat Struct Mol Biol*, 2009. **16**(10): p. 1021-5.
55. Luo, X., et al., MicroRNA signatures: novel biomarker for colorectal cancer? *Cancer Epidemiol Biomarkers Prev*, 2011. **20**(7): p. 1272-86.
56. Michael, M.Z., et al., Reduced accumulation of specific microRNAs in colorectal neoplasia. *Mol Cancer Res*, 2003. **1**(12): p. 882-91.
57. Volinia, S., et al., A microRNA expression signature of human solid tumors defines cancer gene targets. *Proc Natl Acad Sci U S A*, 2006. **103**(7): p. 2257-61.
58. Valeri, N., et al., Modulation of mismatch repair and genomic stability by miR-155. *Proc Natl Acad Sci U S A*, 2010. **107**(15): p. 6982-7.
59. Schetter, A.J., H. Okayama, and C.C. Harris, The role of microRNAs in colorectal cancer. *Cancer J*, 2012. **18**(3): p. 244-52.
60. Ng, E.K., et al., Differential expression of microRNAs in plasma of patients with colorectal cancer: a potential marker for colorectal cancer screening. *Gut*, 2009. **58**(10): p. 1375-81.
61. Cheng, H., et al., Circulating plasma MiR-141 is a novel biomarker for metastatic colon cancer and predicts poor prognosis. *PLoS One*, 2011. **6**(3): p. e17745.

62. Link, A., et al., Fecal MicroRNAs as novel biomarkers for colon cancer screening. *Cancer Epidemiol Biomarkers Prev*, 2010. **19**(7): p. 1766-74.
63. Shibuya, H., et al., Clinicopathological and prognostic value of microRNA-21 and microRNA-155 in colorectal cancer. *Oncology*, 2010. **79**(3-4): p. 313-20.
64. Kulda, V., et al., Relevance of miR-21 and miR-143 expression in tissue samples of colorectal carcinoma and its liver metastases. *Cancer Genet Cytogenet*, 2010. **200**(2): p. 154-60.
65. Nielsen, B.S., et al., High levels of microRNA-21 in the stroma of colorectal cancers predict short disease-free survival in stage II colon cancer patients. *Clin Exp Metastasis*, 2011. **28**(1): p. 27-38.
66. Diaz, R., et al., Deregulated expression of miR-106a predicts survival in human colon cancer patients. *Genes Chromosomes Cancer*, 2008. **47**(9): p. 794-802.
67. Nishida, N., et al., MicroRNA miR-125b is a prognostic marker in human colorectal cancer. *Int J Oncol*, 2011. **38**(5): p. 1437-43.
68. Drebber, U., et al., Altered levels of the onco-microRNA 21 and the tumor-suppressor microRNAs 143 and 145 in advanced rectal cancer indicate successful neoadjuvant chemoradiotherapy. *Int J Oncol*, 2011. **39**(2): p. 409-15.
69. Nagel, R., et al., Regulation of the adenomatous polyposis coli gene by the miR-135 family in colorectal cancer. *Cancer Res*, 2008. **68**(14): p. 5795-802.
70. Akao, Y., Y. Nakagawa, and T. Naoe, let-7 microRNA functions as a potential growth suppressor in human colon cancer cells. *Biol Pharm Bull*, 2006. **29**(5): p. 903-6.
71. Chen, X., et al., Role of miR-143 targeting KRAS in colorectal tumorigenesis. *Oncogene*, 2009. **28**(10): p. 1385-92.
72. Tsang, W.P. and T.T. Kwok, The miR-18a* microRNA functions as a potential tumor suppressor by targeting on K-Ras. *Carcinogenesis*, 2009. **30**(6): p. 953-9.
73. Krichevsky, A.M. and G. Gabriely, miR-21: a small multi-faceted RNA. *J Cell Mol Med*, 2009. **13**(1): p. 39-53.

74. Chang, T.C., et al., Transactivation of miR-34a by p53 broadly influences gene expression and promotes apoptosis. *Mol Cell*, 2007. **26**(5): p. 745-52.
75. Diosdado, B., et al., MiR-17-92 cluster is associated with 13q gain and c-myc expression during colorectal adenoma to adenocarcinoma progression. *Br J Cancer*, 2009. **101**(4): p. 707-14.
76. DeSano, J.T. and L. Xu, MicroRNA regulation of cancer stem cells and therapeutic implications. *AAPS J*, 2009. **11**(4): p. 682-92.
77. Yu, F., et al., let-7 regulates self renewal and tumorigenicity of breast cancer cells. *Cell*, 2007. **131**(6): p. 1109-23.
78. Garzia, L., et al., MicroRNA-199b-5p impairs cancer stem cells through negative regulation of HES1 in medulloblastoma. *PLoS One*, 2009. **4**(3): p. e4998.
79. Godlewski, J., et al., Targeting of the Bmi-1 oncogene/stem cell renewal factor by microRNA-128 inhibits glioma proliferation and self-renewal. *Cancer Res*, 2008. **68**(22): p. 9125-30.
80. Zhang, H., et al., MicroRNA expression profile of colon cancer stem-like cells in HT29 adenocarcinoma cell line. *Biochem Biophys Res Commun*, 2011. **404**(1): p. 273-8.
81. Zhu, R., et al., Ascl2 knockdown results in tumor growth arrest by miRNA-302b-related inhibition of colon cancer progenitor cells. *PLoS One*, 2012. **7**(2): p. e32170.
82. Yu, X.F., et al., miR-93 suppresses proliferation and colony formation of human colon cancer stem cells. *World J Gastroenterol*, 2011. **17**(42): p. 4711-7.
83. Calin, G.A. and C.M. Croce, MicroRNA signatures in human cancers. *Nat Rev Cancer*, 2006. **6**(11): p. 857-66.
84. Calin, G.A., et al., Human microRNA genes are frequently located at fragile sites and genomic regions involved in cancers. *Proc Natl Acad Sci U S A*, 2004. **101**(9): p. 2999-3004.
85. Zhang, H., et al., Genome-wide functional screening of miR-23b as a pleiotropic modulator suppressing cancer metastasis. *Nat Commun*, 2011. **2**: p. 554.

86. Chen, L., et al., VHL regulates the effects of miR-23b on glioma survival and invasion via suppression of HIF-1alpha/VEGF and beta-catenin/Tcf-4 signaling. *Neuro Oncol*, 2012. **14**(8): p. 1026-36.
87. Geng, J., et al., Methylation mediated silencing of miR-23b expression and its role in glioma stem cells. *Neurosci Lett*, 2012. **528**(2): p. 185-9.
88. Jin, L., et al., Prooncogenic factors miR-23b and miR-27b are regulated by Her2/Neu, EGF, and TNF-alpha in breast cancer. *Cancer Res*, 2013. **73**(9): p. 2884-96.
89. Liu, W., et al., miR-23b targets proline oxidase, a novel tumor suppressor protein in renal cancer. *Oncogene*, 2010. **29**(35): p. 4914-24.
90. Majid, S., et al., MicroRNA-23b functions as a tumor suppressor by regulating Zeb1 in bladder cancer. *PLoS One*, 2013. **8**(7): p. e67686.
91. Pellegrino, L., et al., miR-23b regulates cytoskeletal remodeling, motility and metastasis by directly targeting multiple transcripts. *Nucleic Acids Res*, 2013. **41**(10): p. 5400-12.
92. Yuan, B., et al., Down-regulation of miR-23b may contribute to activation of the TGF-beta1/Smad3 signalling pathway during the termination stage of liver regeneration. *FEBS Lett*, 2011. **585**(6): p. 927-34.
93. Zaman, M.S., et al., Inhibition of PTEN gene expression by oncogenic miR-23b-3p in renal cancer. *PLoS One*, 2012. **7**(11): p. e50203.
94. Saini, S., et al., miRNA-708 control of CD44(+) prostate cancer-initiating cells. *Cancer Res*, 2012. **72**(14): p. 3618-30.
95. Shimono, Y., et al., Downregulation of miRNA-200c links breast cancer stem cells with normal stem cells. *Cell*, 2009. **138**(3): p. 592-603.
96. He, H.C., et al., MicroRNA-23b downregulates peroxiredoxin III in human prostate cancer. *FEBS Lett*, 2012. **586**(16): p. 2451-8.
97. Wang, K.C., et al., Role of microRNA-23b in flow-regulation of Rb phosphorylation and endothelial cell growth. *Proc Natl Acad Sci U S A*, 2010. **107**(7): p. 3234-9.
98. Mani, S.A., et al., The epithelial-mesenchymal transition generates cells with properties of stem cells. *Cell*, 2008. **133**(4): p. 704-15.

99. Majid, S., et al., miR-23b represses proto-oncogene Src kinase and functions as methylation-silenced tumor suppressor with diagnostic and prognostic significance in prostate cancer. *Cancer Res*, 2012. **72**(24): p. 6435-46.
100. Chen, L., et al., A lentivirus-mediated miR-23b sponge diminishes the malignant phenotype of glioma cells in vitro and in vivo. *Oncol Rep*, 2014. **31**(4): p. 1573-80.
101. Kai, K., et al., Maintenance of HCT116 colon cancer cell line conforms to a stochastic model but not a cancer stem cell model. *Cancer Sci*, 2009. **100**(12): p. 2275-82.
102. Takahashi, H., et al., Significance of Lgr5(+ve) cancer stem cells in the colon and rectum. *Ann Surg Oncol*, 2011. **18**(4): p. 1166-74.
103. Hsu, H.C., et al., Overexpression of Lgr5 correlates with resistance to 5-FU-based chemotherapy in colorectal cancer. *Int J Colorectal Dis*, 2013. **28**(11): p. 1535-46.
104. Gao, P., et al., c-Myc suppression of miR-23a/b enhances mitochondrial glutaminase expression and glutamine metabolism. *Nature*, 2009. **458**(7239): p. 762-5.
105. Pinto, D., et al., Canonical Wnt signals are essential for homeostasis of the intestinal epithelium. *Genes Dev*, 2003. **17**(14): p. 1709-13.
106. de Lau, W., et al., Lgr5 homologues associate with Wnt receptors and mediate R-spondin signalling. *Nature*, 2011. **476**(7360): p. 293-7.
107. Tian, H., et al., A reserve stem cell population in small intestine renders Lgr5-positive cells dispensable. *Nature*, 2011. **478**(7368): p. 255-9.
108. Kobayashi, S., et al., LGR5-positive colon cancer stem cells interconvert with drug-resistant LGR5-negative cells and are capable of tumor reconstitution. *Stem Cells*, 2012. **30**(12): p. 2631-44.
109. Nakamura, M., et al., Musashi, a neural RNA-binding protein required for Drosophila adult external sensory organ development. *Neuron*, 1994. **13**(1): p. 67-81.
110. Imai, T., et al., The neural RNA-binding protein Musashi1 translationally regulates mammalian numb gene expression by interacting with its mRNA. *Mol Cell Biol*, 2001. **21**(12): p. 3888-900.

111. Kawahara, H., et al., Neural RNA-binding protein Musashi1 inhibits translation initiation by competing with eIF4G for PABP. *J Cell Biol*, 2008. **181**(4): p. 639-53.
112. Kaneko, Y., et al., Musashi1: an evolutionally conserved marker for CNS progenitor cells including neural stem cells. *Dev Neurosci*, 2000. **22**(1-2): p. 139-53.
113. Nishimura, S., et al., Expression of Musashi-1 in human normal colon crypt cells: a possible stem cell marker of human colon epithelium. *Dig Dis Sci*, 2003. **48**(8): p. 1523-9.
114. Potten, C.S., et al., Identification of a putative intestinal stem cell and early lineage marker; musashi-1. *Differentiation*, 2003. **71**(1): p. 28-41.
115. Rezza, A., et al., The overexpression of the putative gut stem cell marker Musashi-1 induces tumorigenesis through Wnt and Notch activation. *J Cell Sci*, 2010. **123**(Pt 19): p. 3256-65.
116. Fargeas, C.A., et al., Characterization of prominin-2, a new member of the prominin family of pentaspan membrane glycoproteins. *J Biol Chem*, 2003. **278**(10): p. 8586-96.
117. Corbeil, D., et al., Expression of distinct splice variants of the stem cell marker prominin-1 (CD133) in glial cells. *Glia*, 2009. **57**(8): p. 860-74.
118. Grosse-Gehling, P., et al., CD133 as a biomarker for putative cancer stem cells in solid tumours: limitations, problems and challenges. *J Pathol*, 2013. **229**(3): p. 355-78.
119. Yin, A.H., et al., AC133, a novel marker for human hematopoietic stem and progenitor cells. *Blood*, 1997. **90**(12): p. 5002-12.
120. Uchida, N., et al., Direct isolation of human central nervous system stem cells. *Proc Natl Acad Sci U S A*, 2000. **97**(26): p. 14720-5.
121. Richardson, G.D., et al., CD133, a novel marker for human prostatic epithelial stem cells. *J Cell Sci*, 2004. **117**(Pt 16): p. 3539-45.
122. Schmelzer, E., et al., Human hepatic stem cells from fetal and postnatal donors. *J Exp Med*, 2007. **204**(8): p. 1973-87.
123. Bussolati, B., et al., Isolation of renal progenitor cells from adult human kidney. *Am J Pathol*, 2005. **166**(2): p. 545-55.

124. Carter, D.A., A.D. Dick, and E.J. Mayer, CD133+ adult human retinal cells remain undifferentiated in Leukaemia Inhibitory Factor (LIF). *BMC Ophthalmol*, 2009. **9**: p. 1.
125. Halasa, M., et al., An efficient two-step method to purify very small embryonic-like (VSEL) stem cells from umbilical cord blood (UCB). *Folia Histochem Cytobiol*, 2008. **46**(2): p. 239-43.
126. Chu, P., et al., Characterization of a subpopulation of colon cancer cells with stem cell-like properties. *Int J Cancer*, 2009. **124**(6): p. 1312-21.
127. Dalerba, P., et al., Phenotypic characterization of human colorectal cancer stem cells. *Proc Natl Acad Sci U S A*, 2007. **104**(24): p. 10158-63.
128. Cayrol, R., et al., Activated leukocyte cell adhesion molecule promotes leukocyte trafficking into the central nervous system. *Nat Immunol*, 2008. **9**(2): p. 137-45.
129. Levin, T.G., et al., Characterization of the intestinal cancer stem cell marker CD166 in the human and mouse gastrointestinal tract. *Gastroenterology*, 2010. **139**(6): p. 2072-2082 e5.
130. Maliepaard, M., et al., Subcellular localization and distribution of the breast cancer resistance protein transporter in normal human tissues. *Cancer Res*, 2001. **61**(8): p. 3458-64.
131. Gupta, N., et al., Down-regulation of BCRP/ABCG2 in colorectal and cervical cancer. *Biochem Biophys Res Commun*, 2006. **343**(2): p. 571-7.
132. Liu, H.G., et al., Expression of ABCG2 and its significance in colorectal cancer. *Asian Pac J Cancer Prev*, 2010. **11**(4): p. 845-8.
133. Zhou, S., et al., The ABC transporter Bcrp1/ABCG2 is expressed in a wide variety of stem cells and is a molecular determinant of the side-population phenotype. *Nat Med*, 2001. **7**(9): p. 1028-34.
134. Zheng, X., et al., Doxorubicin fails to eradicate cancer stem cells derived from anaplastic thyroid carcinoma cells: characterization of resistant cells. *Int J Oncol*, 2010. **37**(2): p. 307-15.
135. Litman, T., et al., The multidrug-resistant phenotype associated with overexpression of the new ABC half-transporter, MXR (ABCG2). *J Cell Sci*, 2000. **113** (Pt 11): p. 2011-21.

136. Barker, N., et al., Identification of stem cells in small intestine and colon by marker gene Lgr5. *Nature*, 2007. **449**(7165): p. 1003-7.
137. Barker, N., et al., Crypt stem cells as the cells-of-origin of intestinal cancer. *Nature*, 2009. **457**(7229): p. 608-11.
138. Yui, S., et al., Functional engraftment of colon epithelium expanded in vitro from a single adult Lgr5(+) stem cell. *Nat Med*, 2012. **18**(4): p. 618-23.
139. Jensen, K.B. and F.M. Watt, Single-cell expression profiling of human epidermal stem and transit-amplifying cells: Lrig1 is a regulator of stem cell quiescence. *Proc Natl Acad Sci U S A*, 2006. **103**(32): p. 11958-63.
140. Powell, A.E., et al., The pan-ErbB negative regulator Lrig1 is an intestinal stem cell marker that functions as a tumor suppressor. *Cell*, 2012. **149**(1): p. 146-58.
141. Cao, L., et al., BMI1 as a novel target for drug discovery in cancer. *J Cell Biochem*, 2011. **112**(10): p. 2729-41.
142. Lessard, J. and G. Sauvageau, Bmi-1 determines the proliferative capacity of normal and leukaemic stem cells. *Nature*, 2003. **423**(6937): p. 255-60.
143. Hosen, N., et al., Bmi-1-green fluorescent protein-knock-in mice reveal the dynamic regulation of bmi-1 expression in normal and leukemic hematopoietic cells. *Stem Cells*, 2007. **25**(7): p. 1635-44.
144. Bertolini, G., et al., Highly tumorigenic lung cancer CD133+ cells display stem-like features and are spared by cisplatin treatment. *Proc Natl Acad Sci U S A*, 2009. **106**(38): p. 16281-6.
145. Zhang, S., et al., Identification and characterization of ovarian cancer-initiating cells from primary human tumors. *Cancer Res*, 2008. **68**(11): p. 4311-20.
146. Oishi, N. and X.W. Wang, Novel therapeutic strategies for targeting liver cancer stem cells. *Int J Biol Sci*, 2011. **7**(5): p. 517-35.
147. Yan, K.S., et al., The intestinal stem cell markers Bmi1 and Lgr5 identify two functionally distinct populations. *Proc Natl Acad Sci U S A*, 2012. **109**(2): p. 466-71.
148. Kreso, A., et al., Self-renewal as a therapeutic target in human colorectal cancer. *Nat Med*, 2014. **20**(1): p. 29-36.

149. Gunes, C. and K.L. Rudolph, The role of telomeres in stem cells and cancer. *Cell*, 2013. **152**(3): p. 390-3.
150. Joseph, I., et al., The telomerase inhibitor imetelstat depletes cancer stem cells in breast and pancreatic cancer cell lines. *Cancer Res*, 2010. **70**(22): p. 9494-504.
151. Marian, C.O., et al., The telomerase antagonist, imetelstat, efficiently targets glioblastoma tumor-initiating cells leading to decreased proliferation and tumor growth. *Clin Cancer Res*, 2010. **16**(1): p. 154-63.
152. Marian, C.O., W.E. Wright, and J.W. Shay, The effects of telomerase inhibition on prostate tumor-initiating cells. *Int J Cancer*, 2010. **127**(2): p. 321-31.
153. Zou, J., et al., Proteome of human colon cancer stem cells: a comparative analysis. *World J Gastroenterol*, 2011. **17**(10): p. 1276-85.
154. Murphy, B.L., et al., Silencing of the miR-17~92 cluster family inhibits medulloblastoma progression. *Cancer Res*, 2013. **73**(23): p. 7068-78.
155. Shigoka, M., et al., Deregulation of miR-92a expression is implicated in hepatocellular carcinoma development. *Pathol Int*, 2010. **60**(5): p. 351-7.
156. Wu, Q., et al., MiR-19b/20a/92a regulates the self-renewal and proliferation of gastric cancer stem cells. *J Cell Sci*, 2013. **126**(Pt 18): p. 4220-9.
157. Kanwar, S.S., et al., The Wnt/beta-catenin pathway regulates growth and maintenance of colonospheres. *Mol Cancer*, 2010. **9**: p. 212.
158. Sharifi, M., et al., Inhibition of microRNA miR-92a induces apoptosis and necrosis in human acute promyelocytic leukemia. *Adv Biomed Res*, 2014. **3**: p. 61.
159. Yu, Y., et al., MicroRNA-21 induces stemness by downregulating transforming growth factor beta receptor 2 (TGFbetaR2) in colon cancer cells. *Carcinogenesis*, 2012. **33**(1): p. 68-76.
160. Kanellopoulou, C., et al., Dicer-deficient mouse embryonic stem cells are defective in differentiation and centromeric silencing. *Genes Dev*, 2005. **19**(4): p. 489-501.

161. Ketting, R.F., et al., Dicer functions in RNA interference and in synthesis of small RNA involved in developmental timing in *C. elegans*. *Genes Dev*, 2001. **15**(20): p. 2654-9.
162. Murchison, E.P., et al., Characterization of Dicer-deficient murine embryonic stem cells. *Proc Natl Acad Sci U S A*, 2005. **102**(34): p. 12135-40.
163. Wang, P., et al., MicroRNA 23b regulates autophagy associated with radioresistance of pancreatic cancer cells. *Gastroenterology*, 2013. **145**(5): p. 1133-1143 e12.
164. Iinuma, H., et al., Clinical significance of circulating tumor cells, including cancer stem-like cells, in peripheral blood for recurrence and prognosis in patients with Dukes' stage B and C colorectal cancer. *J Clin Oncol*, 2011. **29**(12): p. 1547-55.
165. Liu, S., et al., Breast Cancer Stem Cells Transition between Epithelial and Mesenchymal States Reflective of their Normal Counterparts. *Stem Cell Reports*, 2014. **2**(1): p. 78-91.
166. He, S., D. Nakada, and S.J. Morrison, Mechanisms of stem cell self-renewal. *Annu Rev Cell Dev Biol*, 2009. **25**: p. 377-406.
167. Liu, S.Y. and P.S. Zheng, High aldehyde dehydrogenase activity identifies cancer stem cells in human cervical cancer. *Oncotarget*, 2013. **4**(12): p. 2462-75.
168. Huang, C.P., et al., ALDH-positive lung cancer stem cells confer resistance to epidermal growth factor receptor tyrosine kinase inhibitors. *Cancer Lett*, 2013. **328**(1): p. 144-51.
169. Zheng, J., et al., MicroRNA-23b promotes tolerogenic properties of dendritic cells in vitro through inhibiting Notch1/NF-kappaB signalling pathways. *Allergy*, 2012. **67**(3): p. 362-70.
170. Bitarte, N., et al., MicroRNA-451 is involved in the self-renewal, tumorigenicity, and chemoresistance of colorectal cancer stem cells. *Stem Cells*, 2011. **29**(11): p. 1661-71.
171. Pan, Y.Z., M.E. Morris, and A.M. Yu, MicroRNA-328 negatively regulates the expression of breast cancer resistance protein (BCRP/ABCG2) in human cancer cells. *Mol Pharmacol*, 2009. **75**(6): p. 1374-9.

172. Glinka, A., et al., LGR4 and LGR5 are R-spondin receptors mediating Wnt/beta-catenin and Wnt/PCP signalling. *EMBO Rep*, 2011. **12**(10): p. 1055-61.
173. Saoncella, S., et al., Nuclear Akt2 opposes limbal keratinocyte stem cell self-renewal by repressing a FOXO-mTORC1 signaling pathway. *Stem Cells*, 2014. **32**(3): p. 754-69.
174. Grumolato, L., et al., beta-Catenin-independent activation of TCF1/LEF1 in human hematopoietic tumor cells through interaction with ATF2 transcription factors. *PLoS Genet*, 2013. **9**(8): p. e1003603.
175. Yin, X., et al., ATF3, an adaptive-response gene, enhances TGF{beta} signaling and cancer-initiating cell features in breast cancer cells. *J Cell Sci*, 2010. **123**(Pt 20): p. 3558-65.
176. Levi, B.P., et al., Aldehyde dehydrogenase 1a1 is dispensable for stem cell function in the mouse hematopoietic and nervous systems. *Blood*, 2009. **113**(8): p. 1670-80.
177. Marchitti, S.A., et al., Aldehyde dehydrogenase 3B1 (ALDH3B1): immunohistochemical tissue distribution and cellular-specific localization in normal and cancerous human tissues. *J Histochem Cytochem*, 2010. **58**(9): p. 765-83.
178. Chen, Y., et al., Aldehyde dehydrogenase 1B1 (ALDH1B1) is a potential biomarker for human colon cancer. *Biochem Biophys Res Commun*, 2011. **405**(2): p. 173-9.
179. Chen, Z., et al., Suppression of ABCG2 inhibits cancer cell proliferation. *Int J Cancer*, 2010. **126**(4): p. 841-51.
180. Xiao, Z.G., et al., Clinical significance of microRNA-93 downregulation in human colon cancer. *Eur J Gastroenterol Hepatol*, 2013. **25**(3): p. 296-301.
181. Liu, S., et al., MicroRNA93 regulates proliferation and differentiation of normal and malignant breast stem cells. *PLoS Genet*, 2012. **8**(6): p. e1002751.
182. Qiang, X.F., et al., miR-20a promotes Prostate cancer invasion and migration through targeting ABL2. *J Cell Biochem*, 2014.
183. Niu, H., et al., miR-92a is a critical regulator of the apoptosis pathway in glioblastoma with inverse expression of BCL2L11. *Oncol Rep*, 2012. **28**(5): p. 1771-7.

184. Lv, X.B., et al., MiR-92a mediates AZD6244 induced apoptosis and G1-phase arrest of lymphoma cells by targeting Bim. *Cell Biol Int*, 2014. **38**(4): p. 435-43.
185. Cretu, A., et al., Human and rat glioma growth, invasion, and vascularization in a novel chick embryo brain tumor model. *Clin Exp Metastasis*, 2005. **22**(3): p. 225-36.
186. Jan, H.J., et al., Osteopontin regulates human glioma cell invasiveness and tumor growth in mice. *Neuro Oncol*, 2010. **12**(1): p. 58-70.
187. Liu, Q., et al., Targeted delivery of miR-200c/DOC to inhibit cancer stem cells and cancer cells by the gelatinases-stimuli nanoparticles. *Biomaterials*, 2013. **34**(29): p. 7191-203.
188. Bu, P., et al., A microRNA miR-34a-regulated bimodal switch targets Notch in colon cancer stem cells. *Cell Stem Cell*, 2013. **12**(5): p. 602-15.
189. Tang, F., et al., MicroRNA expression profiling of single whole embryonic stem cells. *Nucleic Acids Res*, 2006. **34**(2): p. e9.

Appendix A

SUPPLEMENTARY INFORMATION

A.1 POSITIVELY AND NEGATIVELY CORRELATED GENES WITH ALDH1A1 WITH SHARED TRANSCRIPTIONAL REGULATORY ELEMENTS (TREs) IN NORMAL COLON AND CANCER TISSUE: A BIOINFORMATICS STUDY.

A meta-analysis was performed by Dr. Adam Ertel to identify genes, which have been reported in literature to be upregulated or downregulated with *ALDH1A1* (Colon CSC marker). Results were represented in form of a heatmap for their co-expression pattern with *ALDH1A1* in normal colon, colon cancer and over all samples (**Figure A.1A, A.2A and A.3A**). I gathered the gene list of positively and negatively regulated was fed into DAVID tool to gather information about the genes including full gene names and ENSEMBL and Gene IDs. The gene IDs were used for PAINT analysis to identify shared TREs among the genes in the list. The list of enriched TREs for the upregulated and downregulated genes for three groups of samples (Normal, cancer and overall) are represented in **Figure A.1B, A.1C, A.2B, A.2C, A.3B and A.3C**. The list could further be analyzed for common miRs, which were predicted to target the candidate genes upregulated or downregulated with *ALDH1A1* by using multiple miR target prediction tools such as TARGETSCAN, miRANDA and *rna22*.

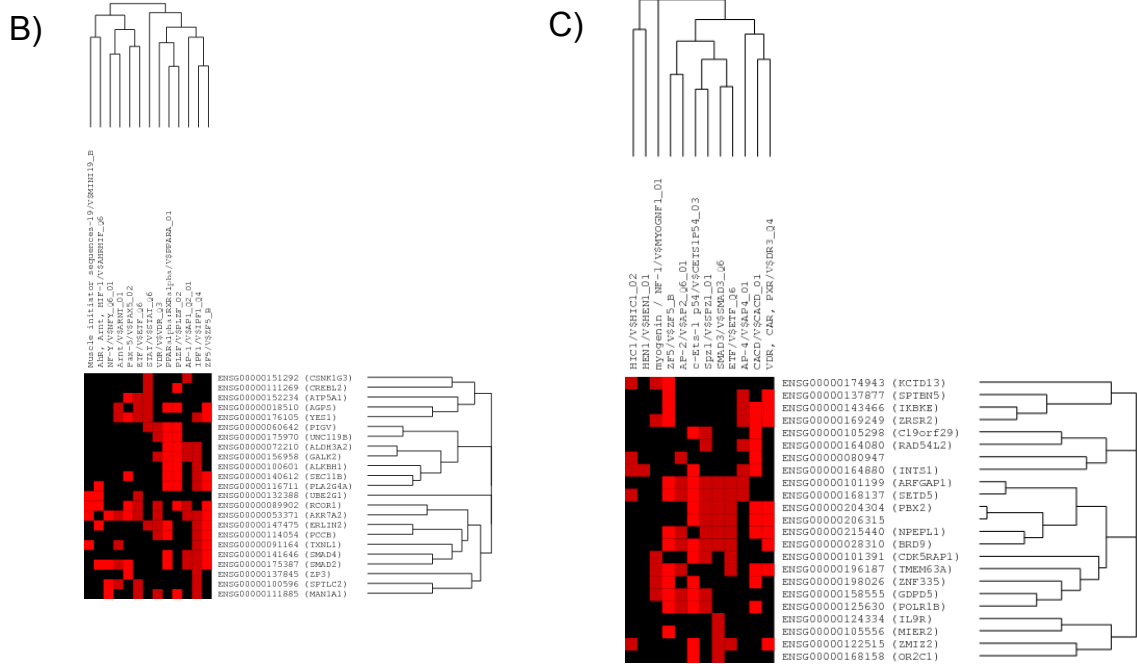
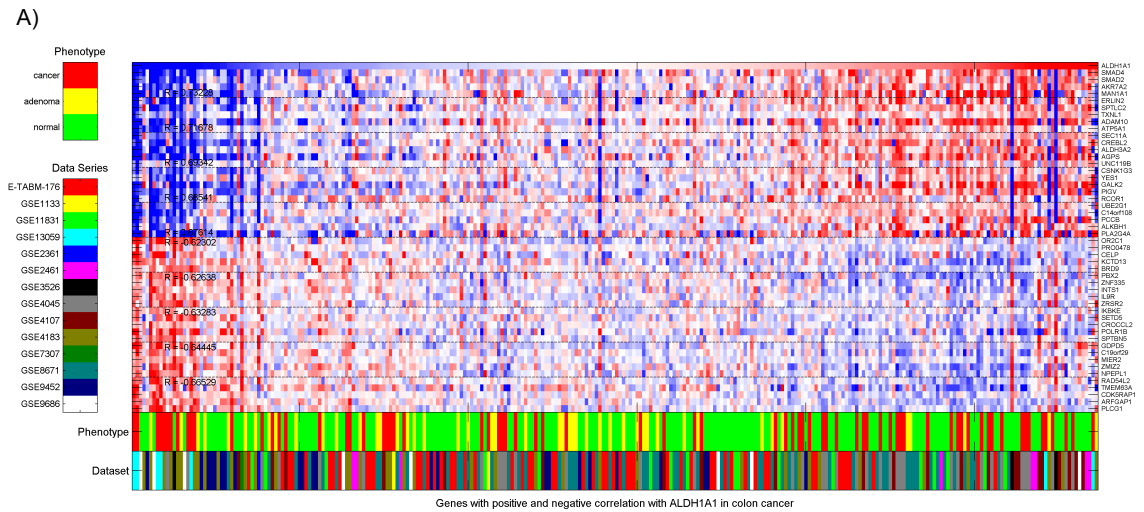


Figure A.2: List of correlated genes with *ALDH1A1* with shared TREs in colon cancer. A) shows meta analysis results in form of a heatmap with the list of genes upregulated or downregulated with *ALDH1A1* expression. PAINT analysis identified enriched TREs among the genelist upregulated (B) and downregulated (C) with *ALDH1A1* expression

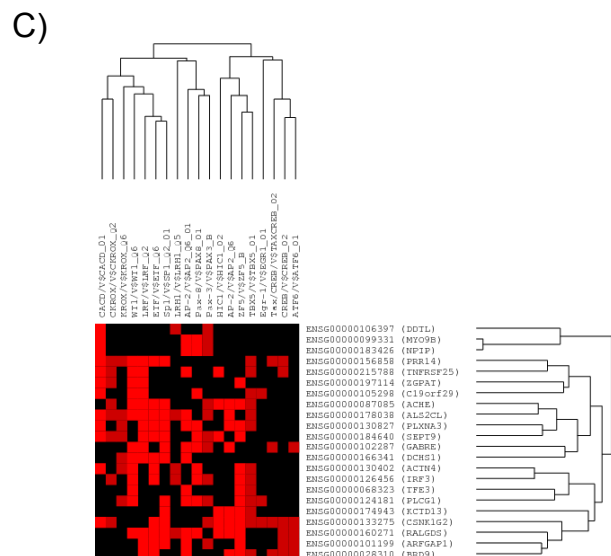
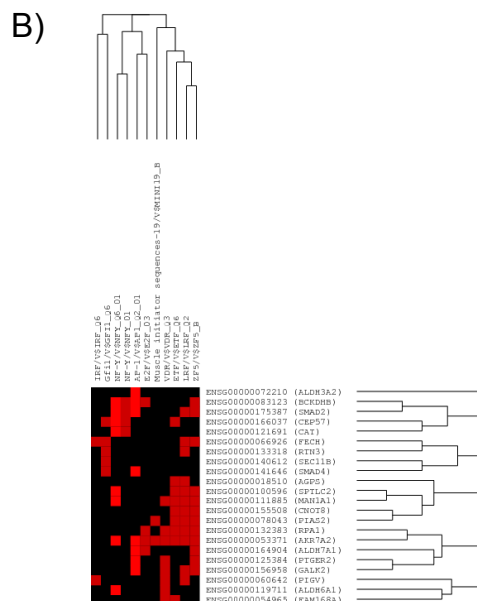
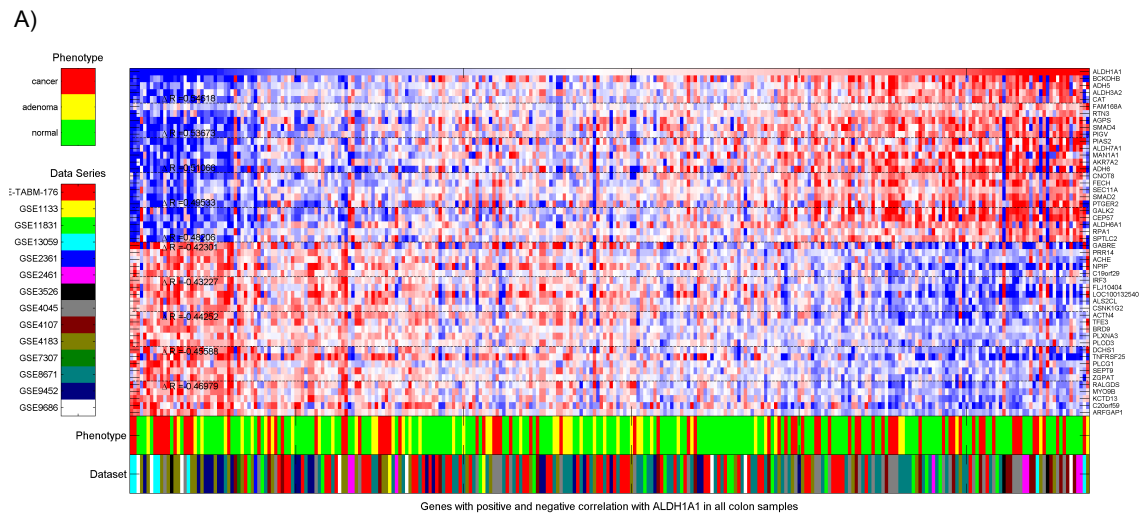


Figure A.3: List of correlated genes with *ALDH1A1* with shared TREs in all samples. A) shows meta analysis results in form of a heatmap with the list of genes upregulated or downregulated with *ALDH1A1* expression. PAINT analysis identified enriched TREs among the genelist upregulated (B) and downregulated (C) with *ALDH1A1* expression

A.2 VALIDATION OF MIR23B OVEREXPRESSION AND KNOCKDOWN IN HT29 CLONES.

SMAD3 is a functional target for miR23b [1] and its protein and mRNA levels were used to validate the levels of miR23b in the overexpressing, knockdown and the control clones of HT29. Western blot analysis showed that SMAD3 levels lowers in miR23b expressing clone as compared to the miR23b knockdown clone, which is quantified and shown in **Figure A.4B**. The mRNA levels of *SMAD3* also correlated with the protein levels (**Figure A.4C**).

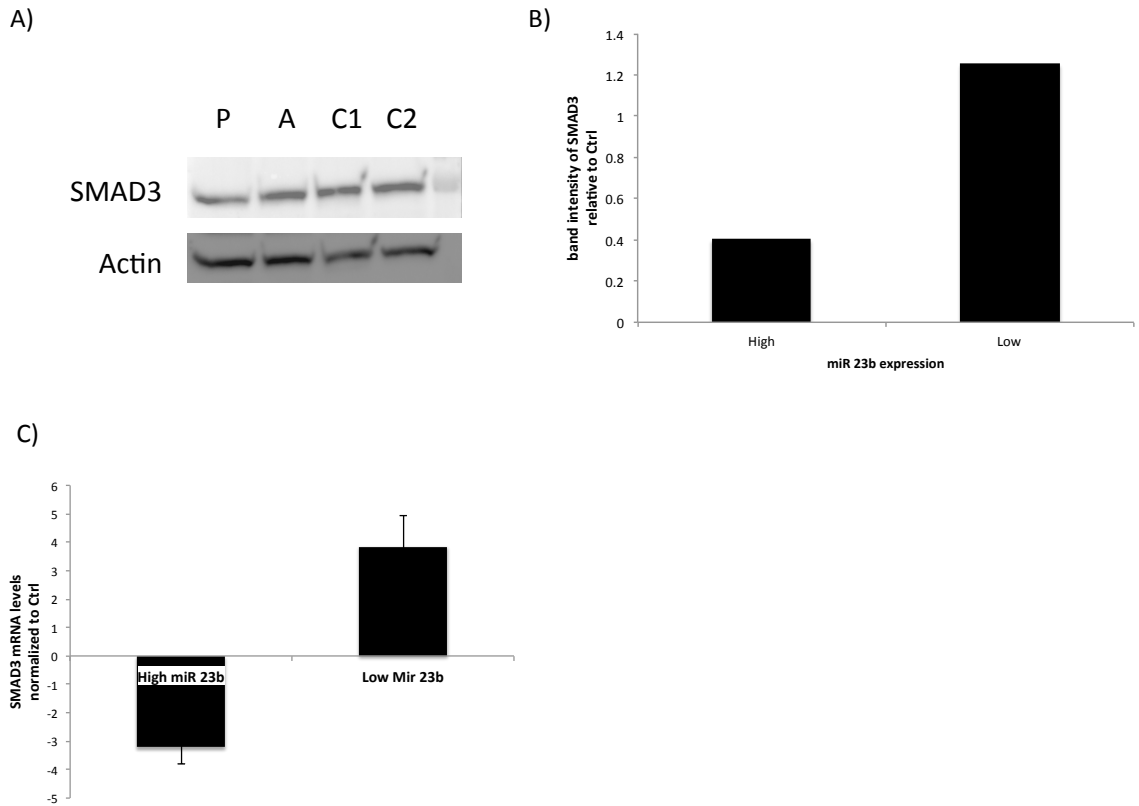
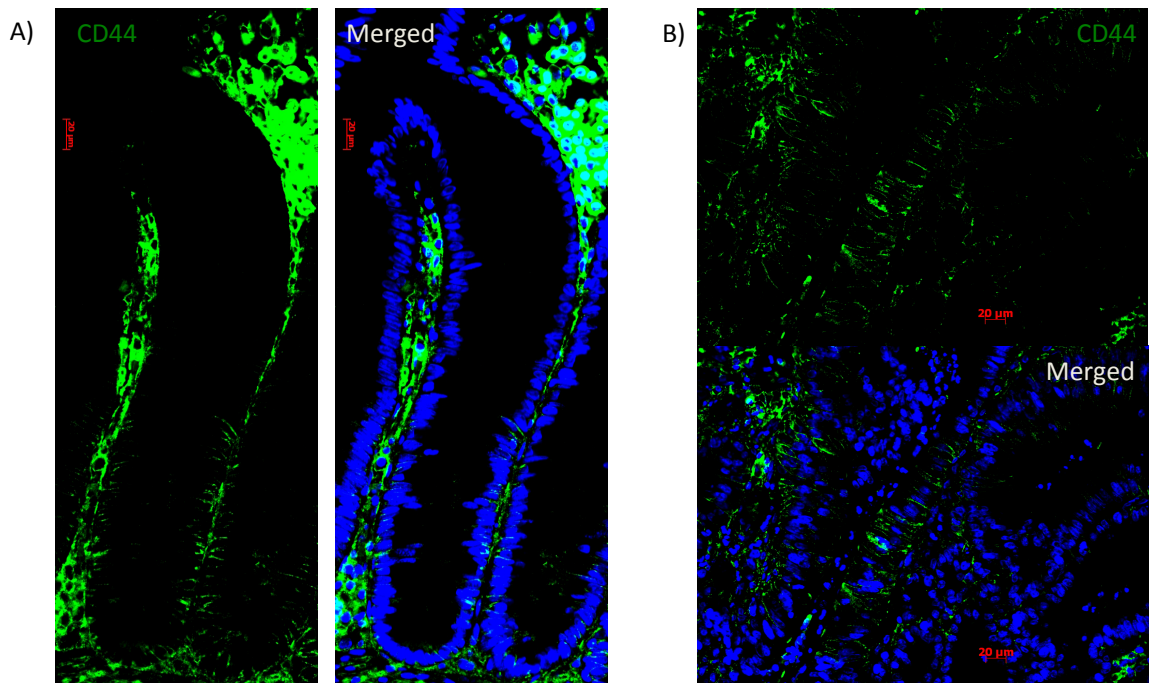


Figure A.4: Validation of miR23b levels in overexpressing and knockdown miR23b clones by looking at its functional target *SMAD3*. A) shows SMAD3 and Actin protein levels in the miR23b overexpressing (P), knockdown (A) and the two control clones (C1 and C2), which was quantified and shown in graph B. C) shows the mRNA levels of *SMAD3* in the overexpressing and knockdown miR23b clones as compared to the control.

A.3 EXPRESSION ANALYSIS OF THREE DIFFERENT CD44 ISOFORMS IN NORMAL COLONIC CRYPT AND TUMOR TISSUES.

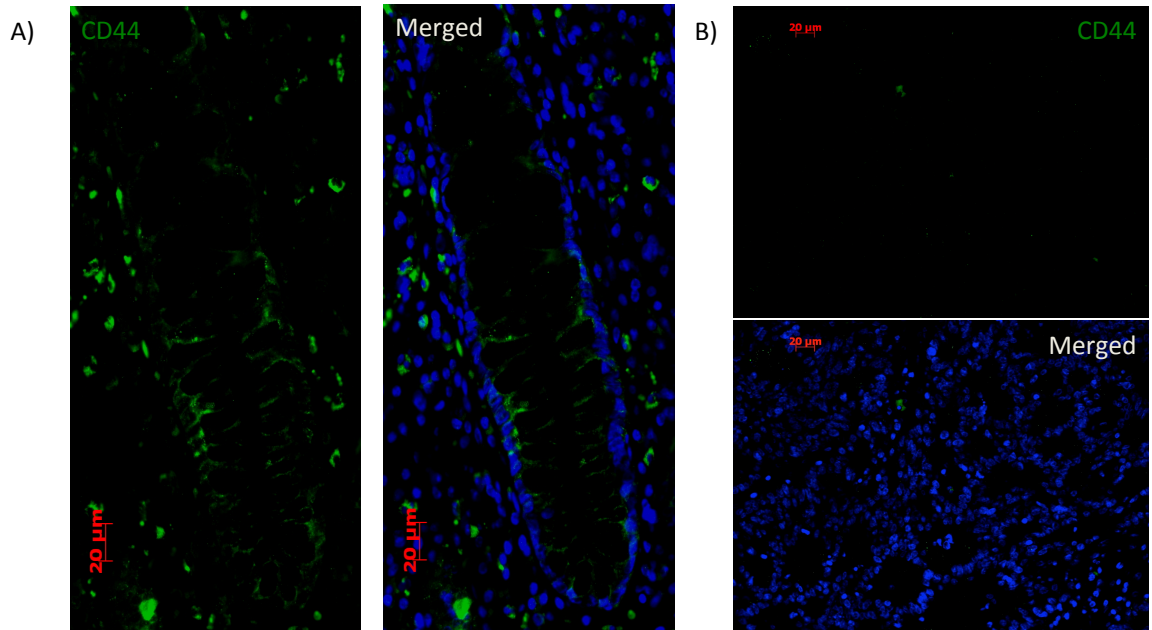
CD44 has been defined as a stem cell marker for the colon. Recently, investigators have pointed out a particular isoform of CD44, which plays a role in the SC compartment of normal and tumor tissue for colon cancer [2]. We conducted a similar study to analyze the expression pattern of various isoforms. SDiX Inc., (Newark, DE) generated antibodies for three different isoforms targeted against different domains of this protein. A preliminary tissue staining experiment was designed where 5 pairs of normal and tumor patient tissue were analysed for the expression of these 3 specific isoforms. Results suggested that the antibody 4077 showed consistent expression in normal and tumor with strong stromal staining across all 5 patients (**Figure A.5**). The antibody 4080 and 4081 gave ambiguous staining pattern in normal and tumor of different patients (**Figure A.6 and A.7**). The summary of the staining pattern is provided in Table 5C, 6C and 7C. This study needs to be extended by increasing the sample size of patients tested and also for presence of co-expression with other stem cell markers such as ALDH1, CD166 and LRIG1.



C)

Catalog no: 77	Normal	Tumor
Patient 1	Stains 1/3 rd of the bottom with a lot of stromal staining	Stains small clusters of cells (basolateral side of the cell)
Patient 2	Bright staining at crypt bottom with a lot of stromal staining	Good staining (basolateral side)
Patient 3	Bright positive staining at 1/3 rd of crypt bottom	Bright positive staining at basolateral side
Patient 4	Bright stain with a lot of stromal staining	Basolateral positive staining
Patient 5	Staining positive in the crypt as well as stroma	Stains positive

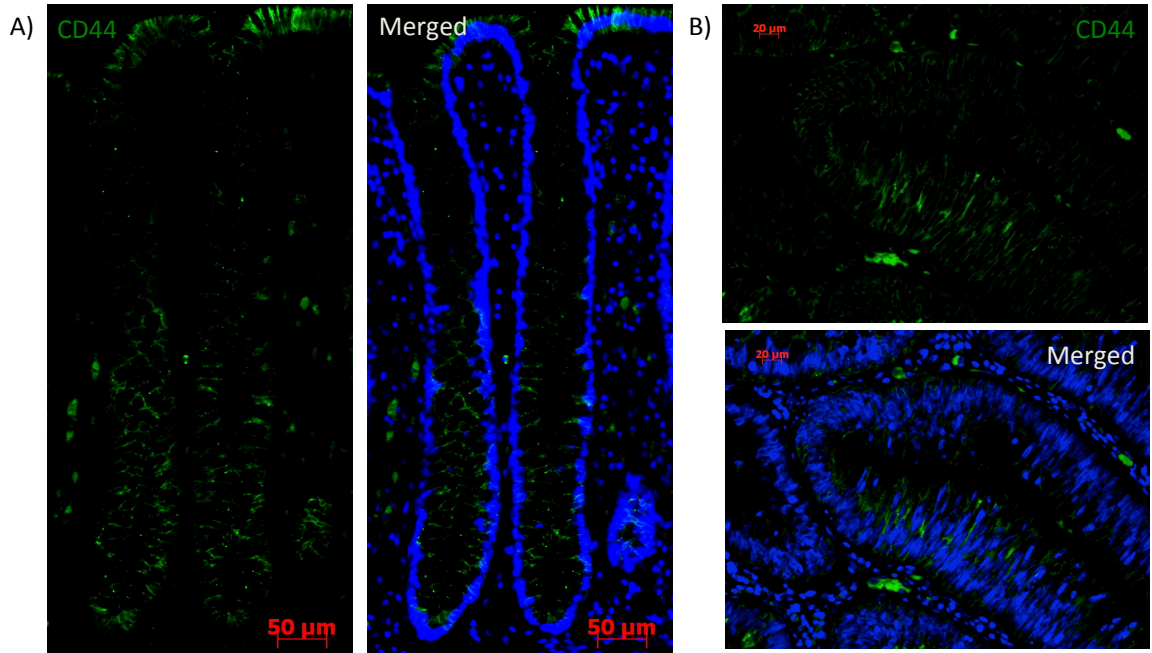
Figure A.5: CD44 staining (4077) of normal and tumor colon tissue. This particular antibody for CD44 stain cells 1/3rd bottom of the normal colonic crypt (A). It also stains specific populations of cells in the colonic tumor tissue (B). Blue represents nuclei stain. C) is a table showing the staining pattern observed across 5 patients tested.



C)

Catalog no: 80	Normal	Tumor
Patient 1	No staining	No staining
Patient 2	Staining at crypt bottom	No staining
Patient 3	Weak staining .	Few cells stain positive
Patient 4	Show non specific staining	Stained positive
Patient 5	Stains at the crypt bottom	No staining

Figure A.6: CD44 staining (4080) of normal and tumor colon tissue. This antibody against CD44 stain cells at the middle and bottom of the normal colonic crypt (A). It shows minimal to weak staining in the colonic tumor tissue (B). Blue represents nuclei stain. C) is a table showing the staining pattern observed across 5 patients tested.



C)

Catalog no: 81	Normal	Tumor
Patient 1	Very very weak staining at high exposure	Positive in adenomatous crypts. Negative In tumor
Patient 2	Weak staining. Mostly background	No staining in tumor
Patient 3	No staining seen in normal	few cells staining positive in tumor
Patient 4	Staining in crypt base	Stained few tumor cells on the apical side
Patient 5	Stained positive in crypt base	Stained cells positive in tumor

Figure A.7: CD44 staining (4081) of normal and tumor colon tissue. CD44 antibody 4081 stain cells towards the lumen as well as base of the normal colonic crypt (A). It also stains specific populations of cells in the colonic tumor tissue (B). Blue represents nuclei stain. C) is a table showing the staining pattern observed across 5 patients tested.

A.4 ANALYSIS OF MRNA LEVELS OF PREDICTED TARGETS FOR DIFFERENTIALLY EXPRESSED MIRS AT THE NORMAL STEM CELL ENRICHED REGION.

MiR7 and miR25 were two of the four miRs, which show differential expression in the crypt bottom as well as in cancer compared to normal tissue. *ADAM12*, *SOX11* and *MeCP2* were identified as common predicted targets for miR7 and miR25 using target prediction tools *rna22*. To test whether these miRs change mRNA expression levels of their predicted targets, colon cancer cell lines HT29 and SW480 cells were transfected with either precursor or antimir for the respective miR and controls. RNA isolated from the cells 48 hours post transfection. Realtime analysis was done for the three genes mentioned above using beta Actin as reference gene. The expression levels for the three genes are represented in **figure A.8**. The mRNA levels of *SOX11* and *ADAM12* were increased significantly in SW480 cells treated with miR25 and miR7 antimirs as compared to the controls. More work has to be done to validate these gene targets by looking at their protein levels via Western blotting and by miR target validation assays such as Luciferase assay.

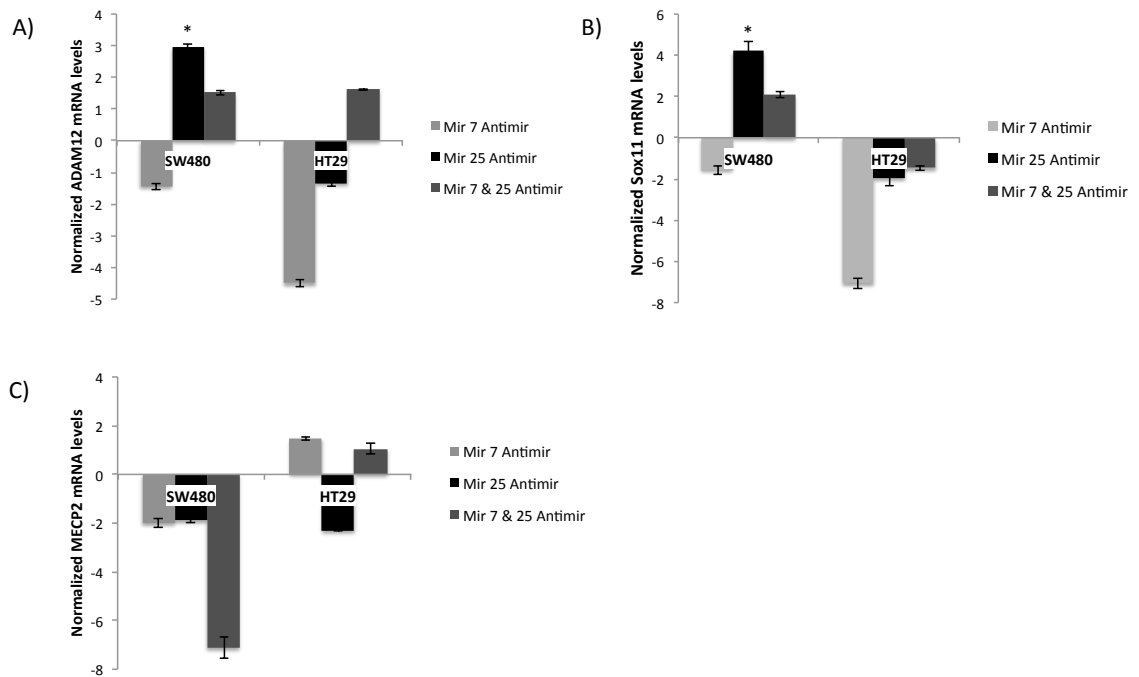


Figure A.8: mRNA levels of common predicted targets of miR25 and miR7. HT29 and SW480 cells were transfected with miR7 antimir, miR25 antimir or both miR7 and miR25, and their respective controls. Bar graphs represents the normalized mRNA levels of *ADAM12* (A), *SOX11* (B) and *MeCP2* (C) in the treated cells as compared to the control. Error bars represent standard error of the mean and * indicates a significant p value < 0.05.

A.5 VALIDATION OF RNA SEQ DATA BY LOOKING AT EXPRESSION OF 3 PREDICTED TARGETS.

RNA SEQ analysis identified ATF2, AKT2 and ATF3 as new predicted targets of miR23b. As this was performed on one replicate, it was important to validate the results. Sets of duplicate experiments were done, where HT29 cells were transfected with miR23b Precursor, Antimir and their respective controls. RNA was isolated 48 hours after transfection and was analyzed for expression levels of ATF2, AKT3 and ATF3 by Real time PCR. Results show that only AKT2 of the three reproduced the trend obtained from RNA SEQ results (**Figure A.9**).

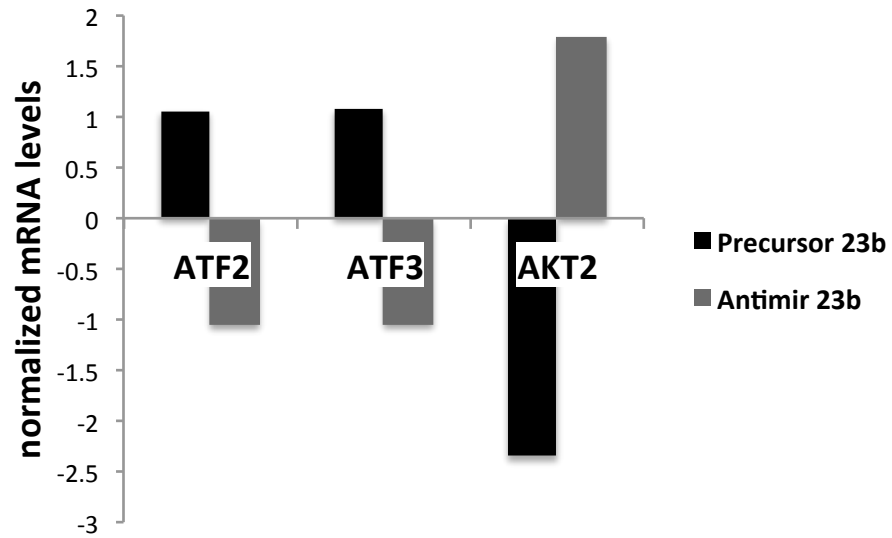


Figure A.9: Expression levels of predicted targets after altered miR23b expression. The graph above represents the average of normalized mRNA levels of the three genes ATF2, ATF3 and AKT2 in the treated HT29 cells (Precursor and Antimir) as compared to the controls.

Table A.1: List of primers of genes used for Real time PCR studies.

GENE	SEQUENCE
<i>ALDH1A1</i>	F: 5' GTTGTCAAACCAGCAGAGCA 3' R: 5' CTGTAGGCCCCATAACCAGGA 3'
<i>LGR5</i>	F: 5' TGCTGGCTGGTGTGGATGCG 3' R: 5' GCCAGCAGGGCACAGAGCAA 3'
<i>LRIG1</i>	F: 5' GGTGAGCCTGGCCTTATGTGAATA 3' R: 5' CACCACCATCCTGCACCTCC 3'
<i>SMAD3</i>	F: 5' CGGCAGTGCCCATTTCCCCTA 3' R: 5' CTAATCCAATCACCTCCAGATT 3'
<i>MeCP2</i>	F: 5' TTGAAGACCTAACCAGGGCCAGAA 3' R: 5' TGGTCAACAGCTTGTCTGGTCAGT 3'
<i>ADAM12</i>	F: 5' CGAGGGGTGAGCTTATGGAAC 3' R: 5' CACTCCGAACAGAGGCACTG 3'
<i>SOX11</i>	F: 5' GGTGGATAAGGATTTGGATTTCG 3' R: 5' GCTCCGGCGTGCAGTAGT 3'
<i>ATF2</i>	F: 5' GGTGCTTTGTAAACACGGCT 3' R: 5' GCAGTCCTTTCTCAAGTTTCC 3'
<i>ATF3</i>	F: 5' GCCATCCAGAACAAGCACCT 3' R: 5' GGCTACCTCGGCTTTTGTGAT 3'
<i>AKT2</i>	F: 5' ATGAATGAGGTGTCTGTTCATCAAAGAAGGC 3' R: 5' TGCTTGAGGCTGTTGGCGACC 3'
<i>GAPDH</i>	F: 5' GAAGGTGAAGGTCGGAGT 3' R: 5' GAAGATGGTGATGGGATTTC 3'
<i>beta ACTIN</i>	F: 5' CACCTTCACCGTTCCAGTTT 3' R: 5' GATGAGATTGGCATGGCTTT 3'

Appendix B

PERMISSIONS

Wallace, Sylvia <SWallace@eb.com> Mon, Apr 21, 2014 at 3:40 PM

To: Vignesh Viswanathan <vignesh@udel.edu>

Encyclopaedia Britannica is happy to grant you permission to use our illustration "human,intestine" only in the Dissertation listed below. We will waive the usual fee and just ask that you use the following credit line in your paper:"By courtesy of Encyclopaedia Britannica ,Inc., copyright 2003; used with permission."

From: Vignesh,Viswanathan [mailto:vignesh@udel.edu],

Sent:Monday, April 21,2014,2:32 PM

To:Wallace,Sylvia

Subject:Re,Content/Copyright,Permissions,S,Viswanathan

Hello Sylvia,

The image is of the large intestine from the following URL

([http://www.britannica.com/EBchecked/media/68639/](http://www.britannica.com/EBchecked/media/68639/Structures-of-the-human-large-intestine-rectum-and-anus-The)

Structures-of-the-human-large-intestine-rectum-and-anus-The). The title of my

dissertation is 'MicroRNAs in normal

and malignant colon stem cells and their possible role in the stem cell origin of colon

cancer'. I am from University Of

Delaware and I intend to publish it end of may or early June.

Regards

Vignesh Viswanathan

PhD Candidate

University of Delaware

On Mon, Apr 21, 2014 at 3:22 PM, Wallace, Sylvia <SWallace@eb.com> wrote:

Dear Mr. Viswanathan,

Your message was passed on to me. I would be happy to help you. Will you please send me the image that you would like to use, your school, the title of your dissertation, and when you plan to publish it?

Best regards,

Sylvia Wallace

Permissions

EB, Inv.

From: Elliff, Ben

Sent: Friday, April 18, 2014 9:30 AM

To: Peppers, Thomas

Subject: Content/Copyright Permissions - Viswanathan

Tom,

I received a call from the customer below as they are interested in using the image **large intestine: mucosa and musculature in humans**, credited to Britannica. They plan to publish the image in the introductory chapter of their dissertation.

Here is their contact information:

Vignesh Viswanathan

vignesh@udel.edu

318-607-2764

Thanks,

Ben

00517288 re:Permission to use a figure in my dissertation

1 message

"Syrra Sanchez" <info@biomedcentral.com> <info@biomedcentral.com> Tue, Apr 1, 2014 at 10:10 PM

To: "vignesh@udel.edu" <vignesh@udel.edu>

Dear Dr Viswanathan

Thank you for contacting BioMed Central.

Reproduction of figures or tables is permitted free of charge and without formal written permission from the publisher or the copyright holder, provided that the figure/table is original, BioMed Central is duly identified as the original publisher, and that proper attribution of authorship and the correct citation details are given as acknowledgement. If you have any questions please do not hesitate to contact me.

Best wishes

Dunncan Suarez

Customer Services

info@biomedcentral.com

www.biomedcentral.com

-----Your Question/Comment -----

Hello,

I am a PhD Candidate and I am writing my dissertation of miRNAs role in colon cancer stem cells. I want to use an image (Figure 1) from one of your open access reviews titled: MicroRNAs in colorectal cancer: translation of molecular biology into clinical application Molecular Cancer 2009, 8:102

It says online that I dont need formal permission if I cite and acknowledge the article properly but I still wanted to make sure if it is right way to do it.

Regards

Vignesh Viswanathan

regarding permissions to use images from website

4 messages

Vignesh Viswanathan <vignesh@udel.edu> Mon, Mar 10, 2014 at 4:20 PM

To: mpotter8@jhmi.edu

Hello Michelle,

I just spoke to you couple of minute back. I am graduate student at the University of Delaware writing my PhD dissertation on colon cancer stem cells and I am seeking your permission to use three images in my introduction chapter which are provided in the website (<http://www.hopkinscoloncancercenter.org>). Here are specific links for the images:

1) Depiction of colorectal stem cells

(http://www.hopkinscoloncancercenter.org/CMS/CMS_Page.aspx?CurrentUDV=59&CMS_Page_ID=2E075D97-85A2-4CBC-A417-8379D1586907)

2) Normal colorectal anatomy

(http://www.hopkinscoloncancercenter.org/CMS/CMS_Page.aspx?CurrentUDV=59&CMS_Page_ID=B6ACAEF5-52D3-4CC1-88CC-CEB21F5ABBCD)

3) TNM classification of colorectal cancer stages

(http://www.hopkinscoloncancercenter.org/CMS/CMS_Page.aspx?CurrentUDV=59&CMS_Page_ID=EEA2CD91-3276-4123-BEEB-BAF1984D20C7)

I look forward to your response.

Regards,

Vignesh Viswanathan

PhD Candidate

University Of Delaware

Michelle Potter <mpotter8@jhmi.edu> Mon, Mar 10, 2014 at 4:27 PM

To: Vignesh Viswanathan <vignesh@udel.edu>

Hello Vignesh,

I forwarded your request to the appropriate person who handles this web site.

Thanks,

Michelle

Michelle Potter

Communications Specialist

Johns Hopkins Kimmel Cancer Center

Office of Public Affairs

901 S. Bond Street Suite 573

Baltimore, MD 21231

(410)R614R2914

www.hopkinskimmelcancercenter.org

Vignesh Viswanathan <vignesh@udel.edu> Mon, Mar 10, 2014 at 4:32 PM

To: Michelle Potter <mpotter8@jhmi.edu>

Thank you Michelle !

Vignesh

Michelle Potter <mpotter8@jhmi.edu> Tue, Mar 11, 2014 at 9:34 AM

To: Vignesh Viswanathan <vignesh@udel.edu>

Good morning,

You may use the images, as long as you cite the Johns Hopkins Colon Cancer Center as the source of the photo.

Many thanks,

Michelle

From: Dan Edelstein <edelstein@jhu.edu>

Date: Monday, March 10, 2014 5:03 PM

To: Michelle Potter <mpotter8@jhmi.edu>

Subject: Re: regarding permissions to use images from website

Hi Michelle,

I'm not actively managing the website, however, please relay to this individual that it is perfectly fine for him to use the images as long as he cites the Johns Hopkins colon cancer center as the source.

Thank you!

Best,

RDan

Sent from my iPhone

On Mar 10, 2014, at 9:26 PM, "Michelle Potter" <mpotter8@jhmi.edu> wrote:

Hi Dan,

I wasn't sure if you still ran the Colon Cancer Web site.

We received a call from the gentleman below in regards to photos. Please see email below.

Thanks,

Michelle

Michelle Potter

Communications Specialist

Johns Hopkins Kimmel Cancer Center

Office of Public Affairs

901 S. Bond Street Suite 573

Baltimore, MD 21231

(410)R614R2914

www.hopkinskimmelcancercenter.org

AMERICAN ASSOCIATION FOR CANCER RESEARCH LICENSE TERMS AND CONDITIONS

May 03, 2014

This is a License Agreement between Vignesh Viswanathan ("You") and American Association for Cancer Research ("American Association for Cancer Research") provided by Copyright Clearance Center ("CCC"). The license consists of your order details, the terms and conditions provided by American Association for Cancer Research, and the payment terms and conditions.

All payments must be made in full to CCC. For payment instructions, please see information listed at the bottom of this form.

License Number 3362060077415

License date Apr 04, 2014

Licensed content publisher American Association for Cancer Research

Licensed content publication Cancer Research

Licensed content title Aldehyde Dehydrogenase 1 Is a Marker for Normal and Malignant

Human Colonic Stem Cells (SC) and Tracks SC Overpopulation during Colon Tumorigenesis

Licensed content author Emina H. Huang, Mark J. Hynes, Tao Zhang et al.

Licensed content date April 15, 2009

Volume number 69

Issue number 8

Type of Use Thesis/Dissertation

Requestor type academic/educational

Format print and electronic

Portion figures/tables/illustrations

Number of

figures/tables/illustrations 3

Will you be translating? no

Circulation 10

Territory of distribution Worldwide

Title of your thesis /

Dissertation MicroRNA dysregulation in normal colon stem cells and its role in colon tumorigenesis

Expected completion date May 2014

Estimated size (number of 200 pages)

Total 0.00 USD

[Terms and Conditions](#)

American Association for Cancer Research (AACR) Terms and Conditions

INTRODUCTION

The Publisher for this copyright material is the American Association for Cancer Research (AACR). By clicking "accept" in

connection with completing this licensing transaction, you agree to the following terms and conditions applying to this transaction. You also agree to the Billing and Payment terms and conditions established by Copyright Clearance Center (CCC) at the time you opened your Rightslink account.

LIMITED LICENSE

The AACR grants exclusively to you, the User, for onetime, non-exclusive use of this material for the purpose stated in your request and used only with a maximum distribution equal to the number you identified in the permission process. Any form of republication must be completed within one year although copies made before then may be distributed thereafter and any electronic posting is limited to a period of one year. Reproduction of this material is confined to the purpose and/or media for which permission is granted. Altering or modifying this material is not permitted. However, figures and illustrations may be minimally altered or modified to serve the new work.

GEOGRAPHIC SCOPE

Licenses may be exercised as noted in the permission process

RESERVATION OF RIGHTS

The AACR reserves all rights not specifically granted in the combination of 1) the license details provided by you and accepted in the course of this licensing transaction, 2) these terms and conditions , and 3) CCC's Billing and Payment terms and conditions.

DISCLAIMER

You may obtain permission via Rightslink to use material owned by AACR. When you are requesting permission to reuse a portion for an AACR publication, it is your responsibility to examine each portion of content as published to determine whether a credit to, or copyright notice of a third party owner is published next to the item. You must obtain permission from the third party to use any material which has been reprinted with permission from the said third party. If you have not obtained permission from the third party, AACR disclaims any responsibility for the use you make of items owned by them.

LICENSE CONTINGENT ON PAYMENT

While you may exercise the rights licensed immediately upon issuance of the license at the end of the licensing process for the transaction, provided that you have disclosed complete and accurate details of your proposed use, no license is finally effective unless and until full payment is received from you, either by the publisher or by the CCC, as provided in CCC's Billing and Payment terms and conditions. If full payment is not received on a timely basis, then any license preliminarily granted shall be deemed automatically revoked and shall be void as if never granted. Further, in the event that you breach any of these terms and conditions, or any of the CCC's Billing and Payment terms and conditions, the license is automatically revoked and shall be void as if never granted. Use of materials as described in a revoked license, as well as any use of the materials beyond the scope of an unrevoked license, may constitute copyright infringement and the publisher reserves the right to take any and all action to protect its copyright in the materials.

COPYRIGHT NOTICE

You must include the following credit line in connection with your reproduction of the licensed material: "Reprinted (or adapted) from Publication Title, Copyright Year, Volume/Issue, Page Range, Author, Title of Article, with permission from AACR".

TRANSLATION

This permission is granted for non-exclusive world English rights only.

WARRANTIES

Publisher makes no representations or warranties with respect to the licensed material.

INDEMNIFICATION

You hereby indemnify and agree to hold harmless the publisher and CCC, and their respective officers, directors, employees and agents, from and against any and all claims arising out of your use of the licensed material other than as specifically authorized pursuant to this license.

REVOCACTION

The AACR reserves the right to revoke a license for any reason, including but not limited to advertising and promotional uses of AACR content, third party usage and incorrect figuresource attribution.

NO TRANSFER OF LICENSE

This license is personal to you and may not be sublicensed, assigned, or transferred by you to any other person without publisher's written permission.

NO AMENDMENT EXCEPT IN WRITING

This license may not be amended except in a writing signed by both parties (or, in the case of publisher, by CCC on publisher's behalf).

OBJECTION TO CONTRARY TERMS

Publishers hereby objects to any terms contained in any purchase order, acknowledgement, check endorsement or other writing prepared by you, which terms are inconsistent with these terms and conditions or CCC's Billing and Payment terms and conditions. These terms and conditions together with CCC's Billing and Payment terms and conditions (which are incorporated herein) comprise the entire agreement between you and publisher (and CCC) concerning this licensing transaction. In the event of any conflict between your obligations established by these terms and conditions, and those established by CCC's Billing and Payment terms and conditions, these terms and conditions shall control.

THESIS/DISSERTATION TERMS

If your request is to reuse an article authored by you and published by the AACR in your dissertation/thesis, your thesis may be submitted to your institution in either in print or electronic form. Should your thesis be published commercially, please reapply.

ELECTRONIC RESERVE

If this license is made in connection with a course, and the Licensed Material or any portion thereof is to be posted to a website, the website is to be password protected and made available only to the students registered for the relevant

course. The permission is granted for the duration of the course. All content posted to the website must maintain the copyright information notice.

JURISDICTION

This license transaction shall be governed by and construed in accordance with the laws of Pennsylvania. You hereby agree to submit to the jurisdiction of the federal and state courts located in Pennsylvania for purposes of resolving any disputes that may arise in connection with this licensing transaction.

Other Terms and Conditions: None v1.0

If you would like to pay for this license now, please remit this license along with your payment made payable to "COPYRIGHT CLEARANCE CENTER" otherwise you will be invoiced within 48 hours of the license date. Payment should be in the form of a check or money order referencing your account number and this invoice number RLNK501269913.

Once you receive your invoice for this order, you may pay your invoice by credit card.

Please follow instructions provided at that time.

Make Payment To:

Copyright Clearance Center

Dept 001

P.O. Box 843006

Boston, MA 02284-3006

For suggestions or comments regarding this order, contact RightsLink Customer

Support: customer@copyright.com or +1-877-622-5543 (toll free in the US) or +1- 978-646-2777. Gratis licenses (referencing \$0 in the Total field) are free. Please retain this printable license for your reference. No payment is required.

SPRINGER LICENSE TERMS AND CONDITIONS

This is a License Agreement between Vignesh Viswanathan ("You") and Springer ("Springer") provided by Copyright Clearance Center ("CCC"). The license consists of your order details, the terms and conditions provided by Springer, and the payment terms and conditions.

All payments must be made in full to CCC. For payment instructions, please see information listed at the bottom of this form.

License Number 3360260739735

License date Apr 01, 2014

Licensed content publisher Springer

Licensed content publication Virchows Archiv

Licensed content title The impact of microRNAs on colorectal cancer

Licensed content author Claudius Faber

Licensed content date Jan 1, 2009

Volume number 454

Issue number 4

Type of Use Thesis/Dissertation

Portion Figures

Author of this Springer

Article No

Order reference number None

Original figure numbers Figure 3

Title of your thesis /

Dissertation MicroRNA dysregulation in normal colon stem cells and its role in colon tumorigenesis

Expected completion date May 2014

Estimated size(pages) 200

Total 0.00 USD

[Terms and Conditions](#)

Introduction

The publisher for this copyrighted material is Springer Science + Business Media. By clicking "accept" in connection with completing this licensing transaction, you agree that the following terms and conditions apply to this transaction (along with the Billing and Payment terms and conditions established by Copyright Clearance Center, Inc. ("CCC"), at the time that you opened your Rightslink account and that are available at any time at

<http://myaccount.copyright.com>).

Limited License

With reference to your request to reprint in your thesis material on which Springer Science and Business Media control the

copyright, permission is granted, free of charge, for the use indicated in your enquiry. Licenses are for one-time use only with a maximum distribution equal to the number that you identified in the licensing process. This License includes use in an electronic form, provided its password protected or on the university's intranet or repository, including UMI (according to the definition at the Sherpa website:

<http://www.sherpa.ac.uk/romeo/>). For any other electronic use, please contact Springer at (permissions.dordrecht@springer.com or

permissions.heidelberg@springer.com).

The material can only be used for the purpose of defending your thesis limited to university use only. If the thesis is going to be published, permission needs to be re-obtained (selecting "book/textbook" as the type of use). Although Springer holds copyright to the material and is entitled to negotiate on rights, this

license is only valid, subject to a courtesy information to the author (address is given with the article/chapter) and provided it concerns original material which does not carry references to other sources (if material in question appears with credit to another source, authorization from that source is required as well).

Permission free of charge on this occasion does not prejudice any rights we might have to charge for reproduction of our copyrighted material in the future.

Altering/Modifying Material: Not Permitted

You may not alter or modify the material in any manner.

Abbreviations, additions, deletions and/or any other alterations shall be made only with prior written authorization of the author(s) and/or Springer Science + Business Media. (Please contact Springer at (permissions.dordrecht@springer.com or permissions.heidelberg@springer.com)

Reservation of Rights

Springer Science + Business Media reserves all rights not specifically granted in the combination of (i) the license details provided by you and accepted in the course of this licensing

transaction, (ii) these terms and conditions and (iii) CCC's Billing and Payment terms and conditions.

Copyright Notice:Disclaimer

You must include the following copyright and permission notice in connection with any reproduction of the licensed material:

"Springer and the original publisher /journal title, volume, year of publication, page, chapter/article title, name(s) of author(s), figure number(s), original copyright notice) is given to the publication in which the material was originally published, by adding; with kind permission from Springer Science and Business Media"

Warranties: None

Example 1: Springer Science + Business Media makes no representations or warranties with respect to the licensed material.

Example 2: Springer Science + Business Media makes no representations or warranties with respect to the licensed material and adopts on its own behalf the limitations and disclaimers established by CCC on its behalf in its Billing and Payment terms and conditions for this licensing transaction.

Indemnity

You hereby indemnify and agree to hold harmless Springer Science + Business Media and CCC, and their respective officers, directors, employees and agents, from and against any and all claims arising out of your use of the licensed material other than as specifically authorized pursuant to this license.

No Transfer of License

This license is personal to you and may not be sublicensed, assigned, or transferred by you to any other person without Springer Science + Business Media's written permission.

No Amendment Except in Writing

This license may not be amended except in a writing signed by both parties (or, in the case of Springer Science + Business

Media, by CCC on Springer Science + Business Media's behalf).
Objection to Contrary Terms

Springer Science + Business Media hereby objects to any terms contained in any purchase order, acknowledgment, check endorsement or other writing prepared by you, which terms are inconsistent with these terms and conditions or CCC's Billing and Payment terms and conditions. These terms and conditions, together with CCC's Billing and Payment terms and conditions (which are incorporated herein), comprise the entire agreement between you and Springer Science + Business Media (and CCC) concerning this licensing transaction. In the event of any conflict between your obligations established by these terms and conditions and those established by CCC's Billing and Payment terms and conditions, these terms and conditions shall control.

Jurisdiction

All disputes that may arise in connection with this present License, or the breach thereof, shall be settled exclusively by arbitration, to be held in The Netherlands, in accordance with Dutch law, and to be conducted under the Rules of the 'Netherlands Arbitrage Instituut' (Netherlands Institute of Arbitration). **OR:**

All disputes that may arise in connection with this present License, or the breach thereof, shall be settled exclusively by arbitration, to be held in the Federal Republic of Germany, in accordance with German law.

Other terms and conditions: v1.3

If you would like to pay for this license now, please remit this license along with your payment made payable to "COPYRIGHT CLEARANCE CENTER" otherwise you will be invoiced within 48 hours of the license date. Payment should be in the form of a check

or money order referencing your account number and this invoice number RLNK501266413.

Once you receive your invoice for this order, you may pay your invoice by credit card.

Please follow instructions provided at that time.

Make Payment To:

Copyright Clearance Center

Dept 001

P.O. Box 843006

Boston, MA 02284-3006

For suggestions or comments regarding this order, contact RightsLink Customer Support: customercare@copyright.com or +1-877-622-5543 (toll free in the US) or

+1-

978-646-2777.

Gratis licenses (referencing \$0 in the Total field) are free. Please retain this printable license for your reference. No payment is required.



Institutional Review Board
FWA00006557

Helen F. Graham Cancer Center & Research
Institute
West Pavilion - Suite 2350
4701 Ogletown Stanton Road
Newark, DE 19713

302-623-4983 phone
302-623-4989 phone
302-623-6863 fax

MEMORANDUM

Steve Kushner, MD
Chairman, IRB #1
Gary Johnson, PhD
Chairman, IRB #2
Jerry Castellano, PharmD, CIP
Corporate Director
Janet Leary-Prowse, MSEd, CIP
IRB Education Specialist
Heidi Derr, BA, CIP
IRB Regulatory Affairs/Auditor
Sonia Martinez-Colon
Executive Assistant
Judy Hutt, BS
Administrative Assistant II

DATE: November 27, 2013
TO: Bruce M. Boman, MD, PhD, MSPH
Oncology Research
Christiana Hospital
FROM: Judy Hutt 
RE: **CCC# 28058 - microRNA Expression
in Colon Cancer Stem Cells:
(DDD# 600277)**

This is to officially inform you that the Continuing Review for your protocol, which was received on **11/27/2013**, was reviewed by Expedited Review and approved by Jerry Castellano, Pharm.D, CIP, Corporate Director of the Christiana Care Health System Institutional Review Board, on **11/27/2013**.

Approval was extended for a period of one year, through **11/26/2014**. A stamped consent form is attached for your records.

Our records indicate this study is OPEN.

If you have any questions or concerns, please contact the IRB Office.

Thank you

This approval verifies that the IRB operates in Accordance with applicable ICH, federal, local and institutional regulations, and with all GCP Guidelines that govern institutional IRB operation.